

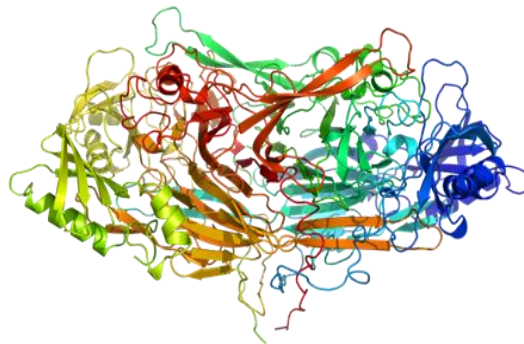


SAPIENZA
UNIVERSITÀ DI ROMA

PhD Course in Biochemistry

Cycle XXXV (2019 – 2022)

**BIOCATALYTIC APPLICATIONS
OF LATHYRUS CICERA AMINE OXIDASE**



PhD candidate

Elisa Di Fabio

Tutor

Prof. Alberto Macone

Coordinator

Prof. Stefano Gianni

Acknowledgements

The experimental work herein reported was carried out at the Department of Biochemical Sciences A. Rossi Fanelli of “Sapienza” University of Rome.

First and foremost, I would like to express all my gratitude to my Tutor prof. Alberto Macone, who deeply introduced me to the research world. I appreciated the faith in my person and my skills, enough to entrust me with the project. Forgetting even one day of those spent in the laboratory will be harsh.

My sincere gratitude goes to prof. Alessandra Bonamore and prof. Alberto Boffi for the opportunity to be part of the research group. Your professionalism, your carefulness and the interest shown towards the project topic have contributed to conquer this path.

Thanks to prof. Giancarlo Fabrizi from Chemistry and Technology of Drugs Department of Sapienza for the valuable collaboration in this research.

My deep gratitude to prof. Francesco Malatesta. I will carry in my emotional baggage the guidance from a presence as firm as you are.

I want to express all my affection and gratitude to the handsome research team I have lived with these years sharing ideals and...pipettes. To PhD Federica Palombarini, Dr. Alessio Incocciati, Dr. Ilaria Vinante, Dr. Valentina Caseli, Stefan Vasile, and Chiara Cappelletti, whom I thank for always being involved in a way that goes beyond the science edges.

Thank to my parents Stefano and Carla, my sister Barbara and all my beloved ones. Thank you to those who know how much I have cared about this route and have never stopped believing in what I have built over the years.

Ad maiora, semper

- Elisa -

*To my soulmate Emilio
and his kind heart*

Index

1) INTRODUCTION	8
1.1 Green Chemistry	8
1.2 Biocatalysis: “Catalytic rather than stoichiometric reagents”	14
1.2.1 Enzymes: properties and features	14
1.2.2 Biocatalysis in pharmaceutical industry	17
1.2.3 Biocatalysis: applications and tools	19
1.2.4 Enzyme immobilization on solid supports.....	20
1.3 Amine Oxidases	24
1.3.1 Amine Oxidases family.....	24
1.3.2 Copper-containing Amine Oxidases	25
1.3.3 <i>Lathyrus cicera</i> Amine Oxidase	31
2) AIM OF THE WORK	34
3) MATERIALS AND METHODS	37
3.1 Chemicals.....	37
3.2 LCAO chromatography-free purification protocol.....	37
3.3 LCAO activity.....	39
3.4 Enzymatic synthesis of aldehydes.....	39
3.5 HPLC analysis of aldehydes	40
3.6 GC/MS analysis of aldehydes	40
3.7 Purpald® colorimetric assay	41
3.8 LCAO immobilization on solid supports	41
3.9 Synthesis and characterization of 1-benzyl-7-methoxy-1,2,3,4- tetrahydroisoquinolin-6-ol	45

3.10 LCAO stability in non-aqueous media.....	47
4) RESULTS AND DISCUSSION.....	49
4.1 LCAO purification	49
4.2 Exploring LCAO activity towards aliphatic and aromatic amines ..	54
4.3 Biocatalytic production of aldehydes.....	60
4.4 Immobilization of LCAO.....	71
4.5 Characterization and performance study of LCAO-MMPs	75
4.6 Biocatalytic application of immobilized LCAO	78
4.7 LCAO stability in non-aqueous media.....	88
5) CONCLUSIONS	94
6) BIBLIOGRAPHY.....	97
7) APPENDIX I.....	109
8) APPENDIX II.....	115
9) APPENDIX III.....	130
10) APPENDIX IV	131
11) APPENDIX V.....	132
12) APPENDIX VI	133

CHAPTER 1

INTRODUCTION

1.1 Green Chemistry

To date, chemistry has assumed a fundamental role in almost all aspects of modern society. The tendency towards a better quality of life is increasing the demand and the use of ever more advanced amounts of chemicals. However, the last decades of the 20th century have seen growing concerns about the impact of chemical products on the environment, such as increased levels of greenhouse gases, the fertilizers present in waterways, and stratospheric ozone depletion. The perplexity about the chemical industry, reflecting the more negative effects such as global warming and dramatic pollution rates, has been consolidating over time. It now represents a serious global issue that has required a revolution and a reassessment of production processes.

The scarcity of resources is a concept that took on a meaning originally with the oil crises of the 1970s, first in 1973 with the Yom Kippur War and later with the Iranian Revolution (1979). Due to the sharp rise in the international oil price market, the concept of "limit" came overwhelmingly in the Western world and everyday life, and economic growth lost the vigor of the 1950s and 1960s. While society had benefited from the post-war growth up to that point, governments had now introduced energy-saving measures. Due to the austerity

policies applied in many states, the industrial system no longer knew the growth rates recorded in previous decades. Especially from 1979, a technological revolution increased the energy efficiency of western economies: in the field of research, new energy sources began to be investigated [1].

The concept of sustainability, however, began to spread only in the 1980s and was officially adopted in the Brundtland report, called *Our Common Future*, published in 1987 by the World Commission on Environment and Development (WCED). The Brundtland report, still valid today, defined a strategy, known as *sustainable development*, which addressed the global problems caused by the unsustainable consumption of industrialized countries [2]. Any plan of action had to make a serious commitment to finding alternatives to fossil fuels and to redesigning machinery to use less energy. From then on, environment and development have no longer been such distant ideologies: there is no development if environmental resources are deteriorating.

The Brundtland report made governments aware of the critical issues and challenges that had to be faced in the immediate future (scarcity of resources and food, effects on ecosystems, and industrial regression risk). In the years to come, various measures have been taken to confine the repercussions of chemical processes. The first approach was made in 1969 by Coca-Cola Company, which originally conceived the Life Cycle Assessment (LCA) [3]. For a correct assessment of the environmental impact of a product, each phase of the process must be considered, from the moment the starting materials are obtained to when they are processed into the final product, which will ultimately be disposed of or recycled. This analysis identifies which aspects are necessary to promote sustainability. Depending on the goal of the industry,

edges can cover the entire supply chain (cradle-to-grave) or be set on raw materials extraction and processing (cradle-to-gate), or just on the manufacturing domain (gate-to-gate). This valuation grew over the decades to promote a "cradle-to-cradle" model to industries.

The turning point, however, came between the end of the 1980s and the early 1990s, when the scientific community defined metrics for assessing the environmental footprint of processes. Atom Economy is a metric first introduced in 1991 by Barry Trost [4]. This theoretical number is given by dividing the molecular weight of the desired product by the total mass of all substances formed in the stoichiometric equation, without considering the contribution of chemicals and solvents in the reaction mixture. Atom Economy evaluates, before performing any experiment, the approximate conversion efficiency of a chemical process through the stoichiometric quantities of starting materials and the desired product. Unlike the chemical yield, for which high levels may still represent significant rates of by-products, the optimal value of Atom Economy is 100%. A higher conversion of reactant atoms into the products means a smaller percentage is transformed into undesired derivatives and environmental and economic effects of waste disposal decrease [5]. The following year, Roger Sheldon first published on the Environmental (Impact) Factor [6]. Sheldon observed that the synthesis of 1 kg of phloroglucinol led to the production of 40 kgs of solid chromium-containing waste starting from the carcinogen trinitrotoluene (TNT). By investigating other processes, he realized kilos of waste were generated for other fine chemicals, bulk chemicals, and APIs. He proposed the E factor as a new parameter indicating the yield of an organic reaction when taking the produced waste and the toxicity of chemicals into account [7]. It is the ratio between the mass expressed in kilos of waste and the products, and its optimal value is zero.

A low E factor means lower production of waste and, consequently, a more negative impact on the environment.

Over time, alternative metrics [8, 9] have been proposed, such as Mass Efficiency [10], Mass Intensity [11], and Environmental Quotient [12]. However, Atom Economy and Environmental Factor were crucial in comprehending that the balance between desired products and refuse is favored if less waste is generated [13]. Immediately after, this ideology culminated in the innovative *modus operandi* named Green Chemistry [14]. The term was coined in the early 1990s by Paul Anastas, Director of Yale University's Center for Green Chemistry and a member of the United States Environmental Protection Agency. Green Chemistry is an ethical approach encouraging the design and development of materials, technologies, and chemical processes with a lower impact on the environment than traditional methods. In its most recent definition, this methodology contemplates mainly the quantitative reduction of waste generated and directs manufacturing towards less hazardous and polluting procedures and substances. From then on, the new order of priority for industry and research has relied on specific indications aiming at eco-sustainability. These guidelines merged into the 12 principles of Green Chemistry, published in 1998 by Paul Anastas and his colleague John Warner [15].



Applying sustainable chemistry principles does not mean limiting activity of companies. The aim remains to guarantee the production growth, as highlighted for the 12 principles of Green Chemistry summarized in the acronym PRODUCTIVELY [16].

P	Prevent waste
R	Renewable material
O	Omit derivatization steps
D	Degradable chemical products
U	Use safe synthetic methods
C	Catalytic reagents
T	Temperature, pressure ambient
I	In-process monitoring
V	Very few auxiliary substances
E	E-factor, maximise feed in product
L	Low toxicity
Y	Yes, it is safe

Waste prevention is the first of the 12 principles and the postulate upon which the entire philosophy of Green Chemistry rests. Humans, as living beings, will always be responsible for emissions. Rather than seeking remedies, eco-friendly production must focus on waste prevention. With a minimum amount of waste, lessening the environmental impact can be operated on several fronts, e.g. by making the waste more easily degradable or by consuming less energy for its disposal. The other postulates suggest several precautions to avoid the formation of large quantities of waste, perhaps toxic. A synthesis carried out with auxiliary and safer reaction media, or by reducing/eliminating the use of organic solvents, is beneficial for the environment and human health. A method designed to maximize the incorporation of all starting materials into the final product avoids losses. Another indication is to choose raw materials rather than exhaustible ones and to monitor the real-time quantity of dangerous substances formed. Thus, if a process follows the first postulate of Green Chemistry, the other principles are respected accordingly. When the synthesis of a molecule leads to an application, green chemistry allows its production with minimal environmental implications [17].

1.2 Biocatalysis: “Catalytic rather than stoichiometric reagents”

Biocatalysis is a Green Chemistry postulate fulfilling 10 out of the 12 principles, and it has emerged as the key to achieve green procedures [18]. The term refers to the use of biocatalysts as an alternative to metal- and organocatalysis. Enzymes employed for this synthetic schedule can be used as isolated preparations of wild-type or genetically modified variants, or in whole cells, either as native cells or as recombinant expressed proteins inside host cells [19].

1.2.1 Enzymes: properties and features

Enzymes are the basis of life processes. Humankind has employed these natural catalysts for hundreds of years [20], first unconsciously as part of the microbial processes (in wine, vinegar, cheese, and bread making), then aware that the enzyme hallmarks allowed for their diffusion in the most heterogeneous fields.

At the dawn of this transition, most enzymes belonged primarily to hydrolases or amidases [21]. As a result, reactions consisted mainly of the resolution of primary and secondary chiral alcohols, amines, or carboxylic acids.

Currently, biocatalysis is the point of reference in sustainable development and has found application in innumerable fields, ranging from pharmaceuticals to polymer synthesis, in addition to food, flavors, fragrances, beverage, textile, and agricultural industries. In a short time, this strategy has affected almost

every production process. The food industry [22], for instance, is based on biocatalytic applications to produce cheese, aspartame, and syrups, but also to extract bioactive compounds and eliminate food safety hazards. Some biocatalysts are also ideal candidates for biofuel production through biorefining [23]. Ene-reductase is a robust alternative to metal- and organocatalyzed double-bond reductions adopted by the flavors and fragrances industry [24]. Polyethylene terephthalate (PET) depolymerization from waste bottles is probably among the most impactful hydrolase applications as terephthalic acid monomer can be rehabilitated in the production cycle to reconstitute the polymer [25].

Biocatalysis is of great interest to the industrial scenery because its application makes processes in line with the concept of sustainability. Combining environmental and worker safety with progress is a challenge facilitated by the unique features of biocatalysts.

Enzymes are biodegradable compounds obtained from inexpensive renewable sources such as microorganisms or plants. Preferring a synthetic pathway based on enzymatic catalysis lowers the cost of goods in terms of energy and materials [21]. In addition, the protein is stored stably and without special precautions in its natural environment until the extraction.

The benefits are evident if biocatalysis is compared to reactions adopting precious and polluting metals. Palladium and platinum have been used for decades to catalyze hydrogenation reactions. To date, green options replace metal catalysts. For instance, the immobilization of old yellow enzyme (YqjM) and glucose dehydrogenase leads to the asymmetric hydrogenation of C=C bonds in SpinChem reactors [26].

Biocatalysts react under mild reaction conditions at low temperatures, atmospheric pressure, and in economic and easy-to-find solvents. Unlike chemical routes, biotransformations occur in batch reactors without requiring costly specific devices [27].

Replacing stoichiometric reagents with catalytic cycles improves the efficiency of a reaction, shortening synthetic routes [28]. A case in point concerns the development of the enzymatic process devised by Merck to synthesize the sodium salt of Montelukast, a drug administered for the treatment of asthma. Compared to the chemical pathway, the involvement of an engineered alcohol dehydrogenase accelerates production [29]. Catalytic cycles also generate fewer by-products and wastes.

The natural medium where enzymes perform their activity is water, which can be considered the ecological solvent par excellence. Processes carried out by biocatalysts avoid stoichiometric amounts of reagents and reduce/eliminate organic and toxic solvents. GlaxoSmithKline, for instance, has opted for an alcohol dehydrogenase from *Rhodococcus erythropolis* to convert p-chloroacetophenone into the optically active (S)-enantiomer in a two-phase system composed of water and a long chain alkane [30].

All these features reduce hazards across all the life-cycle stages. In addition to being economically profitable, biocatalysis emerges as a valid alternative for the industry when the interest is a safer, more sustainable, and highly selective process.

1.2.2 Biocatalysis in pharmaceutical industry

According to Roger Sheldon, the pharmaceutical stood out as the sector with the highest Environmental Factor (**Table 1**) among the chemical industries and emerged as the biggest waste producer [31].

Sector	Product tonnage	E factor (kg waste per kg product)
Oil refining	10 ⁶ -10 ⁸	< 0.1
Bulk chemicals	10 ⁴ -10 ⁶	<1 to 5
Fine chemicals	10 ² -10 ⁴	5 to > 50
Pharmaceuticals	10-10 ²	25 to > 100

Table 1 Chemical industry E factors evaluation by evaluation by R.A. Sheldon
E factors, green chemistry and catalysis: an odyssey (2008)

Given the estimates, the pharmaceutical field could not fail to include a renewal aimed at sustainability [19, 27, 32]. Over time, biocatalysis has merged into pharmaceutical chemistry, permitting it to become a rapidly eco-sustainable growing field. The applications are widespread. Panke and coworkers reported a biocatalytic route comprising invertases and an epimerase to synthesize D-psicose. [33]. Both boceprevir [34] and telaprevir [35], and proton-pump inhibitor esomeprazole, are synthesized by oxidases. L-3,4-dihydroxyphenylalanine (L-DOPA) is obtained by *Erwinia herbicola* cells expressing a tyrosine phenol lyase [36].

High turnover number and enormous reaction rate acceleration distinguish biotransformations unequivocally. Because enzymes are not consumed in the reactions, and can be used several times, even a small quantity is needed. This property is the basis of the effectiveness of enzymes.

In addition, the flexibility of biocatalysts breaks down the barrier defined by the molecular structure of a drug. The pharmacological targets are specific

regions of cellular macromolecules with complex three-dimensional geometry. Thus, they recognize and interact only with other complementary molecules. The flexible structure of the enzymes adapts to the target, which reshapes the active site, then returns to its conformation without having undergone permanent changes.

Traditional organic synthesis often leads to racemic mixtures. In most cases only one of the two enantiomers owns the desired biological activity. Isolating and purifying the drug from the mixture requires high temperatures and extremely acidic or basic pH, as well as polluting solvents and metal catalysts to remove from the reaction environment. Conversely, developing enzymatic resolutions makes the process specific and selective: enzymes achieve high yields due to regio-, stereo-, and chemoselectivity. These latter features lead to more straightforward synthetic pathways with no functionalization steps needed, resulting in reduced waste. To date, regioselective C-H allogenation are efficiently catalyzed by Flavin-dependent tryptophan halogenases [37].

Unlike chemical counterparts, biocatalysts show a three-dimensional structure with multiple contact points for the substrate of interest, allowing for high selectivity. Furthermore, nature has evolved into a state where a plant or a microorganism is equipped with an enzyme, or several enzymes, synthesizing different products. Consequently, some biocatalysts extracted for synthetic purposes can accept and convert even analogous substrates.

1.2.3 Biocatalysis: applications and tools

Biocatalysis is now a proven methodology. The advent of guidelines promoted by Green Chemistry and the advancement of industrial processes have contributed not only to the rapid growth of biocatalysis but also to its consideration as a winning strategy. The rising need for valuable alternatives to traditional methods has led to biocatalysts' experimentation within systems that best fit process requirements.

The choice to carry out catalytic reactions in alternative solvents arises mainly from the awareness of being able to increase enzyme performance [38]. Given the propensity for hydrolytic side reactions and protein unfolding, aqueous solvents are not the ideal medium for some biotransformations. In organic media, on the other hand, the enzyme seems to increase its stability and carries out reactions commonly prevented by thermodynamic and kinetic restrictions [39]. The organic medium also facilitates the catalytic mechanisms for most compounds commonly insoluble in water, giving rise to easily recoverable products. Enantiopure 2-chloro- and 2-bromo-propionic acids, used as intermediates for the synthesis of phenoxypropionic herbicides and of some pharmaceuticals, have been obtained from yeast lipase-catalysed enantioselective butanolysis in anhydrous solvents [40].

In enzyme cascades, or multi-enzymatic reactions, series of catalyses occur with isolated or immobilized enzymes in a one-pot fashion [41]. Reactions take place sequentially on the same vessel allowing for capital costs reduction, improvement of equilibrium, *in situ* substrate supply, and product removal. The biotransformation product is no longer isolated but becomes a substrate itself, ready to be converted in turn. Domino systems mimic metabolic pathways or can be inserted in a multistep synthesis to obtain high structural

complexity molecules starting from simple building blocks. Enzymatic cascades are now widespread. A case in point concerns the conversion of 5-methoxymethylfurfural into 2,5-furandicarboxylic acid along a three oxidoreductases path [42]. The latter compound is the building block for those polyesters expected to replace fossil fuels.

Starting from 2000s, a new approach has aimed at modelling the biocatalyst structure through studies on enzyme access and resorting to the most sophisticated engineering techniques (bioinformatics, computational tools, proteins and strains engineering, recombinant DNA technologies, and DNA sequencing). These features propelled biocatalysis through its so-called “four-waves development” [19, 43, 44]. In a short period, basic engineering techniques switched to silicon protein models of the emerging design-make-test cycle depicted by the fourth phase [43]. Prospecting novel functions of a protein, after introducing a series of mutations, is now conceivable. The mutant enzyme is distinguished in the acquisition of new properties (solubility, substrate specificity, stability, conformation) compared to native molecule, responding to needs that that protein had not evolved naturally.

1.2.4 Enzyme immobilization on solid supports

The strategies described in the previous section (§ “*Biocatalysis: applications and tools*”) make a contribution in enhancing the production efficiency. Indeed, despite the advances made in recent decades, some large-scale biotransformations remain challenging [21]. In addition to being expensive when produced in large quantities, not all enzymes are available, and low operational stability may occur. Some biocatalysts depend on pricey cofactors representing an additional expense for the industry [45]. Identifying an

enzyme, optimizing it, and finally exploring its activity can take an extremely long time, to the point of no longer being economically profitable. Enzyme loss during biotransformation is another reality to be addressed. Although it is not consumed at the end of the reaction, an enzyme that is not recovered is no longer functional and remains as an impurity in the product.

The recombinant expression of the enzyme in a microbial host, the application of engineering techniques altering the properties of the biocatalyst, or the development of co-factor restoring systems are basic strategies adopted to stem a specific issue.

Great attention is now paid to enzyme immobilization on solid supports [46] since it improves the process efficiency operating on several fronts at the same time, and it collects a fair amount of interest if the company aims for larger productions. As highlighted in the previous section, the immobilization figures as the lowest common denominator of almost all biocatalytic strategies.

Confining the enzyme to a specific and isolable region will allow the enzyme to be recovered at the end of the reaction and reused several times, increasing its performance [47]. The benefits are not limited to recycling, which already marks a revolution. The possibility of reusing the same enzyme for a new biocatalytic cycle drastically lowers production costs, especially in a large-scale context. Indeed, the tireless contribution of the biocatalyst, as well as fewer fermentation and processing steps, contain the production price. When immobilized efficiently to the support on which it fits the best, the enzyme is more stable [47]. Recovering the product is effortless, and no additional purification cost occurs since the product stream is protein-free. Thus, from the biocatalytic point of view, enzyme immobilization can easily be recognized as one of the greenest tools [48, 49].

The first industrial use of immobilized enzymes was reported in 1967 by Chibata and co-workers who immobilized *Aspergillus oryzae* amino acylase for the resolution of synthetic D/L amino acids into the corresponding optically active enantiomers [50].

There is no universally accepted method capable of immobilizing molecules as structurally and functionally diverse as enzymes. Thus, it is necessary to identify the most efficient support and choose the most suitable immobilization technique among carrier-bound attachment, encapsulation, or cross-linked enzyme aggregates (CLEAs) [51].

Heterogeneous solid supports evolved quickly and include resins, magnetic particles, functionalized beads, liposomes, hydrogels, chitosan, metal oxides, polymers and many others. CLEAs, which arise from the aggregation of the enzyme via a precipitating reagent, is the only model in which the enzyme becomes its own solid support.

Since abandoning an ongoing development is an economical risk for the company, few immobilized enzymes have come to be commercialized. The high production costs, the complexity of design process, and the possible reduced efficiency (since bonds with solid support may constrain the catalytic function) [48] prevent the distribution of these specialized formulations.

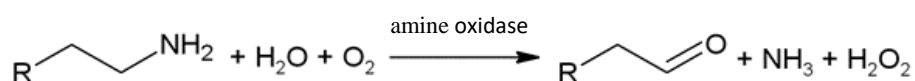
For a considerable period, hydrolases, which are co-factors independent, have shown great potential in the immobilized state [52, 53]. However, reactions cannot be limited to hydrolysis because additional intermediates and products are required for biocatalytic applications. The scenario, indeed, has rapidly changed and is welcoming valuable biotransformations, including C-C bond formation, asymmetric synthesis, and oxidations [54, 55, 56] for efficient biocatalytic applications. These catalytic mechanisms deserve a thorough

analysis. In this regard, amine oxidases are receiving increasing attention because of their potential. Mainly, they have been identified and engineered for the resolution and functionalization of chiral amines [57, 58] and their immobilized form found application in biosensors' design [59, 60].

1.3 Amine Oxidases

1.3.1 Amine oxidases family

Amine oxidases belong to the class of oxidoreductases and are widespread among living organisms. The oxidative cleavage of many biologically significant alkylamines into the corresponding aldehyde is coupled to the reduction of molecular oxygen to hydrogen peroxide and the release of ammonia, according to the following equation.



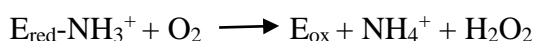
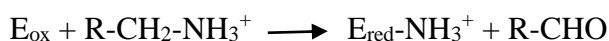
Amine oxidases are divided into two subfamilies based on the prosthetic group involved in the catalytic mechanism, that is a flavin moiety or a copper ion. These biocatalysts are classified as monoamine oxidases or FAD-AOs (flavin-containing amine oxidase) and amine oxidase (copper-containing) AOCs [61].

Monoamine oxidases catalyze the oxidative deamination of monoamine neurotransmitters and monoamines ingested in food.

Copper-containing amine oxidases are classified in turn into three subclasses. Lysyl oxidase is also known as protein-lysine 6-oxidase and catalyzes the deamination of lysine molecules into highly reactive aldehydes that form cross-links in extracellular matrix protein. Primary-amine oxidases are identified as “semicarbazide-sensitive amine oxidases”, and diamine oxidases as "amine oxidase, copper-containing, 1" (AOC1).

1.3.2 Copper-containing Amine Oxidases

Copper-containing Amine Oxidases (AOCs) are ubiquitous and involved in the most heterogeneous regulations of eukaryotes and prokaryotes [62]. The oxidative deamination of alkylamines consists of a transamination followed by the transfer of two electrons to molecular oxygen which is reduced to H₂O₂, as reported below.



The roles assumed by copper-containing amine oxidases are varied. In bacteria the catabolism of primary amines represents the source of those nutrients, such as carbon and nitrogen, necessary for the microorganism growth [62]. In plants, hydrogen peroxide is involved in multiple cell signalling pathways, including wound-healing and cell reinforcement during pathogen invasion and cell wall maturation and differentiation [63]. In addition, excessive metabolism of polyamines seems a response in plants upon exposure to cadmium or excess salt [64]. AOCs inactivate histamine and other polyamines in humans [65]. In higher eukaryotic organisms these enzymes accumulate in the digestive tract and in the placenta at high levels. Placenta trophoblasts secrete copper-containing amine oxidases in the blood stream of pregnant women [66], and their lowered concentrations in the plasma is probably a preeclampsia indicator.

X-ray crystallography studies performed on a series of copper-containing amine oxidases show that these enzymes are dimers composed of 70-90 kDa subunits. Each monomer has three domains D2, D3 and D4 (**Figure 1**) [67]. The D4 domain consists of two antiparallel β -sheets, wrapped up in a β -

sandwich, while the two smaller domains, D2 and D3, which lie on the surface of D4, are formed by two α -helices and four antiparallel β -sheets. Most of the interactions between the two subunits occurs at the interface of the β -sandwich regions of the D4 domain. Prokaryotic enzymes possess an additional D1 domain.

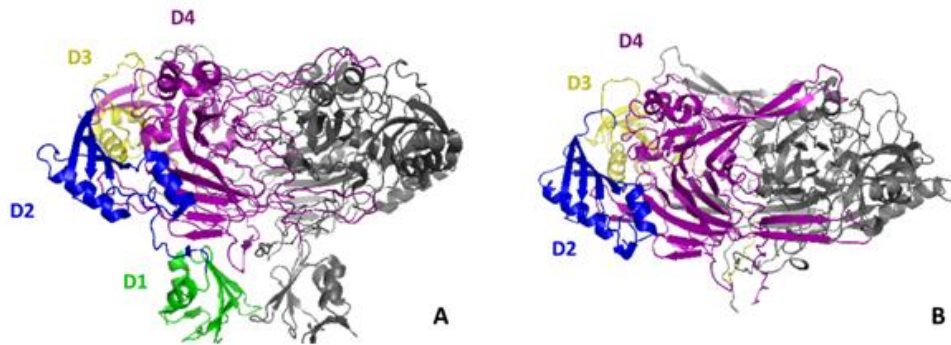
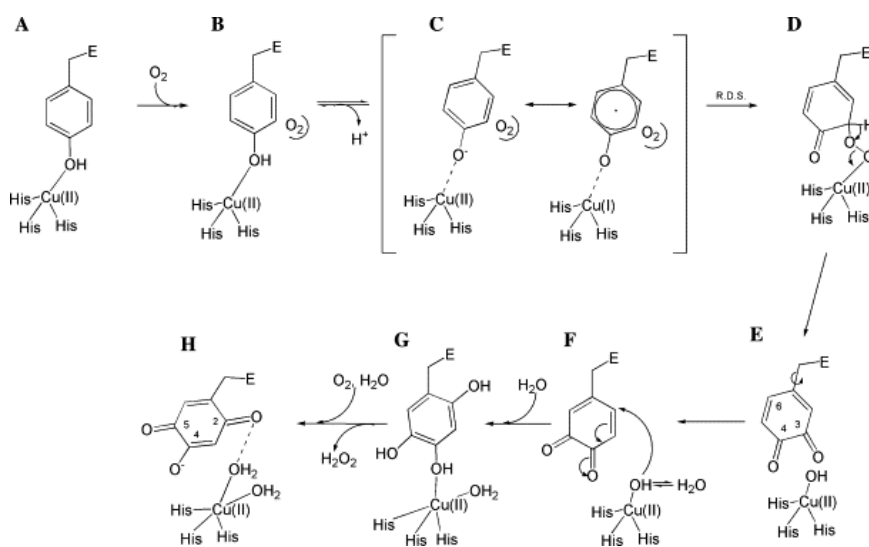


Figure 1 Crystallographic resolution of copper-containing amine oxidase in prokaryotes (A) and eukaryotes (B) *B.J. Brazeau et al.: Copper-containing amine oxidases. Biogenesis and catalysis; a structural perspective (2004)*

The resolution of X-ray crystallography structures also showed that copper-containing amine oxidases exhibit a high structural homology. Ten AOCs from different sources retain thirty-three residues in the catalytic site, although the primary sequence identity is relatively low (<25%) [68]. Bovine serum amine oxidase (BSAO) shares a high degree of identity (83%) with AOCs vascular adhesion protein-1 (VAP-1) [69]. Even a higher homology (91%) correlates pea seedling amine oxidase (PSAO) and lentil seedling amine oxidase (LSAO) [70]. Furthermore, thirty amino acids of the N-terminal sequences of *Lathyrus odoratus* and *Lathyrus cicera* amine oxidases show 100% identity with PSAO [71]. This indicates copper-containing amine oxidases as highly preservative proteins along the pro-evolution line.

In the 1990s, an organic prosthetic group was identified in AOCs [72]. 2,4,5-trihydroxyphenylalanine-quinone (TPQ) derives from the post-translational oxidation of a tyrosine residue near the active site at the level of a preserved sequence [68]. At first, TPQ generation seemed to be a self-processing event only requiring the addition of O₂ and Cu (II) but no auxiliary enzymatic activity or reducing equivalents. Brazeau et al. [67], however, reported the plausible TPQ biogenesis mechanism (**Scheme 1**), in which the cofactor is firstly converted to dopaquinone and then to topaquinone in a Cu₂⁺-dependent manner.



Scheme 1 TPQ biogenesis mechanism based on the results of experiments involving *Hansenula polymorpha* amine oxidase in solution and X-ray crystallographic studies of AGAO. B.J. Brazeau et al.: *Copper-containing amine oxidases. Biogenesis and catalysis; a structural perspective* (2004)

The catalytic site is also well preserved [68]. It is located inside a crack at the level of the β -sandwich of the D4 domain and binds the two cofactors. The Cu (II) atom is coordinated by the side chains of three histidine residues and two water molecules. As already mentioned, the active site provides two different

reactions: both the TPQ synthesis and the two electron oxidation of primary amines. TPQ cofactor has been identified in two conformations (**Figure 2**) [73]. The “off-copper” TPQ represents the catalytically productive conformer as the nucleophilic site (C5 atom of TPQ ring) points away from the copper centre and toward the amine substrate channel. The “on-copper” TPQ conformer acts as a copper binding because the rotation of the TPQ ring is followed by a water molecule displacement. Thus the nucleophilic site is no more accessible to the substrate.

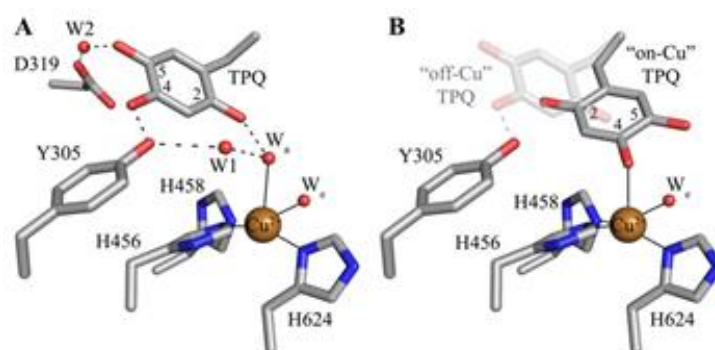


Figure 2 Crystal structures of the *Hansenula polymorpha* amine oxidase type-1 active site with TPQ in an (A) “off-copper” or (B) “on-copper” conformation. V. Klema *et al.*: *The Role of Protein Crystallography in Defining the Mechanisms of Biogenesis and Catalysis in Copper Amine Oxidase* (2012)

For decades, research has investigated the alkylamine deamination by copper-containing amine oxidases. Below is a recent plausible pattern of the ping-pong mechanism that may occur in most AOCs (**Figure 3**) [74]. As shown, the involvement of both the mobility and oxidation state of TPQ in the deamination is now evident. The ping-pong mechanism comprises two half-reactions. Firstly, an aminotransferase mechanism occurs: the oxidized enzyme reacts with the primary amine generating Cu (II)-quinone ketimine, the substrate Schiff base; the latter, after a proton abstraction, is converted into a Cu (II)-quinolaldimine, the product Schiff base. After hydrolysis and

aldehyde release, an aminoquinol species is formed (aminoresorcinol). Molecular oxygen reoxidizes the reduced cofactor to iminoquinone, passing through the radical form (Cu(I)-semiquinolamine) of the cofactor corresponding to the “on-TPQ” conformer. Hydrolysis and ammonia release restore the TPQ oxidative form.

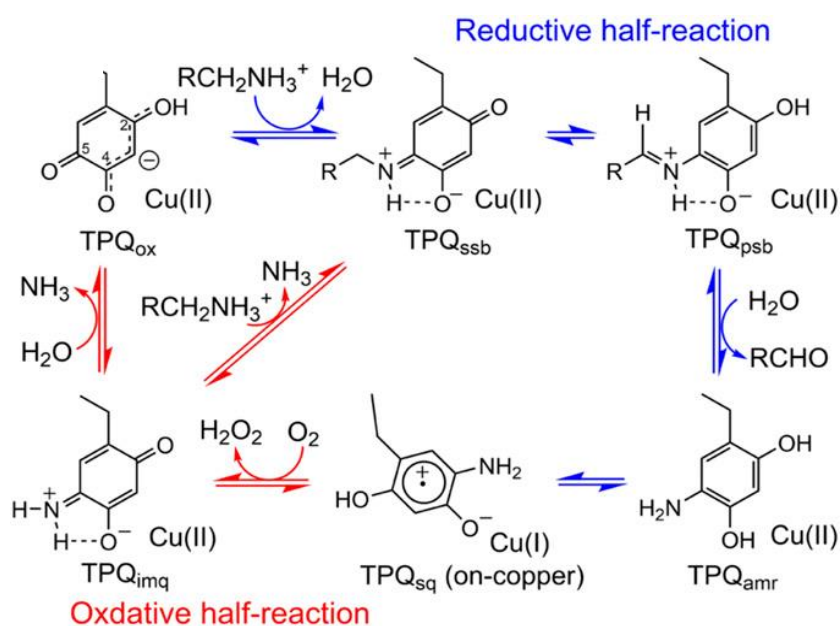


Figure 3 Catalytic mechanism in *Arthrobacter globiformis* amine oxidase. T. Murakawa *et al.*: *In crystallo* thermodynamic analysis of conformational change of the topaquinone cofactor in bacterial copper amine oxidase (2019)

Bacterial AOCs

Spectroscopic analysis and crystallography on bacteria models allowed to define the structure and activity of this enzymatic subfamily. From the data collected, a better comprehension of the mechanisms of biogenesis and catalysis occurred, in addition to the roles assumed by metal ions, inhibitors,

and oxygen. The aforementioned ping-pong mechanism was obtained by thermodynamic analyzes on *Arthrobacter globiformis* [74].

Human AOCs

AOCs are involved in different metabolic pathways in mammals. Thus, a thorough investigation of the catalytic site could be the point of reference for developing a potential pharmacological therapy [65]. Vascular adhesion protein-1 (hVAP-1) is involved in several disorders, including autoimmune and inflammatory diseases. Inhibitors targeting hVAP-1 avoid its translocation to the endothelial cell surface from intracellular storage granules at sites of inflammation. The pro-inflammatory protein histamine is degraded in human tissues by diamine oxidases DAOs, and ensuring the control of this pathway modulates severe allergic reactions. An alteration in polyamines metabolism raises their levels in cells, which may undergo carcinogenicity. Diabetes mellitus, Alzheimer's disease, and other inflammatory disorders seem to be associated with changes in AOCs activity.

Plant AOCs

Remarkable applications are promoted by plant copper-containing amine oxidases. The most characterized are *Pisum sativum*, *Lens esculenta*, *Cicer arietinum*, and the subject of this project *Lathyrus cicera* [71, 72, 75, 76]. Histaminase purified from pea seedling lowers the oxidative tissue damage induced by ROS generated during anaphylactic reactions [77]. Carboxymethyl starch: chitosan monolithic matrices containing grass seedling diamine oxidase (PSDAO) have been developed to mimic the behaviour of novel delivery systems, which may be employed in the treatment of inflammatory bowel diseases [78]. The design entailed by Boffi et al. comprises biosensors in which an engineered *Zea mays* amine oxidase and a mouse spermine oxidase, both

flavin-dependent, are entrapped in a photo-crosslinkable gel onto an electrode surface to determine spermine and spermidine content [59].

1.3.3 *Lathyrus Cicera Amine Oxidase*

Lathyrus cicera Amine Oxidase LCAO is a copper-containing enzyme expressed mainly in the shoots of the aforementioned legume.

LCAO structure and activity

Unlike other AOCs of bacteria and higher organisms, both the primary sequence and the crystallographic structure of LCAO have yet to be determined. However, given the high structural homology highlighted for other plant AOCs (§ section “*Copper-containing Amine Oxidases*”), it would not be surprising that *Lathyrus cicera* AO has also preserved a similar structure during its evolution.

LCAO inactivation began to be investigated around 2000 and attributed to co-product hydrogen peroxide. The peak of oxidized TPQ cofactor whitens under anaerobic conditions, and three characteristic absorption bands representative of the Cu^+ - semiquinolamine radical appear [79]. The subsequent radical decay into the inactive state of the enzyme is either not observed or less reduced in the presence of catalase, even under anaerobic conditions or with an amino substrate excess [80]. The explanation rests in hydrogen peroxide inactivating a conserved residue in the reduced enzyme after the fast turnover phase.

As stated in following studies, some aldehydes share an inactivation mechanism as irreversible inhibitors of plant copper-containing amine oxidases [81]. Indeed, even in the absence of H_2O_2 , the distinctive spectrum of the enzyme in the inactive state may still be observed. 2-bromoethylamine, 2-

chloroethylamine, and 1,2-diaminoethane are suicidal substrates for plant AOCs. The oxidation of these latter alkylamines involves the formation of a reversible enzyme-killer product complex followed by an irreversible inactivation state. The irreversible condition is due to the aldehyde binding the TPQ-derived free radical catalytic intermediate that forms a stable 6-membered ring. In the case of aldehydes resulting from the deamination of 1,4-diamino-2-butyne and 1,5-diamino-2-pentyne, a lysine residue in the active site is bound. Even though each amino substrate modifies the amino acid differently, the inactivation is permanent.

Pietrangeli's team evaluated the activity of some copper-containing amine oxidases toward natural polyamines and analogous substrates [76]. Unlike bovine serum AO, LCAO and other plant copper-containing amine oxidases show higher turnover numbers towards putrescine and several aromatic amines. The limited pH dependence of $k_{\text{cat}}/k_{\text{M}}$ means hydrophobic interactions predominate over polar ones as a more stable semiquinone intermediate is generated in plant amine oxidases.

Applications of LCAO

Lathyrus cicera Amine Oxidase accumulates mainly in the shoot apoplast, in which hydrogen peroxide promotes cell signalling and mediates defense and growth mechanisms [63], but until now this enzyme has showed great potential from a biocatalytic point of view. LCAO has been employed as a detection tool for human saliva amines responsible for halitosis, alternatively to expensive and complex chromatographic procedures [82]. A polyacrylamide gel electrophoresis, in which peroxidase is previously entrapped, evaluates the proteolysis of *Lathyrus cicera* amine oxidase to simulate its delivery in stomach and intestines [83]. To determine the biogenic amines content in beer

and wine, Di Fusco et al. [84] designed electrochemical biosensors on whose LCAO acts as the detection component. In the perspective of elaborating a novel strategy for tetrahydroisoquinolines synthesis, *Lathyrus cicera* amine oxidase and *Thalictrum flavum* norcoclaurine synthase have been employed in an enzymatic cascade. In the one-pot two steps synthesis developed by Bonamore and co-workers (**Figure 4**) [85], dopamine cyclizes with the aldehyde generated *in situ* by different amines. The Pictet-Spengler enantioselective cyclization, catalyzed by norcoclaurine synthase, is a valid alternative to produce the (S)-enantiomer forms of the corresponding tetrahydroisoquinolines.

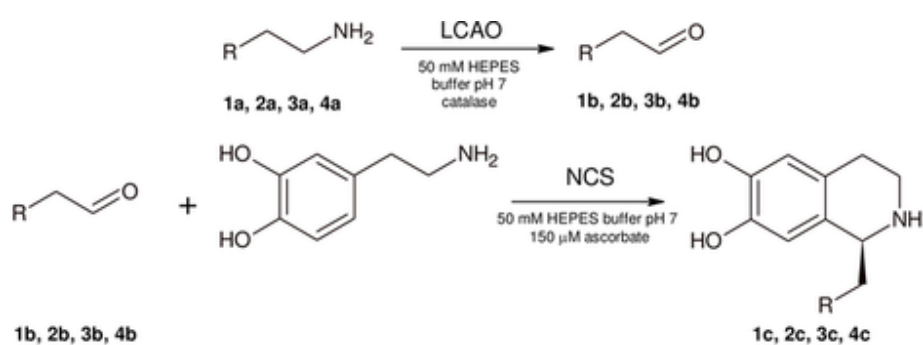


Figure 4 Enzymatic cascade for the synthesis of tetrahydroisoquinolines.
A. Bonamore et al.: A Novel Enzymatic Strategy for the Synthesis of Substituted Tetrahydroisoquinolines (2016)

CHAPTER 2

AIM OF THE WORK

Enzymes are the basis of all biological processes. The study of biotransformations is of current and growing interest due to their direct employment in the development of industrial processes with low environmental impact.

This project herein reported is set in the context of biocatalysis and aims at exploring *Lathyrus cicera* amine oxidase potential.

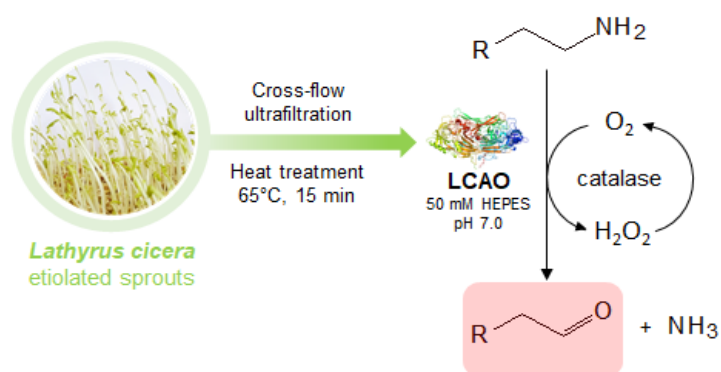
This enzyme has a quite relaxed substrate specificity, as well as high stability, and remarkable purification yields. To date this enzyme has been used for different purposes including the direct dosage of polyamines in human saliva or as a part of a biosensor for the analysis of polyamines in oenological matrices. LCAO has also been used in a domino process for the synthesis of substituted tetrahydroisoquinolines.

The aim of this Ph.D. thesis is to explore the biocatalytic potential of *Lathyrus cicera* amine oxidase. To this purpose the following objectives will be pursued:

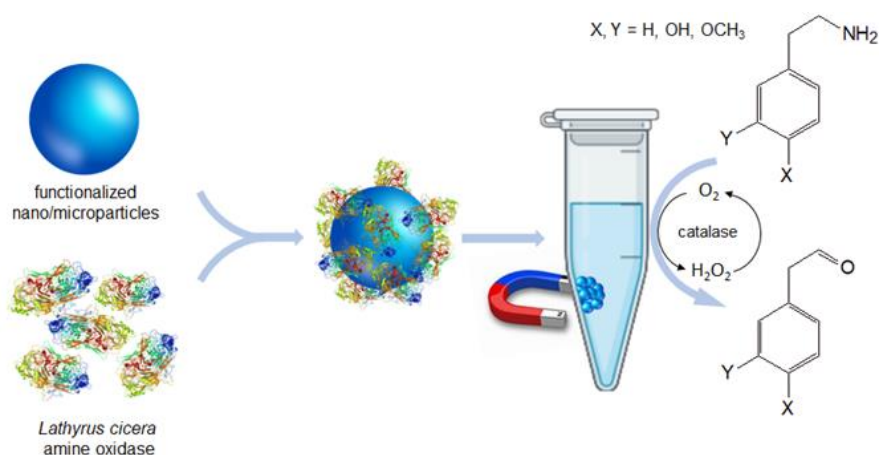
- I. Development of a new protocol for the purification of the enzyme from *Lathyrus cicera* shoots aiming at scale-up the process. To achieve this goal, cross-flow ultrafiltration will be used. Unlike dead-end filtration, cross-flow filtration is a continuous procedure by which the solution does not settle on the surface of the membrane, but passes through it

tangentially. The tangential stream avoids the formation of the filter cake and lets the filter unit operational. The opportunity of scaling the purification step is also facilitated by the extensive filtering surface of the membrane, reaching up to square meters in some apparatus, and the connection in series of devices at different cut-offs to process larger volumes.

- II. Exploring the biocatalytic potential of LCAO by developing a general method for the synthesis of pure aldehydes starting from differently substituted aliphatic and aromatic primary amines. The synthesis of these aldehydes is particularly interesting for several reasons: (i) they are not commercially available; (ii) some of them are biogenic aldehydes that can be used as pure standards for measurements in human and animal tissues; (iii) they can be used in domino reactions as substrates of other enzymes to produce intermediates of active pharmaceutical ingredients. Specifically, LCAO activity will be tested on a set of selected amino substrates, ranging from primary aromatic ethyl/propyl amines to linear amines/diamines, to evaluate their kinetic parameters. The conversion into the corresponding aldehydes will also be evaluated.



- III. Immobilizing LCAO on various supports including magnetic particles. Typically, immobilization improves the overall catalytic performance, allowing enzyme recycling, and a reduction in the overall process costs. Among the different support materials, magnetic nanoparticles are considered the future of enzyme immobilization, due to their exceptional ease of handling, recovery, and reuse. Immobilized LCAO will also be used for the biocatalytic production of different substituted phenylacetaldehydes according to the following scheme:



- IV. Testing free and immobilized LCAO stability in non-aqueous media, including biphasic systems. Carrying out the reaction in alternative media could be advantageous for future biocatalytic applications as it would allow testing water insoluble substrates.

CHAPTER 3

MATERIALS AND METHODS

3.1 Chemicals

Reagents and solvents obtained from commercial suppliers were used without further purification. All chemicals were purchased from Merck KGaA (Darmstadt, Germany). CDCl_3 (99.80% D) was obtained from Eurisotop (Saint Aubin, France).

3.2 LCAO chromatography-free purification protocol

Lathyrus cicera seeds (300 g) were soaked for 12 h in tap water and then spread in a monolayer on trays lined with moistened filter paper. The trays were covered tightly with aluminium foils. The germinated seeds were watered every 2 days with 100 mL of tap water. After 10 days, the etiolated seedlings (about 500 g) were harvested above the roots, cut in small pieces (about 2 mm) and washed with 1 L of ice-cold deionized water for 15 min. After washing, the ground plant sample was kept in 1.5 L of ice-cold extraction buffer (50 mM pH 5.5 phosphate buffer containing 0.3 M NaCl) for 30 min and then filtered through a 20 Micron Nylon Mesh and squeezed by hand to remove the debris. To allow quantitative recovery, the pellet was extracted again as described above and the resulting crude mixtures were combined. To remove insoluble

material, the crude enzyme extract (3 L) was clarified by disposable Sartolab® Vacuum Filters System (Polyethersulfone, 0.22 µm) using 30 g of Sartoclear Dynamics® Lab Filter Aid (Sartorius) containing highly pure diatomaceous earth (Celpure® C300–pharmaceutical grade) prewetted with ultrapure water. The buffer was exchanged with 20 mM phosphate buffer pH 6.5 through diafiltration by means of crossflow ultrafiltration using a single Vivaflow 200 module (Sartorius) with a 50 kDa cutoff, coupled to a Masterflex L/S pump system. The same device was also used to concentrate the enzyme extract to 100 mL. The feed flow rate was set to 40 mL/min both in concentration and diafiltration modes. As the last purification step, the sample was subjected to heat treatment at 65 °C for 15 min. Denatured proteins were removed by centrifugation (12000 rpm, 20 min, 20 °C). All purification steps were monitored by SDS-PAGE (12% SDS) and measuring the enzyme's specific activity. Enzyme activity (LCAO Units) was used to determine the recovery after each purification step. Total soluble protein concentration was determined using the Bradford method with bovine serum albumin as a standard. LCAO content throughout the purification procedure was also monitored by high-performance size exclusion chromatography (HP-SEC). HP-SEC was performed using an Agilent Infinity 1260 HPLC apparatus equipped with a UV detector. Separation was carried out using an Agilent AdvanceBio SEC 300 Å, 7.8 x 150 mm, 2.7 µm, LC column connected to an AdvanceBio SEC 300 Å, 7.8 x 50 mm, 2.7 µm, LC guard column. Isocratic analysis was carried out with 20 mM phosphate buffer pH 6.5 containing 150 mM NaCl as mobile phase. The flow rate was 0.7 mL/min over an elution window of 7 min. Protein elution was followed using UV detection at 220 nm and 445 nm (TPQ-phenylhydrazine adduct).

3.3 LCAO activity

LCAO activity was assayed by a coupled diamine oxidase/oxidase spectrophotometric test at 25 °C with 10 mM putrescine in 20 mM phosphate buffer in the presence of 150 nM enzyme. H₂O₂ produced by LCAO was monitored following horseradish peroxidase catalyzed coupling of 4-aminoantipyrine (AAP) and sodium 3,5-dichloro-2-hydroxybenzenesulfonate (DCHBS) as oxygen acceptor. The enzymatic activity, which led to the formation of colored product, was measured at 515 nm for 60 s and expressed as U/mL per mg protein. Initial rates of reaction at the various substrate concentrations were determined at three different pHs, and the kinetic parameters were calculated by non-linear regression fitting of the data to the Michaelis–Menten equation $V = V_{\max}[S]/(K_M+[S])$. All curve fitting was carried out using Kaleidagraph software (Synergy Software, Reading, PA, USA).

3.4 Enzymatic synthesis of aldehydes

The biocatalytic synthesis of aldehydes was carried out starting from the corresponding primary amines in the presence of LCAO. Twenty different substituted ethyl amines were tested. A 5 mM solution of amino substrate was prepared in 50 mM HEPES buffer pH 7.0 in the presence of 250 U/mL of catalase from bovine liver (Sigma-Aldrich) to a final volume of 10 mL. LCAO was added to a final concentration of 2 U/mL and the reaction was carried out at room temperature under stirring. To ensure constant catalytic efficiency, the enzyme is supplied (5 U) at regular time intervals (30 min). The substrate consumption was monitored by HPLC or GC/MS, whereas aldehyde formation was monitored by purpald® assay.

3.5 HPLC analysis of aldehydes

Aromatic amines consumption was followed by HPLC using an Agilent Infinity 1260 HPLC apparatus equipped with UV and fluorometric detectors. The separation was carried out using a Halo C18 AQ column (3 x 150 mm, 2.7 μm) connected to the C18 AQ guard column (3 x 5 mm, 2.7 μm). The elution was performed at a flow rate of 0.8 mL/min, with solvent A (0.1% trifluoroacetic acid in water) and solvent B (0.1% trifluoroacetic acid in acetonitrile). The mobile phase was linearly increased from 0% to 100% of solvent B in 15 min and then run isocratically for 5 min. Afterward, buffer A was reintroduced in the mobile phase up to 100%, and the column was allowed to equilibrate for 10 min. The elution profile of aromatic amines was monitored by setting the UV detector at 280 nm.

3.6 GC/MS analysis of aldehydes

Aliphatic amine consumption was followed by GC/MS. Derivatization with ethyl chloroformate (ECF) was conducted in a single step by adding to 0.1 mL of the reaction mixture 20 μL of NaOH 7M, and 20 μL of ECF dissolved in 0.5 mL of dichloromethane. The biphasic system was stirred vigorously for 2 min, saturated with NaCl and extracted sequentially with 1 mL of diethyl ether and 1 mL of ethyl acetate. The organic extracts were combined, dried under nitrogen flow, resuspended in dichloromethane, and analyzed by GC/MS. GC/MS analyses were performed with an Agilent 6850A gas chromatograph coupled to a 5973N quadrupole mass selective detector (Agilent Technologies, Palo Alto, CA, USA). Chromatographic separations were carried out with an Agilent HP-5MS fused silica capillary column (30 m x 0.25 mm id) coated with 5% phenyl - 95% dimethylpolysiloxane (film thickness 0.25 μm) as

stationary phase. Injection mode: splitless at a temperature of 280 °C. Column temperature program: 100 °C for 2 min and then to 300 °C at a rate of 15 °C/min and held for 5 min. The carrier gas was helium at a constant flow of 1.0 mL/min. The spectra were obtained in the electron impact mode at 70 eV ionization energy; ion source 280 °C; ion source vacuum 10^{-5} Torr. Mass spectrometric analysis was performed in the range m/z 50 to 500 at a rate of 0.42 scans s^{-1}).

3.7 Purpald® colorimetric assay of aldehydes

Substrate conversion efficiency was calculated through the reaction of the newly formed aldehyde with 4-amino-5-hydrazino-1,2,4-triazole-3-thiol (purpald®), a reagent for the colorimetric detection of aldehydes. A volume of 50 μ L of the reaction mix were added to 1 mL NaOH 2 M containing 5 mg of purpald®, vortexed for 5 min and read at 550 nm after 15 min. The calibration was carried out using phenylacetaldehyde commercial standard in the concentration range 0.28–7 mM.

3.8 LCAO immobilization

LCAO immobilization was performed using different commercial solid supports (DEAE resin, amino- and carboxy-functionalized magnetic microparticles, chloromethyl latex beads, and amino-functionalized Turbobeads), using standard protocols provided by the manufacturers, optimizing the incubation times as well as the amount of protein to be bound. The amount of immobilized enzyme was measured by the Bradford assay by

determining the concentration of soluble protein before and after the immobilization procedure.

DEAE fast flow resin: 2.47 g of Sepharose fast flow resin (Ge Healthcare) were washed twice with deionized water, activated with 0.5 M sodium chloride, and equilibrated with 10 mL of 50 mM sodium phosphate pH 7.0. LCAO (180 U - 3.2 mg) and 0.2% glutaraldehyde (final concentration) were then added, and the mix was left in gentle agitation for 1 h. The resin was extensively washed with 50 mM sodium phosphate pH 7.0, resuspended in the same buffer to a final volume of 6 mL, and stored at 4 °C.

Chloromethyl latex beads: 0.25 mL of chloromethyl latex beads solution (Thermo Fisher Scientific) were activated with 1 mL 25 mM MES buffer pH 6.0, then centrifuged at 6000 rpm for 20 min. The beads (30 mg) were resuspended in 1 mL 25 mM MES buffer pH 6.0 containing 1.7 mg of LCAO (94 U) and incubated overnight at room temperature under gentle stirring. Then, the particle solution was centrifuged for 15 min at 5000 rpm and the beads were washed twice with 2 mL PBS and stored at 4 °C in 2 mL of the same buffer containing 0.1% glycine and 1% Tween 20.

Carboxy-functionalized magnetic microparticles (COOH-MMPs): 0.2 mL of carboxy- functionalized magnetic microparticles (Merck KGaA) were washed with 2 mL 0.1 M MES buffer pH 5.3. Magnetic particles (4 mg) recovered using the LifeSep magnetic separation unit (Dexter Magnetic Technologies, Inc.) were resuspended in 2 mL of the same buffer containing 1-ethyl-3-(3-dimethylaminopropyl) carbodiimide EDC (10 mM) and left under gentle stirring for 30 min at room temperature. The activated particles were washed with 50 mM sodium phosphate pH 7.3. Immobilization took place by adding 2.7 mg of LCAO (150 U) dissolved in 2 mL of the washing buffer and leaving

the particles under stirring at room temperature for 3 h. The mix was washed with phosphate buffer and then resuspended in 2 mL 50 mM sodium phosphate pH 7.0 containing 30 mM glycine (quencher) and 0.5% Tween 20. After 30 min under gentle stirring, the microparticles were recovered, washed with phosphate buffer, and stored at 4 °C in 50 mM sodium phosphate pH 7.0 containing 0.1% Tween 20.

Amino-functionalized magnetic Turbobeads: 30 mg of Turbobeads nanoparticles (Merck KGaA) were washed with deionized water, recovered using the LifeSep magnetic separation unit, resuspended in 1 mL 0.1 M MES buffer pH 6.0 and then sonicated for 1 min. The nanoparticles were extensively washed in the sonication buffer, resuspended in 2 mL of the same buffer containing 10% glutaraldehyde, and stirred for 1.5 h. The particles were then washed with 50 mM phosphate buffer pH 7.3 and incubated with 1.5 mg of LCAO (82 U) under gentle stirring at room temperature. After 3 h, the reaction was quenched exchanging the buffer with 50 mM phosphate pH 7.3 containing 30 mM glycine and 0.5% tween 20. After an additional 30 min, the particles were recovered, washed with phosphate buffer, resuspended in 2 mL 50 mM phosphate buffer pH 7.0 containing 0.1% tween 20, and stored at 4 °C.

Amino-functionalized magnetic microparticles (NH₂-MMPs): 0.2 mL of amino-functionalized magnetic microparticles solution (Merck KGaA) were activated twice with 0.1 M MES buffer pH 6.0. After separation using the LifeSep magnetic separation unit, the particles (10 mg) were resuspended in the same buffer containing 10% glutaraldehyde and left under stirring for 1 h at room temperature. The magnetic beads were then recovered, washed with 50 mM phosphate buffer pH 7.3, and resuspended in 1 mL of the same buffer containing different amounts of LCAO (from 1 to 5 mg; 55–275 U). After 2.5 h, the reaction was quenched exchanging the buffer with 50 mM sodium

phosphate pH 7.3 containing 30 mM glycine and 0.5% Tween 20. After further 30 min under gentle stirring, the magnetic particles were washed with 50 mM sodium phosphate pH 7 and 0.1% Tween 20 and stored at 4 °C in the same buffer.

3.9 Synthesis of aldehydes catalyzed by immobilized LCAO

The biocatalytic synthesis of the seven different aldehydes was carried out starting from the corresponding primary amines in the presence of LCAO immobilized on the surface of NH₂-MMPs (LCAO-MMPs). A 20 mM solution of amine substrate was prepared in 50 mM sodium phosphate buffer pH 7.0 in the presence of 30 U of LCAO-MMPs and 250 U/mL of catalase to a final volume of 15 mL. At the end of each reaction cycle, the particles were recovered using the magnetic separation unit, extensively washed with phosphate buffer pH 7, and reused for the next reaction cycle. The substrate consumption was monitored by GC/MS, whereas aldehyde formation was monitored by purpald® assay and GC/MS.

GC/MS analysis: amino substrates were analyzed as ethoxy carbonyl derivatives. Derivatization with ethyl chloroformate (ECF) was conducted by adding to 50 µL of the reaction mixture, 25 µL of NaOH 7 M, and 25 µL ECF dissolved in 50 µL of dichloromethane. The biphasic system was stirred vigorously for 2 min, saturated with NaCl, and extracted with 125 µL of ethyl acetate. After centrifugation, 100 µL of the organic phase were analyzed by GC/MS using methyl-C17 as the internal standard. GC/MS analyses were performed with an Agilent 6850A gas chromatograph coupled to a 5973N quadrupole mass selective detector (Agilent Technologies, Palo Alto, CA, USA). Chromatographic separations were carried out with an Agilent HP-5ms

fused silica capillary column (30 m x 0.25 mm id) coated with 5% phenyl–95% dimethylpolysiloxane (film thickness 0.25 μ m) as a stationary phase. Injection mode: splitless at a temperature of 280 °C. Column temperature program: 70 °C for 4 min and then to 240 °C at a rate of 25 °C min⁻¹ and held for 4 min. The carrier gas was helium at a constant flow of 1.0 mL min⁻¹. The spectra were obtained in the electron impact mode at 70 eV ionization energy; ion source 280 °C; ion source vacuum 10⁻⁵ Torr. Mass spectrometric analysis was performed in the range m/z 50–500 at a rate of 0.42 scans s⁻¹.

Purpald® colorimetric assay: aldehyde production was monitored by a colorimetric assay already described, following the reaction between the newly synthesized aldehyde and 4-Amino-5-hydrazino-1,2,4-triazole-3-thiol (*Purpald*®)

3.10 Synthesis and characterization of 1-benzyl-7-methoxy-1,2,3,4-tetrahydroisoquinolin-6-ol

1-benzyl-7-methoxy-1,2,3,4-tetrahydroisoquinolin-6-ol was synthesized starting from the amino substrate **1a** as described above. The immobilized enzyme was reused up to 8 times. After each reaction cycle, LCAO-MMPs were recovered and reused, while the newly synthesized aldehyde (15 mL 20 mM) was stored at -20 °C. At the end of the last cycle, the reaction fractions of each cycle were pooled, the pH was adjusted to 6.0, and the ionic strength of the buffer was increased to 0.3 M. The amino substrate **6a** was added stoichiometrically to the compound **1b** and the phosphate mediated Pictet-Spengler cyclization was carried out for 2 h at 50 °C in the presence of 30% acetonitrile.

GC/MS analysis

The production of the benzyloisoquinoline alkaloid was monitored by GC/MS after ECF derivatization. 50 μl of the reaction mixture was added to 25 μl of NaOH 7M and 25 μl of ethyl chloroformate dissolved in 50 μl of dichloromethane. The biphasic system was stirred vigorously for 2 min, saturated with NaCl, and extracted sequentially with 250 μl of diethyl ether and 250 μl of ethyl acetate. The organic extracts were combined, dried under nitrogen flow, resuspended in dichloromethane, and analysed by GC/MS. Column temperature program: 70 °C for 1 min and then to 300 °C at a rate of 15 °C min^{-1} and held for 10 min.

Purification

At the end of the reaction, the crude was allowed to cool at room temperature and extracted with dichloromethane. The combined organic layers were dried over Na_2SO_4 , filtered, and concentrated under reduced pressure at 30 °C before being purified by preparative TLC using Macherey-Nagel TLC glass plates, silica gel layer, 1.0 mm, eluting with a mixture of n-hexane/EtOAc/MeOH (2/8/1 v/v) ($R_f = 0.15$) to give compound as yellow solid.

NMR analyses

Identification of tetrahydroisoquinoline was performed by NMR analysis of the purified compound ^1H and ^{13}C NMR (400.13 and 100.03 MHz) analyses were recorded with an Avance 400 spectrometer, equipped with a Nanobay console and Cryoprobe Prodigy probe (Bruker Italia S. r. l., Milano, Italy). About 20 mg of the compound were dissolved in 0.7 mL of CDCl_3 , transferred into an NMR tube, and analyzed. The resulting ^1H NMR and ^{13}C NMR spectra were processed using Bruker TOPSPIN TopSpin 3.5pl2 software.

HPLC analysis

To calculate reaction yield, the crude was analyzed by HPLC. An HPLC-DAD apparatus (Perkin Elmer, Milan, Italy), equipped with an LC Series 200 pump, a Series 200 DAD, and a Series 200 autosampler, including Perkin Elmer TotalChrom software for data tracking was used. Analyses were performed at 280 nm with a Luna RP-18, 3 μ column in isocratic elution consisting of acetonitrile (65%) and water acidified by 5% of formic acid (35%), at a flow rate of 1.0 mL min⁻¹. Tetrahydroisoquinoline was identified by comparing retention time to that of an authentic standard. Peak area was used to calculate analyte concentrations in the samples by reference to the standard curve attained by pure substance chromatography, under identical conditions. DAD response was linear within the calibration ranges with correlation coefficients exceeding 0.997.

IR spectra were recorded with a Jasco FT/IR-6800 spectrophotometer. Melting points were determined with a Büchi B-545 apparatus and are uncorrected.

3.11 LCAO stability in non-aqueous solvents

Free LCAO and LCAO–MMPs stability in water-miscible solvents Each sample was prepared by dissolving 10 μ L (2 Units) of LCAO solution in 1 mL of different percentages of water-miscible solvents (acetonitrile, acetone, ethanol, methanol, or isopropanol). The sample was kept closed under constant stirring at room temperature over time and LCAO activity was evaluated at regular intervals by a peroxidase-coupled spectrophotometric assay.

Free LCAO and LCAO–MMPs stability in water/organic solvent 1:1 Each sample was prepared by adding 1 mL of a LCAO solution (2 Units) to 1 mL of

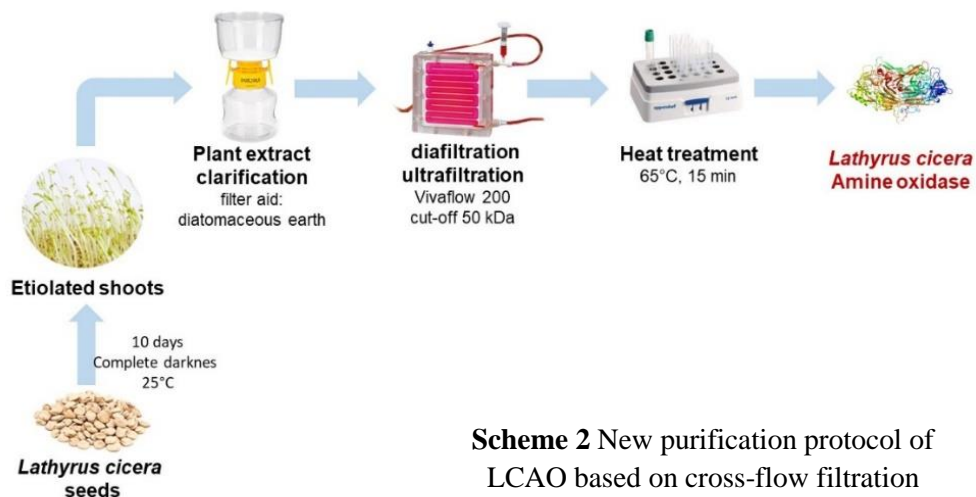
a water-immiscible solvent (hexane, diethyl ether, dichloromethane, or ethyl acetate). The sample was kept closed under constant stirring at room temperature over time and LCAO activity was evaluated at regular intervals by a peroxidase-coupled spectrophotometric assay.

CHAPTER 4

RESULTS AND DISCUSSION

4.1 LCAO purification

The present project reports the development of a new protocol for LCAO purification, which has significant advantages over the generally used one, as it is chromatography-free, fast, and easily scalable. Sprouts of *Lathyrus cicera* were selected because they show higher specific activity than other common *Leguminosae*, such as *Pisum sativum*, *Lens culinaris*, and *Phaseolus vulgaris* (data not shown). The protocol involves the combined use of diatomaceous earth filter aid and tangential ultrafiltration for the purification of recombinant proteins. Now, for the first time, these techniques are being used on plant material for the purification of LCAO (**Scheme 2**).



Scheme 2 New purification protocol of LCAO based on cross-flow filtration

According to this purification strategy, the crude plant extract is vacuum filtered using diatomaceous earth as a filter aid. This step replaces the classic centrifugation steps which are time-consuming and limit the amount of plant material that can be processed. As shown in **Table 2**, this allows an almost total recovery of the enzymatic activity with a concomitant increase in specific activity. The subsequent diafiltration/ultrafiltration step has a dual objective: (i) exchange the buffer, bringing the pH and ionic strength values to those that guarantee greater stability of the enzyme and, (ii) concentrate the enzyme itself. In addition, in this case, all the enzymatic activity is maintained and there is a 12-fold increase in the specific activity. Tangential ultrafiltration replaces classical dialysis and concentration steps, making the whole process fast and efficient. This process can be easily scaled up using suitable crossflow systems equipped with cassettes with larger membrane areas, able to filter larger volumes (up to thousands of liters). Considering that tangential flow filtration devices and cassettes can be cleaned and reused several times, the system is also economical. Since the stability of the enzyme is not affected by temperatures up to 60 °C (**Figure 5A**), the last purification step consists of a mild heat treatment, which leads to a 22-fold increase in specific activity, comparable to that obtained by classical chromatographic purification.

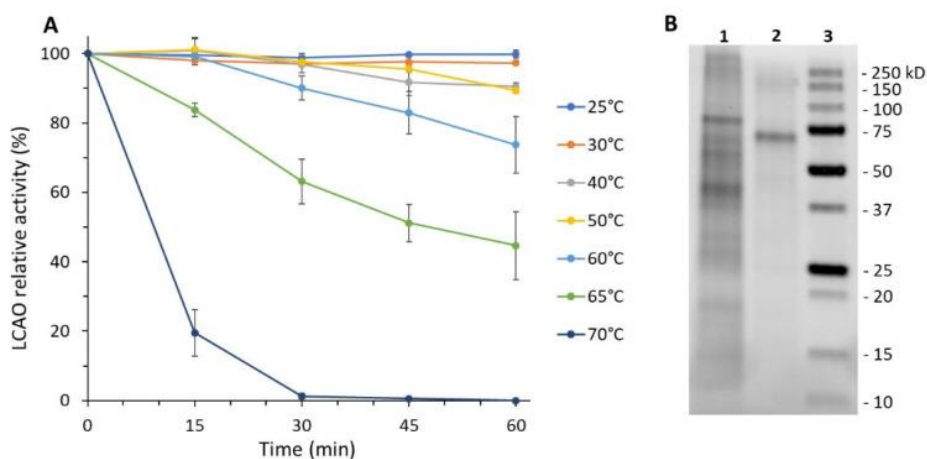


Figure 5 Heat treatment was used as the last step of LCAO purification. **(A)** Thermal stability of LCAO in the range 25-70 °C. **(B)** SDS-PAGE of LCAO after the treatment at 65 °C for 15 min. Lane 1: insoluble fraction; lane 2: soluble fraction; lane 3: protein

Purification Step	Total Activity (Units)	Total Protein (mg)	Specific Activity (units × mg ⁻¹ Protein)	Recovery (%)	Purification (-fold)
Crude extract	2630	2706	0.97	100	1
Filtration on Celpure® C300	2590	1546	1.68	98.47	1.73
Vivaflow200 diafiltration/ultrafiltration	2606	217	12.01	99.08	12.38
Heat treatment (65 °C)	2100	97.3	21.58	79.85	22.24

Table 2 Purification procedure for *Lathyrus cicera* amine oxidase. The recovery (%) was determined by evaluating the total activity (enzyme units) after each purification step.

As demonstrated by SDS-PAGE and HP-SEC analysis (**Figure 5B, Figures 6 and 7**), LCAO is highly purified (>95%).

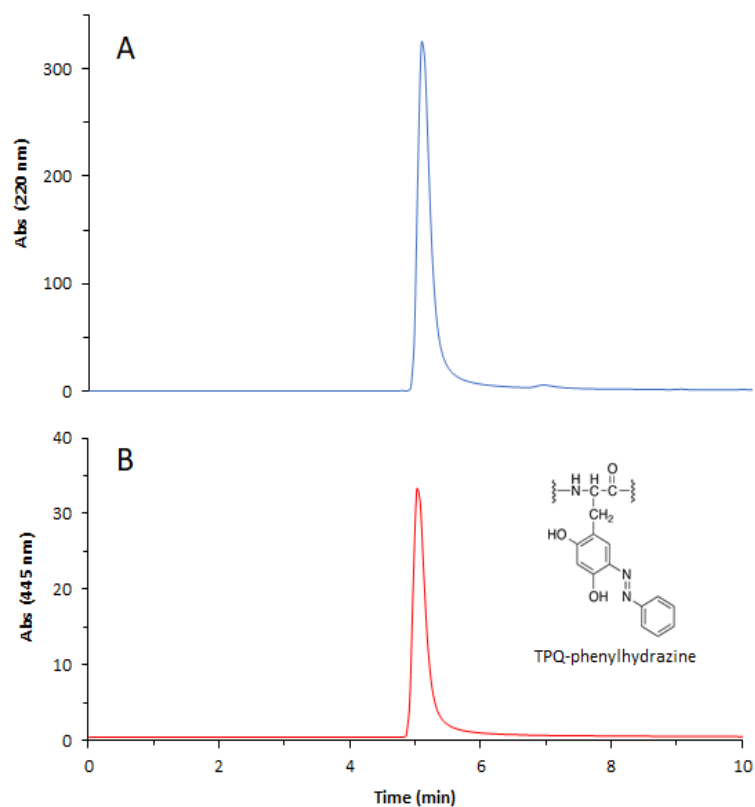


Figure 6 HP-SEC analysis of purified LCAO **A)** chromatographic profile following the UV signal at 220 nm; **B)** chromatographic profile following the UV signal of TPQ-phenylhydrazine adduct (445 nm).

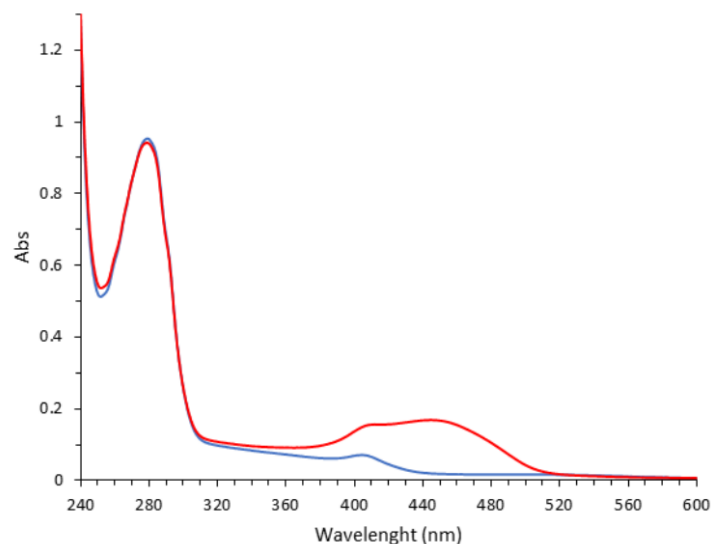


Figure 7 UV-vis spectrum of purified LCAO. UV-vis spectra were acquired with (red line) or without (blue line) phenylhydrazine that covalently binds TPQ cofactor at the active site of LCAO. the TPQ- phenylhydrazine adduct formation leads to a spectrum change in the visible region (400-500 nm).

The whole purification procedure takes about 7 h compared to the 16 h needed for the previously used protocol (data not shown). The purified protein is stable for up to 6 months, sterile filtered at 4 °C (**Figure 8**).

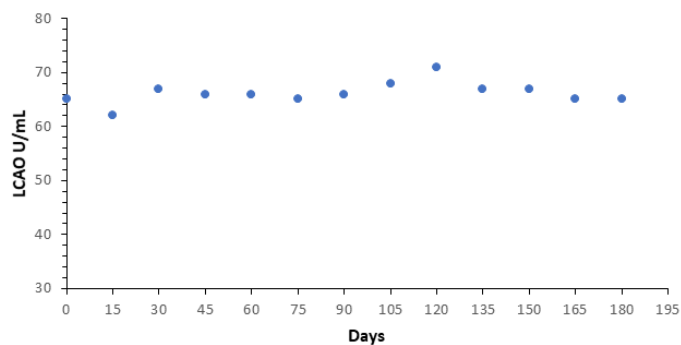
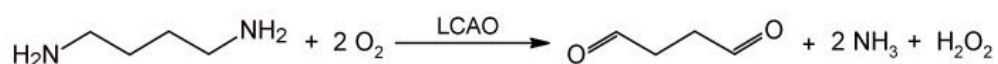


Figure 8 Overtime stability of LCAO. Highly purified LCAO was sterile filtered and stored at 4°C. Enzyme activity was assayed regularly over 6 months. During this time frame, the enzymatic activity does not change.

4.2 Exploring LCAO activity towards aliphatic and aromatic primary amines

LCAO typically uses as a substrate of choice small polyamines such as putrescine, cadaverine, and spermidine, which are oxidatively deaminated with the production of hydrogen peroxide (**Scheme 3**).



Scheme 3 LCAO catalyzed conversion of putrescine into the corresponding aldehyde

Similarly, to other copper amine oxidases, it has been reported that this enzyme is also able to accept substrates of a different nature (e.g., histamine, tyramine, benzylamine, etc.) although with lower catalytic performances [76, 86]. We, therefore, decided to test the enzymatic activity of LCAO against a larger number of substrates to obtain a variety of aldehydes that may be used as intermediates for the synthesis of molecules with potentially interesting pharmacological profiles. Since this biocatalytic process occurs in aqueous media, aldehydes can be actually used in domino processes by adding other enzymes that use them as substrates [85, 86, 87] or in other organic transformations that can be carried out directly in water [88, 89, 90]. In this study, we tested the activity of LCAO toward different classes of commercially available primary amines: 14 substituted β -ethylamines, three substituted γ -propylamines and three linear amines (**Table 3**).

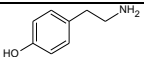
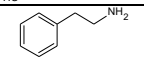
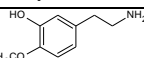
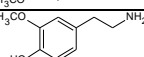
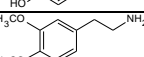
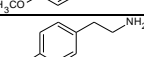
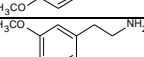
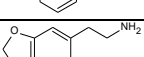
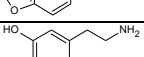
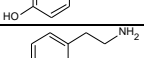
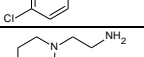
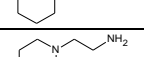
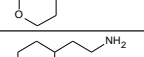
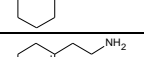
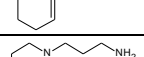
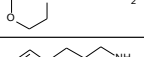
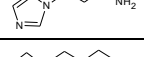
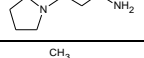
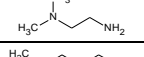
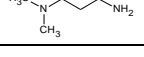
n.	structure	pH 7				pH 8			
		K_M (mM)	k_{cat} (s^{-1})	k_{cat}/K_M ($M^{-1}s^{-1}$)	relative activity (%)	K_M (mM)	k_{cat} (s^{-1})	k_{cat}/K_M ($M^{-1}s^{-1}$)	relative activity (%)
1a		0.60	29.24	49.00	100	0.49	13.30	26.94	100
2a		1.20	18.35	14.25	62.8	0.60	9.16	15.92	68.9
3a		1.58	0.27	0.21	0.9	1.66	0.17	0.10	1.3
4a		1.31	2.00	1.53	6.8	1.35	0.96	0.69	7.2
5a		1.00	1.54	1.53	5.3	1.80	2.31	1.26	17.4
6a		5.37	2.53	0.45	8.7	5.60	4.02	0.70	30.2
7a		0.47	6.20	13.04	21.2	1.20	1.80	1.48	13.5
8a		3.83	2.95	0.77	10.1	1.44	1.21	0.78	9.1
9a		ND	ND	0.49	ND	ND	ND	ND	ND
10a		3.38	10.15	3.15	34.7	1.30	1.98	1.45	14.9
11a		0.42	5.53	0.79	18.9	0.70	0.73	0.23	5.5
12a		6.46	5.63	0.72	19.3	0.75	0.17	0.41	1.3
13a		1.44	1.06	0.79	3.6	0.70	0.29	0.80	2.2
14a		1.90	1.47	12.93	5.0	0.23	0.19	1.04	1.4
15a		17.00	1.27	0.07	4.3	ND	ND	0.00	ND
16a		0.61	2.77	4.92	9.5	0.25	0.40	1.60	3.0
17a		2.30	5.08	2.14	17.4	ND	ND	0.46	0.0
18a		0.23	1.27	2.05	4.3	0.11	2.20	2.19	16.5
19a		8.80	17.9	1.29	61.2	0.33	0.73	5.47	5.5
20a		2.59	3.51	5.35	12.0	2.12	11.8	20.00	88.7

Table 3 Steady-state kinetic parameters for LCAO-catalyzed oxidative deamination of primary amines at pHs 7.0 and 8.0.

LCAO kinetic parameters were determined at pH 6, 7, and 8. The enzyme is inactive at pH 6, while it is active at pH 7 on all the tested substrates with the exception of compound **9a**, which can be considered a poor substrate. This molecule is processed slowly by the enzyme, and it was not possible to accurately measure the kinetic parameters. This could be probably due to the presence of the hydroxyl groups in the catechol moiety. The enzyme is active in the absence of substituents on the aromatic ring (**2a**), in the presence of substituents in the para position (**1a**, **10a**), or when the catechol –OH are singly or both methylated (**3a–9a**). Besides phenylethylamines, LCAO can also transform non-aromatic or heterocyclic ethyl- or propylamines (**11a–17a**) as well as linear amines (**18a–20a**). Conversely, the enzyme is generally less performing at pH 8. At this pH value, compounds **9a**, **15a** and **17a** are not transformed at all. To date, LCAO crystal structure is not yet available, and it is challenging to establish the structural determinants of the interaction between the enzyme and these unnatural substrates. Although the catalytic performance of LCAO toward all the tested amino substrates is lower than that measured for putrescine, the natural substrate ($k_{\text{cat}} = 262 \text{ s}^{-1}$ and $k_{\text{M}} = 2.7 \times 10^{-4} \text{ M}$) [76], the kinetic data indicate that this enzyme can actually be used for synthetic purposes. Below, the kinetic plots of LCAO catalyzed deamination at pH 7.0 of compounds 1a-8a, 10a-20a (**Figures 9-12**). Initial rates of reaction were determined at the various substrate concentrations in the presence of 150 nM LCAO (20 μg , 1 U), at 25°C by means of a coupled LCAO-peroxidase spectrophotometric assay.

The formation of the colored product was followed at 515 nm for 1 min. Each point in the plot is the mean value of 3 replicates (SD values were always less than 5%). V_0 is expressed as $\mu\text{M min}^{-1}$.

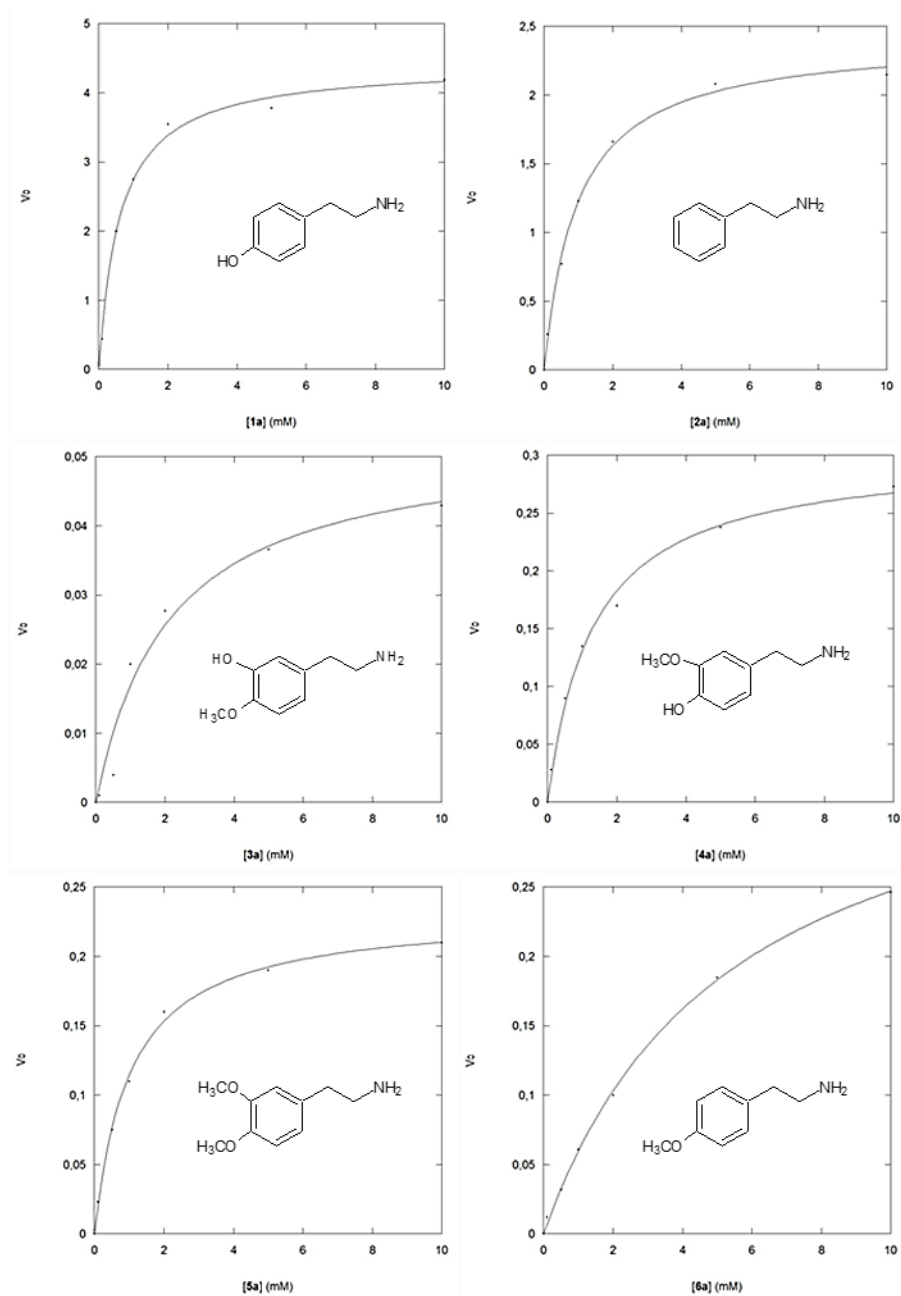


Figure 9 Kinetic plots of LCAO deamination at pH 7.0 of compounds **1a** – **6a**.
 V_0 : $\mu\text{M min}^{-1}$. Concentration range: 0.1-10 Mm.

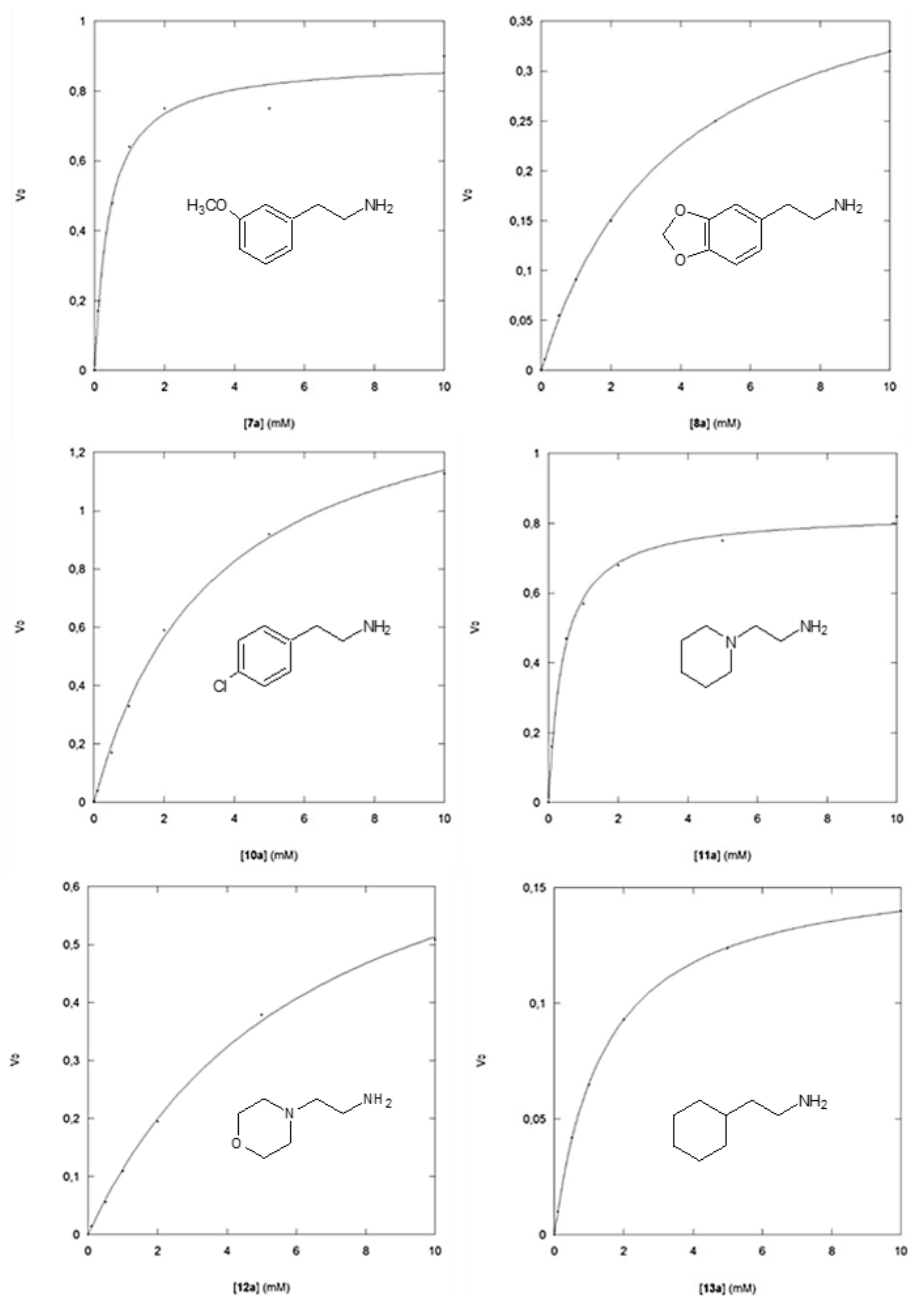


Figure 10 Kinetic plots of LCAO deamination at pH 7.0 of compounds **7a-8a** and **10a-13a**. V_0 : $\mu\text{M min}^{-1}$. Concentration range: 0.1-10 Mm.

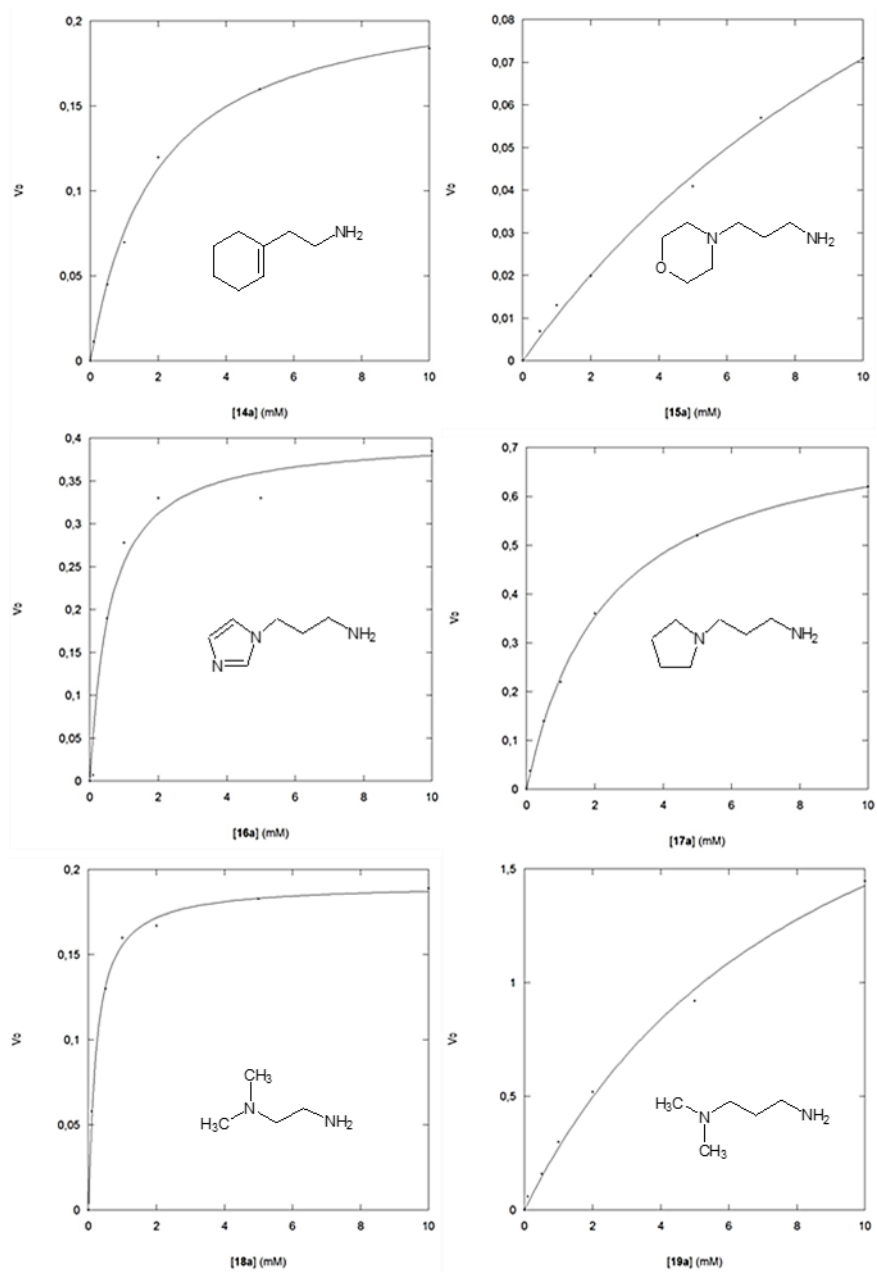


Figure 11 Kinetic plots of LCAO deamination at pH 7.0 of compounds **14a** – **19a**.

V_0 : $\mu\text{M min}^{-1}$. Concentration range: 0.1-10 Mm.

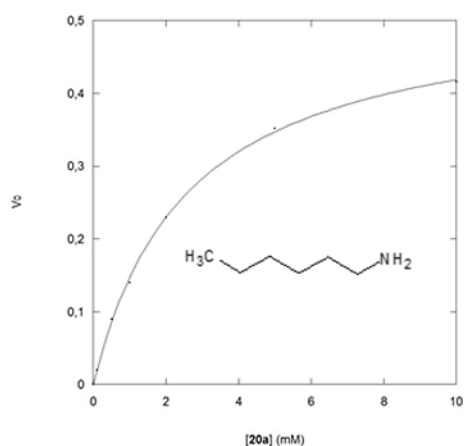
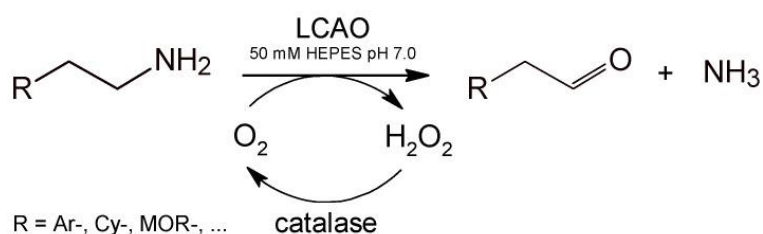


Figure 12 Kinetic plot of LCAO deamination at pH 7.0 of compound **20a**.

V_0 : $\mu\text{M min}^{-1}$. Concentration range: 0.1-10 Mm.

4.3 Biocatalytic production of aldehydes

Considering that LCAO shows the best catalytic performance at pH 7, the synthesis of the aldehydes was carried out at this pH value starting from the corresponding primary amines (**Scheme 4**).



Scheme 4 Biocatalytic conversion of primary amines (compounds **1a-20a**) into the corresponding aldehydes (compounds **1b-20b**) in the presence of LCAO and catalase

In the biocatalytic production of aldehydes, LCAO is coupled with catalase, which decomposes hydrogen peroxide, a co-product of the reaction, to water

and oxygen. Hydrogen peroxide must be quickly removed from the reaction medium because it can inactivate the proteins and oxidize the substrates and the reaction products. Thus, catalase preserves LCAO activity, while contributing to the recycling of oxygen which is co-substrate of the reaction.

The production of the aldehydes was monitored by the purpald® colorimetric assay that, unlike the time-consuming GC and HPLC methods, is typically fast, while preserving high specificity and sensitivity. The assay was set up using the commercially available phenylacetaldehyde as a standard (**Figures 13-14**).

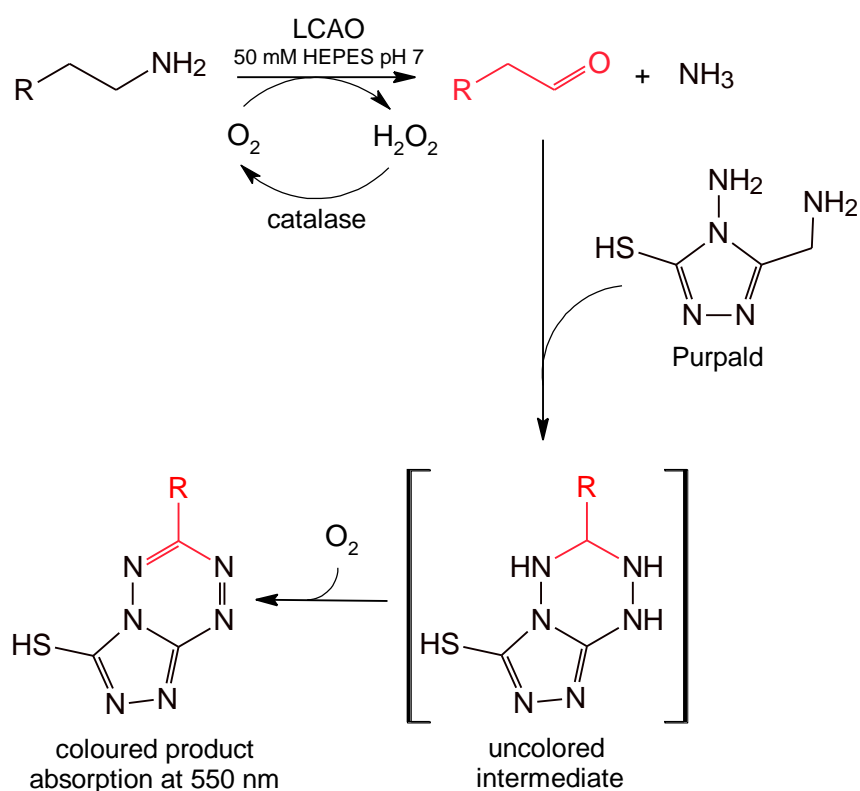


Figure 13 Purpald® reaction with aldehydes leading to the formation of a colored product (550nm).

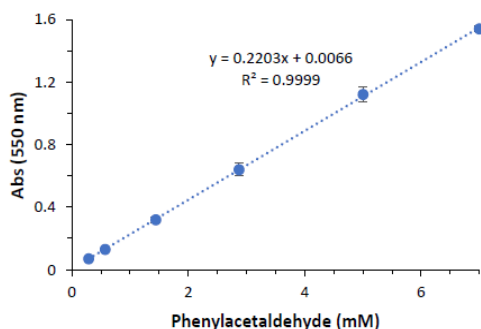


Figure 14 Purpald® calibration plot was performed using commercial phenylacetaldehyde (0.28-7.0 mM) as standard.

The reaction products were also characterized by GC/MS by comparison with the fragmentation profiles of the NIST2017 database (**Figures 15-19**). Retention times are reported in **Table 4**.

compound	HPLC (280 nm) Retention time (min)	GC/MS (ECF derivative) Retention time (min)	Compound	GC/MS Retention time (min)
1a	4.05	/	1b	12.23
2a	11.44	/	2b	8.47
3a	4.57	/	3b	11.55
4a	4.42	/	4b	11.48
5a	5.13	/	5b	11.82
6a	5.43	/	6b	9.27
7a	5.46	/	7b	9.07
8a	5.35	/	8b	10.34
10a	6.22	/	10b	8.61
11a	/	19.89	11b	7.67
12a	/	15.07	12b	7.64
13a	/	11.02	13b	7.00
14a	/	11.28	14b	5.67
15a	/	16.33	15b	7.31
16a	6.23	/	16b	9.36
17a	/	10.87	17b	11.62
18a	/	9.64	18b	4.27
19a	/	10.11	19b	4.30
20a	/	9.34	20b	4.98

Table 4 Retention times of compounds **1a-20a** and **1b-20b**. Aliphatic/aromatic amines characterization performed by GC/MS / HPLC. Products have been characterized by GC/MS after extraction with ethyl acetate.

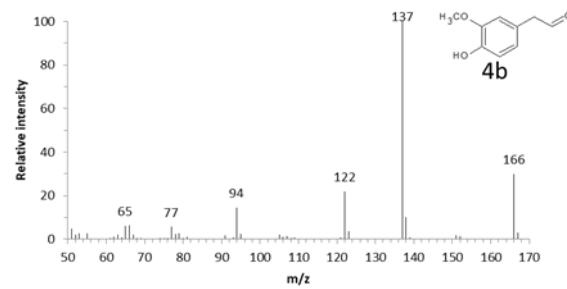
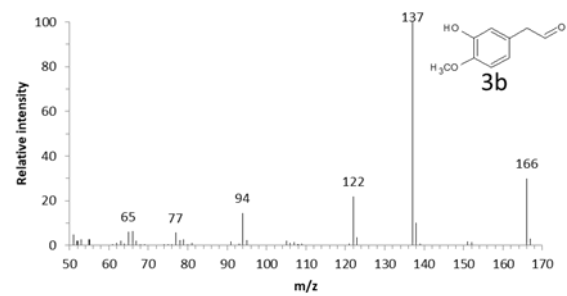
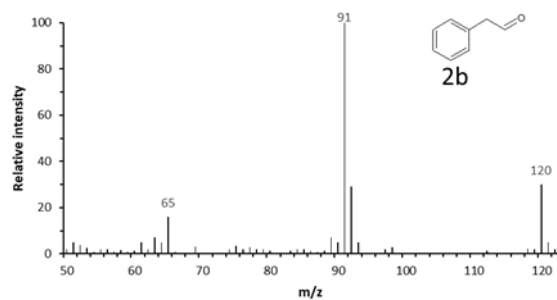
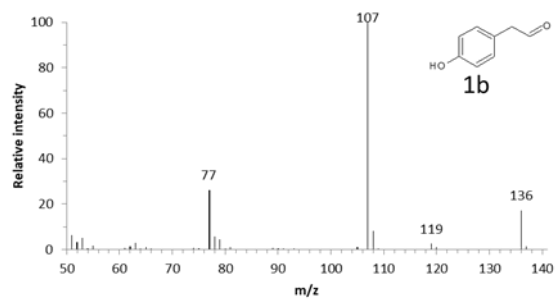


Figure 15 Mass spectra of compounds **1b-4b** after extraction with ethyl acetate

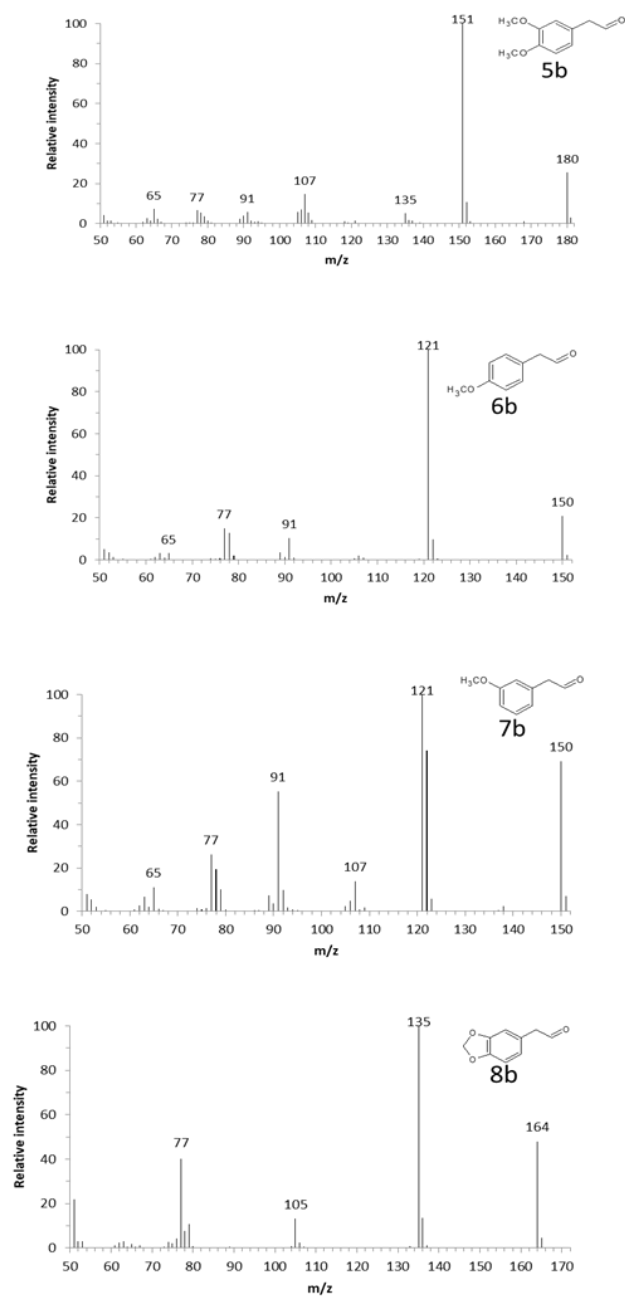


Figure 16 Mass spectra of compounds **5b-8b** after extraction with ethyl acetate

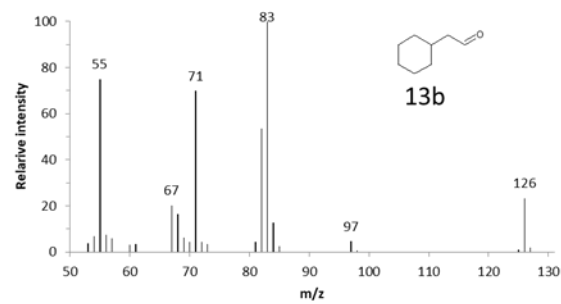
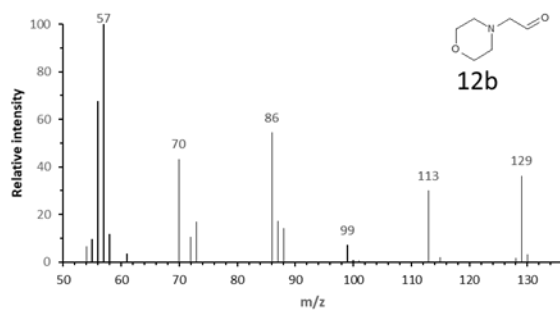
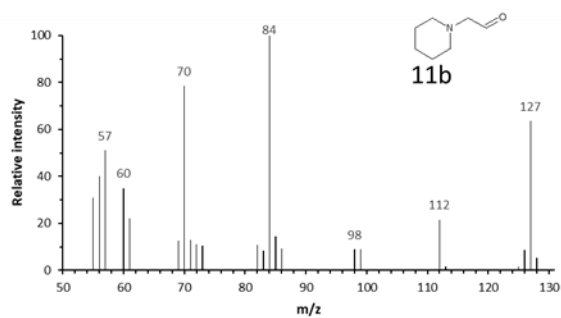
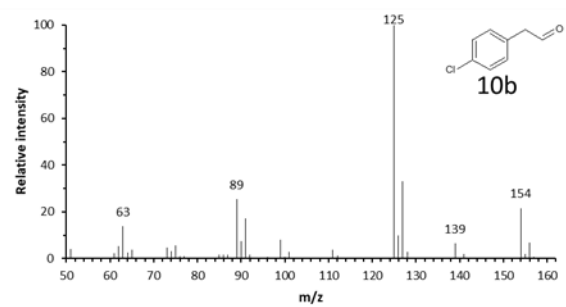


Figure 17 Mass spectra of compounds **10b-13b** after extraction with ethyl acetate

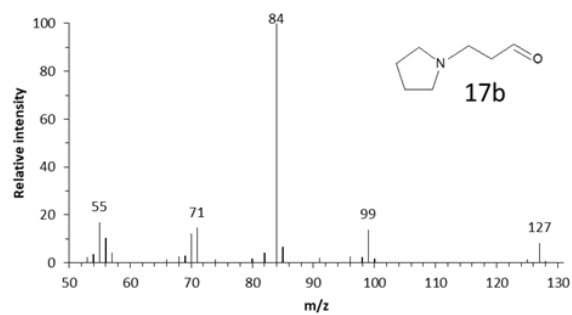
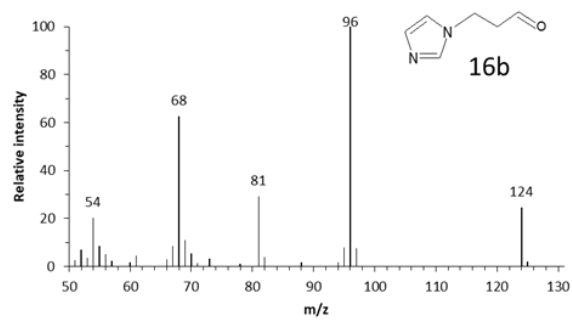
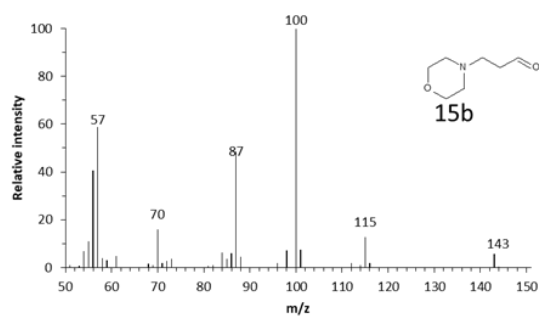
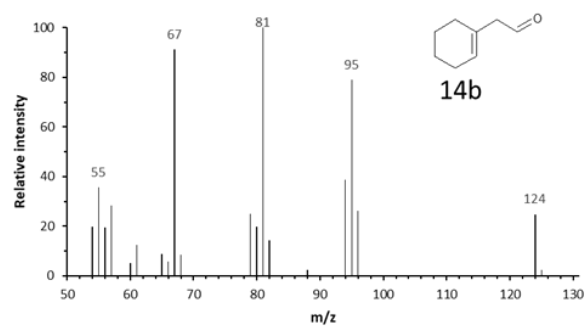


Figure 18 Mass spectra of compounds **14b-17b** after extraction with ethyl acetate

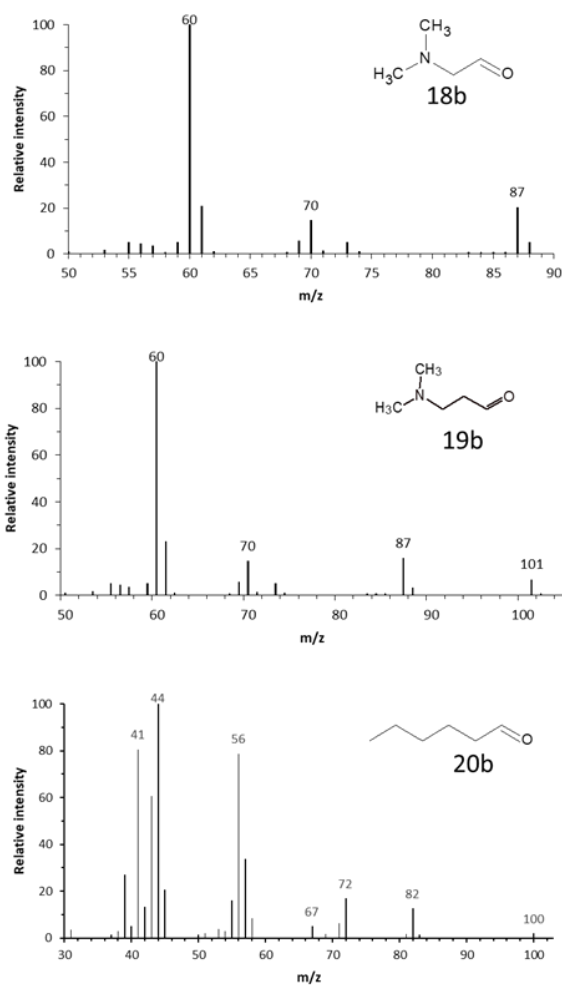


Figure 19 Mass spectra of compounds **18b-20b** after extraction with ethyl acetate

As shown in **Table 5**, all the tested amines are almost completely converted into the corresponding aldehydes (**1b-20b**) in a time ranging from 0.5 to 3 hours. The formation of byproducts, such as imine derivatives (deriving from the reaction between aldehydes and primary amines or ammonia), which typically form at pH 4–5, is not observed at pH 7.

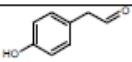
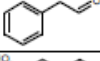
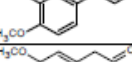
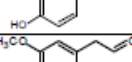
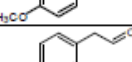
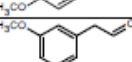
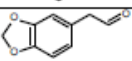
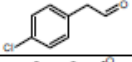
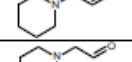
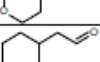
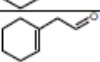
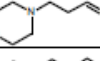
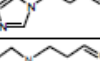
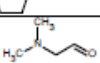
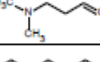

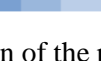
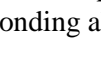
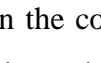
n.	reaction product	Conversion (%)			
		0.5 h	1 h	2 h	3 h
1b		87	99		
2b		63	98		
3b		13	22	54	95
4b		23	38	62	97
5b		17	33	72	96
6b		34	47	75	98
7b		41	56	83	99
8b		29	41	69	95
10b		98			
11b		67	98		
12b		56	87	99	
13b		25	54	78	98
14b		27	60	74	97
15b		60	79	96	
16b		45	82	96	
17b		43	76	97	
18b		27	47	66	98
19b		99			
20b		68	99		

Table 5 Conversion of the primary amines **1a–8a**, **10a–20a** to the corresponding aldehydes **1b–8b**, **10b–20b**.

The enzyme is efficient in the conversion of linear amines (compounds **19a** and **20a**), structurally similar to the natural substrate, and with para-substituted phenylethylamines (compounds **1a** and **10a**). For these compounds, the transformation occurs within an hour. To ensure constant catalytic efficiency, the enzyme is supplied at regular time intervals (30 min). This is necessary

because, over longer reaction times, the newly synthesized aldehydes may partially inactivate the enzyme. Considering the intrinsic reactivity and instability of aldehydes, this biosynthetic method is particularly suitable for their use as short-living intermediates in domino processes where the aldehydes can be quickly processed in enzymatic cascades [85, 87]. However, to evaluate the scalability of the process, we applied the synthesis protocol described above to the conversion of a 10-fold amount of **2a** to the corresponding aldehyde. In addition, in this case, we had an almost total conversion. The extraction of aldehyde from the aqueous reaction media resulted in yield of isolated product of 43 mg (71.6%, purity > 95%) (**Figures 20-21**).

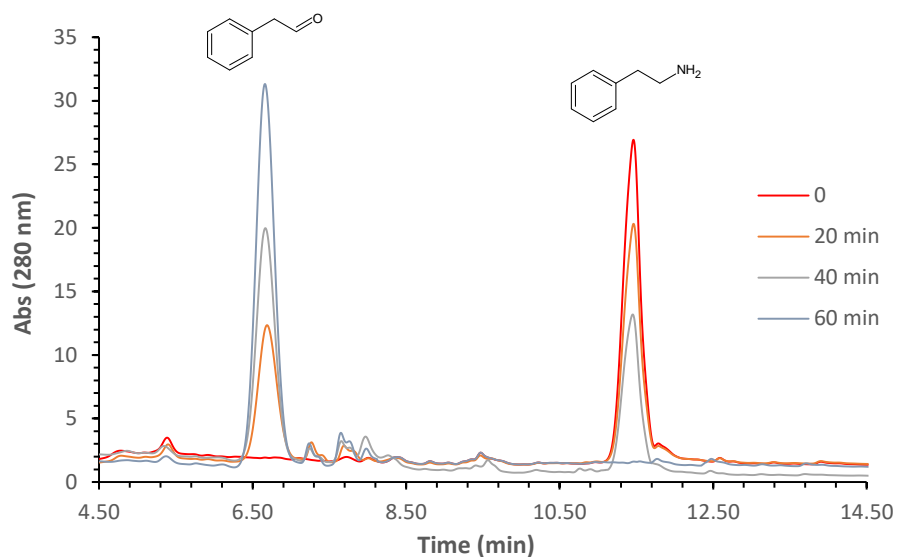


Figure 20 Enzymatic synthesis of phenylacetaldehyde (compound **2b**) by HPLC analysis.

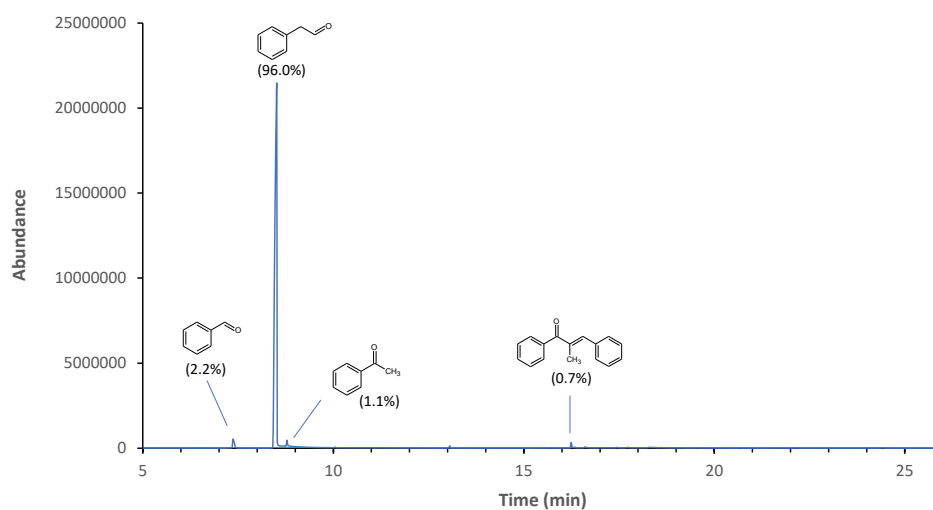


Figure 21 A scale-up of the synthesis of **2b** was performed and the isolated compound was analyzed by GC/MS to test its purity (96%). (16.27 min): aldol dimerization product. (7.42 min) and (8.45 min) probably originate from LCAO-catalyzed transformation of amines present as impurities in **2a**.

4.4 Immobilization of LCAO

Cu-containing amine oxidases are enzymes highly expressed in *Leguminosae* sp. Among them, *Lathyrus cicera* is an extremely abundant source of this enzyme, where it is produced at high yields and accumulates in the apoplastic space of the etiolated sprouts. As reported above we demonstrated that LCAO can be purified using an easily scalable chromatography-free protocol. The purified enzyme is naturally active on biogenic primary amines, but it can be also used for the biocatalytic synthesis of a wide range of aliphatic and aromatic aldehydes, starting from the corresponding amines. Typically, biotransformation of non-natural substrates requires more enzyme with respect to the natural substrates, and this could be a problem when considering a large-scale synthesis. In this regard, LCAO immobilization may overcome this issue, by allowing its recycling/reuse, and at the same time, by avoiding the possible inactivation due to the accumulation of the aldehyde. Optimal immobilization strategies have to be tailored for each specific enzyme; thus, we tested which solid support was the most suitable for immobilizing LCAO. As a first step, we selected a series of resins and differently functionalized magnetic and non-magnetic particles, to test the binding capacity of the enzyme and its activity. Specifically, we chose different types of solid supports: a DEAE Sepharose resin, chloromethyl latex microparticles, and three different magnetic beads (COOH- or NH₂-functionalized microparticles (COOH-MMPs and NH₂-MMPs), and TurboBeads amine nanoparticles).

The surface lysine residues of the enzyme are used to covalently bind the selected supports using different strategies. Glutaraldehyde and 1-ethyl-3-(3-dimethylaminopropyl) carbodiimide hydrochloride (EDC) crosslinkers were used for amine-functionalized supports (DEAE, NH₂-MMPs, and TurboBeads amine nanoparticles) and COOH-MMPs, respectively; chloromethyl latex

nanoparticles do not require crosslinker agents as they display on their surface chloromethyl groups which yield a stable covalent bond with amino groups of LCAO, in a one-step process under mild aqueous conditions. As shown in **Figure 22**, all the selected supports were able to bind the enzyme which, in all cases, was active.

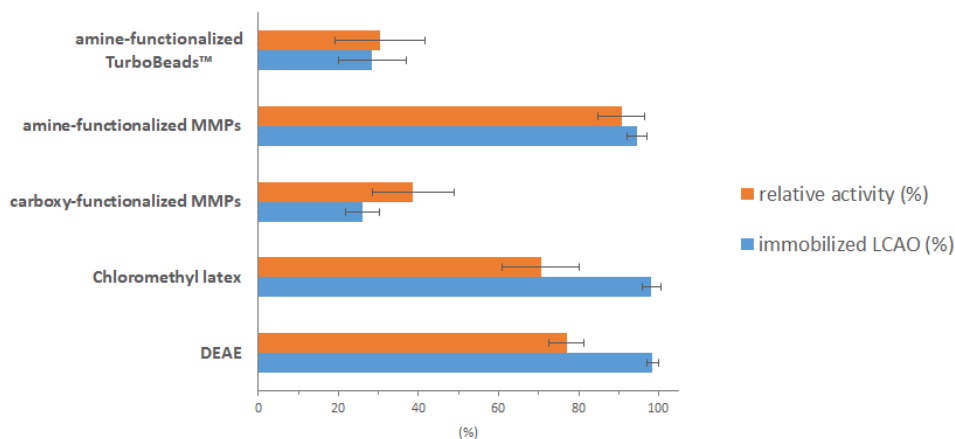


Figure 22 LCAO immobilization on different supports. Data are presented as mean \pm SD (n = 3).

Greater difficulties were encountered with the TurboBeads magnetic nanoparticles that, due to the low diameter (≤ 50 nm), are quite difficult to handle and tend to aggregate. This results in a low degree of protein binding, even though the linked enzyme is still active. A similar result was obtained when using the COOH-MMPs. In this case, although the relative activity is higher than expected based on the immobilized enzyme, this system is not convenient due to the large loss of protein that occurs during the crosslinking process. LCAO immobilization occurred efficiently on all the other tested solid supports. On chloromethyl latex nanoparticles and DEAE Sepharose resin very similar results were obtained: about 100% of the enzyme was bound with an enzymatic activity of about 70–80%. Both systems have advantages:

chloromethyl latex beads are easy to prepare while DEAE resin can be packed on a column to generate a kind of flow reactor, in which the amino substrate present in the mobile phase can be converted into the aldehyde by the crosslinked enzyme. The best performance in terms of immobilization and activity was achieved with NH₂-MMPs. In this case, the amount of immobilized enzyme is comparable to chloromethyl latex and DEAE resin, while the relative activity is definitely higher (>90%). These results can be explained by the use of glutaraldehyde as the crosslinker: it typically promotes the formation of multipoint bonds with the enzyme while allowing it to maintain high conformational mobility, likely mimicking its free form. The superparamagnetic property of these micro-sized magnetic beads is useful because individual microparticles become magnetized only when exposed to an external magnetic field, but no magnetization occurs when the field is removed. These unique features can be exploited for enzyme separation from the reaction mixture and its reuse, making them competitive especially for large-scale industrial uses. Given these results, the NH₂-MMPs were selected as the support of choice for LCAO immobilization.

LCAO-catalyzed oxidative deamination can be easily followed by monitoring hydrogen peroxide by a spectrophotometric assay coupled with peroxidase. The latter, in the presence of AAP and DCHBS, generates a typical purple-colored adduct. This assay can be promptly used to check LCAO immobilization on the surface of MMPs. As shown in **Figure 23B**, the solution turns purple starting from the particles that gather when a magnetic field is applied.

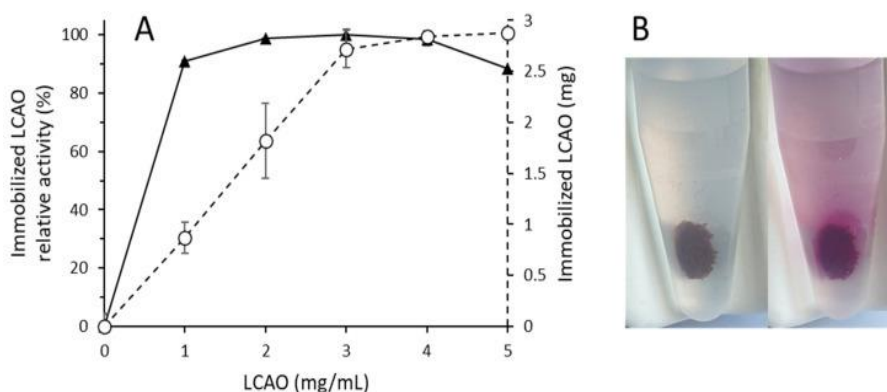


Figure 23 LCAO immobilization on NH₂-MMPs. **(A)** Effect of LCAO concentration on the immobilization on NH₂-MMPs (data are presented as the mean \pm SD of two experiments). **(B)** LCAO immobilized on NH₂-MMPs in the absence (left) or the presence (right) of the reagents used for the peroxidase coupled assay. The purple halo around the microparticles grouped by the effect of the magnet indicates that LCAO is immobilized on them.

Alongside these qualitative data, we carried out a quantitative analysis of the immobilization process. The immobilization was performed according to the manufacturer's instructions, starting from a fixed concentration of particles (10 mg) and glutaraldehyde (10%), varying the amount of enzyme. The parameters used to evaluate the efficiency of the process were the amount of protein bound and its relative activity. Soluble LCAO activity at its optimum (pH 7, 25 °C) was considered 100%. As shown in **Figure 23A**, we tested enzyme concentrations ranging from 1 to 5 mg/mL measuring at the same time the activity of immobilized LCAO.

In our experimental setting, MMPs are saturated using 3 mg of protein. A further increase in enzyme concentration did not improve the immobilization yield. In addition, in the range of 1–4 mg, the relative activity of the immobilized LCAO was close to 100%. Further increase in enzyme concentration resulted in a 15% loss of LCAO activity that may be explained

by reduced accessibility of the substrate to the active site, probably due to a crowding of the enzyme on the surface of the support. Based on these results, the best immobilization yield is achieved by using 3 mg of the free enzyme. The LCAO-MMPs thus obtained were used for the performance study.

4.5 Characterization and performance study of LCAO-MMPs

The effect of reaction pH on the relative activity of both soluble and immobilized enzymes was investigated at different pH values (**Figure 24A**). As previously demonstrated [**Table 3**], soluble LCAO has an optimum pH towards its natural substrate putrescine between 7 and 8 while is significantly less active at pH 5.5 and 6. The immobilized enzyme does not show a shift in the optimum pH, while at pH different from 7, the activity is always higher than in the free enzyme (T-test, $p < 0.05$). This might be due to the change in the electrostatic charge of the enzyme after immobilization. Based on these results, the performance study was carried out at this pH value.

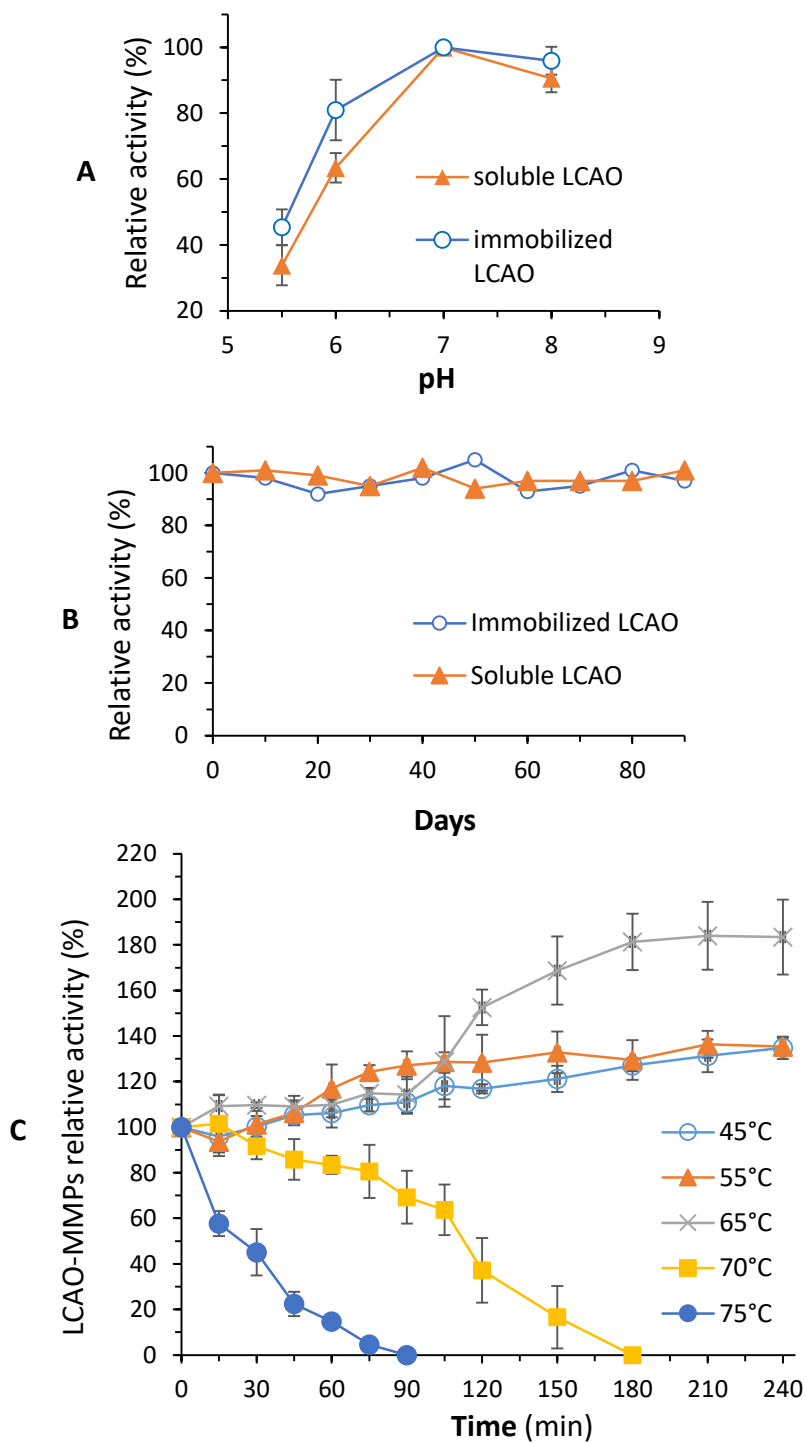


Figure 24 Effect of immobilization of LCAO on reaction pH (A), storage stability (B), and thermostability (C). Data are presented as mean \pm SD (n = 3).

The enzyme immobilization method was reliable as three different batches of immobilized enzyme prepared by the procedure described gave comparable results in terms of crosslinked protein ($94.57\% \pm 2.6$) and relative activity ($90.67\% \pm 5.86$) (Figure 1). As shown in **Figure 24B**, both soluble and immobilized LCAO stored at 4 °C retain their activity for up to 90 days. These results also prove that there is no protein leakage over time.

LCAO is stable at 50–60 °C up to 1 h and here we checked whether the immobilized enzyme retains this thermal stability profile (**Figure 24C**). The results are shown in Figure 3C, where the stability is measured in a temperature range of 45–75 °C. The immobilization procedure resulted in enhanced thermal stability of LCAO, which means an increase in the resistance of the immobilized enzyme towards heat-induced conformational changes. Immobilized LCAO is stable for at least 4 h up to 65 °C, after 2 h at 70 °C it still retains 50% activity, and it is still 50% active after 30 min at 75 °C. This might be explained because the glutaraldehyde treatment enables the formation of covalent bonds that restrict the enzyme unfolding through multipoint linkage. In addition, a 35% enhancement of apparent activity is observed after 4 h at 45 and 55 °C, which further increases to 83% when the enzyme is incubated at 65 °C. This might be the result of specific interactions between magnetic microparticles and enzymes, substrates, or reaction media that could occur at higher temperatures.

One of the main reasons for the immobilization of an enzyme for biocatalytic purposes is its reusability and this is important to reduce the overall costs in any industrial application. While free LCAO can be used once, immobilized LCAO can be recycled efficiently. As shown in **Figure 25**, the enzyme can be reused up to 15 times with its natural substrate putrescine ($10.87 \pm 1.83\%$ relative activity at cycle 15).

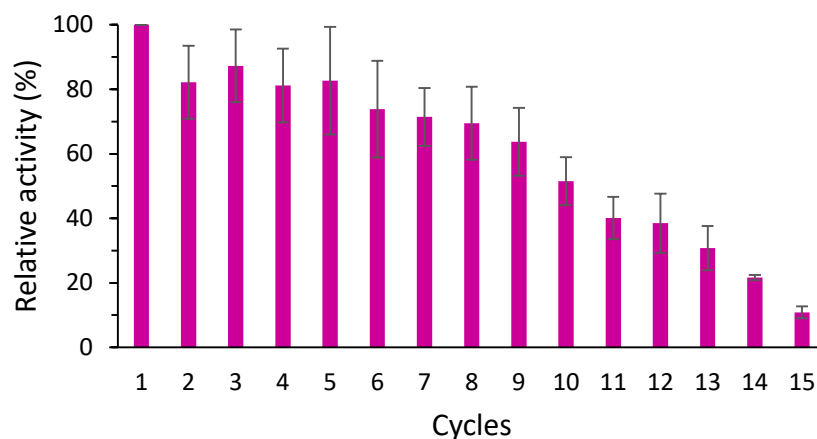
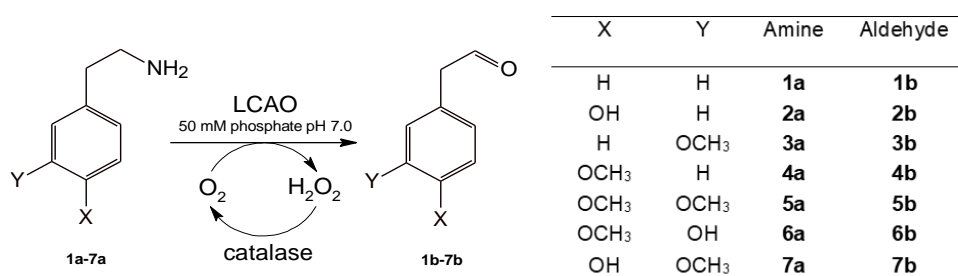


Figure 25 Reusability of LCAO immobilized on NH₂-MMPs. The reaction was carried out with putrescine as a substrate in the presence of catalase. Data are presented as mean \pm SD (n = 3).

The loss of activity observed during the cycles could be due to the partial inactivation of the enzyme caused by the accumulation of the aldehyde product which can react with the amino groups on the surface of the enzyme itself. However, the immobilized enzyme is more stable with respect to the free one probably because these surface amino groups are already involved in the crosslinking with the MMPs.

4.6 Biocatalytic application of the immobilized LCAO

The greater stability of the immobilized enzyme paves the way for its better use for biocatalytic purposes. Free LCAO has a relaxed substrate specificity, being able to process variously substituted aromatic and aliphatic primary amines [Table 3]. In this paper, we aim to test whether the immobilized enzymes can be used for the biocatalytic production of aldehydes starting from a selection of aromatic ethylamines according to Scheme 5.



Scheme 5 Biocatalytic conversion of primary amines (**1a–7a**) into the corresponding aldehydes (**1b–7b**) in the presence of LCAO and catalase.

As a first step, we determined the Michaelis–Menten constant of the immobilized enzyme towards compounds **1a–7a** comparing them with the natural substrate putrescine. The k_M values are reported in **Table 6** and compared with those previously obtained with the free enzyme.

Substrate	k_M Free LCAO (mM)	k_M LCAO-MMPs (mM)
putrescine	0.27	0.36
1a	1.20	0.51
2a	0.60	0.79
3a	0.47	1.81
4a	5.37	4.74
5a	1.00	2.19
6a	1.58	0.64
7a	0.47	0.47

Table 6 Michaelis–Menten constant of free and immobilized LCAO towards **1a–7a** and putrescine.

The immobilized LCAO is active on all the substrates being able to convert all the amines tested in the corresponding aldehydes. K_M values for LCAO-MMPs are in the same low millimolar range of free enzyme and the small differences observed may be due to a series of factors including stabilization of the enzyme in more active conformations, different accessibility to the catalytic site, and different diffusion rate of substrates on the surface of the nanoparticle.

Based on these data, we tested whether immobilized LCAO could be eligible for scaling up the biocatalytic production of more complex aldehydes (**Scheme 5**). LCAO can oxidatively deaminate a variety of aliphatic and aromatic primary amines with almost total conversion. In that case (§ “Enzymatic synthesis of aldehydes”, Material and Methods), we used an amine concentration equal to 5 mM as the accumulation of reaction product aldehyde tended to inactivate the enzyme. To overcome this drawback, more units of LCAO were added at regular intervals until the reaction was completed. The immobilized enzyme is less susceptible to inactivation by the accumulation of the reaction products, probably because its surface amino groups are instead used to bind to the magnetic microparticle.

A strong indication of this behavior comes from the actual studies on the natural putrescine substrate (see **Figure 25**), where the increased stability of the enzyme allowed up to 15 reaction cycles. Based on this observation and on the kinetic parameters reported in **Table 6**, we decided to scale up the process using an initial 20 mM amine concentration (15 mL final volume) in the presence of catalase, then using the same condition at each reaction cycle. The results are shown in **Figure 26** and **Table 7**.

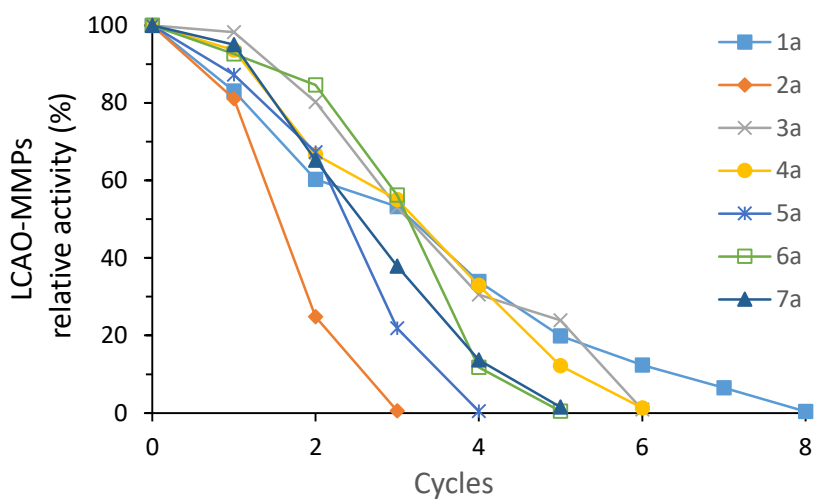


Figure 26 Reusability of LCAO immobilized on NH₂-MMPs using compounds **1a–7a** as substrates in the presence of catalase. Data are presented as the mean of two experiments.

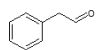
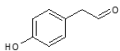
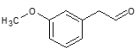
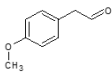
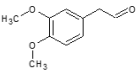
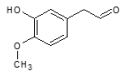
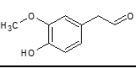
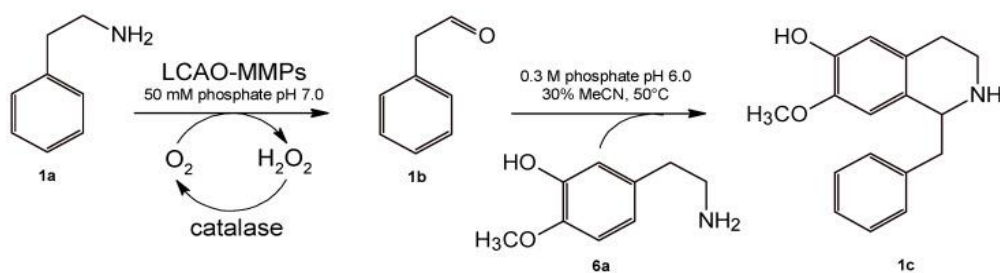
Reaction product	Cycles	Conversion (%)	Total amount (mg)
 1b	8	92.85	267.4
 2b	3	89.46	109.5
 3b	6	91.50	247.05
 4b	6	88.83	239.85
 5b	4	89.93	194.25
 6b	5	90.82	226.15
 7b	5	89.48	222.8

Table 7 Reusability of LCAO immobilized on NH₂-MMPs in the synthesis of **1b–7b**.

LCAO-MMPs quantitatively convert all tested substrates, although the number of times they can be reused varies. The conversion at the end of each reaction cycle was evaluated by determining the concentration of aldehyde by means of a colorimetric assay with Purpald®. The overall conversion at the end of all cycles is about 90% for all tested substrates, with an aldehyde production ranging between 100 and 270 mg depending on the substrate used. These values show an increase in aldehyde yield up to 45 times higher than the previously published method with the free enzyme [Table 5]. These yields can be further increased by excluding the last reaction cycle. In the last cycle, in fact, the residual relative activity is always very low while the quantity of amine is equal to that of the previous cycles (20 mM). This implies that the complete transformation is slower and that the aldehyde formed, over long reaction times, can generate by-products that reduce the overall yields. Therefore, excluding the last cycle, a purer product would be obtained, albeit in a smaller quantity. With this protocol, the aldehydes are obtained in aqueous media ready to be used in domino processes, without further extraction and purification.

In this regard, as a proof of concept, we used one of the aldehydes thus produced to synthesize a new non-natural benzyloquinoline alkaloid. In nature, the first committed step for the synthesis of benzyloquinoline alkaloids is the Pictet–Spengler cyclization between p-OH phenylacetaldehyde and dopamine, catalyzed by norcoclaurine synthase [85]. Pesnot et al. found that this reaction can be catalyzed by phosphate ions as well, although yielding the racemic product [91]. This can be a very convenient method for the synthesis of racemic benzyloquinolines, as metabolic engineering and total chemical synthesis approaches, though occasionally applied, fail to meet industry standards in sustainability and efficiency. Other research groups have

shown that the phosphate biomimetic catalysis may be suitable for the synthesis of different benzyloquinolines, starting from dopamine (or analogs with a free OH in position 3) and a series of variously substituted aldehydes. Based on these findings, we decided to synthesize a benzyloquinoline (**1c**), starting from **1b** (produced with LCAO-MMPs) and **6a** using phosphate ions as a catalyst (**Scheme 6**).



Scheme 6 Biomimetic synthesis of
1-benzyl-7-methoxy-1,2,3,4-tetrahydroisoquinolin-6-ol

This reaction takes place in the same reaction pot as the aldehyde (after removing the immobilized enzyme), lowering the pH to 6 and increasing the ionic strength of the buffer (up to 0.3 M). Under these conditions, in the presence of acetonitrile as co-solvent and at a temperature of 50 °C, the Pictet–Spengler reaction takes place. In about 2 h the reaction is complete providing **1c** with a yield of 80%. Reaction yield was determined based on HPLC analyses, according to the method already described, in collaboration with prof. Giancarlo Fabrizi from Chemistry and Technology of Drugs Department of Sapienza. In **Figure 27**, the GC/MS characterization of compound **1c** is reported, whereas the HPLC-DAD analysis and the NMR characterization are reported in **figures 28** and **29-30**, respectively (in collaboration with prof. Giancarlo Fabrizi from Chemistry and Technology of Drugs Department of Sapienza).

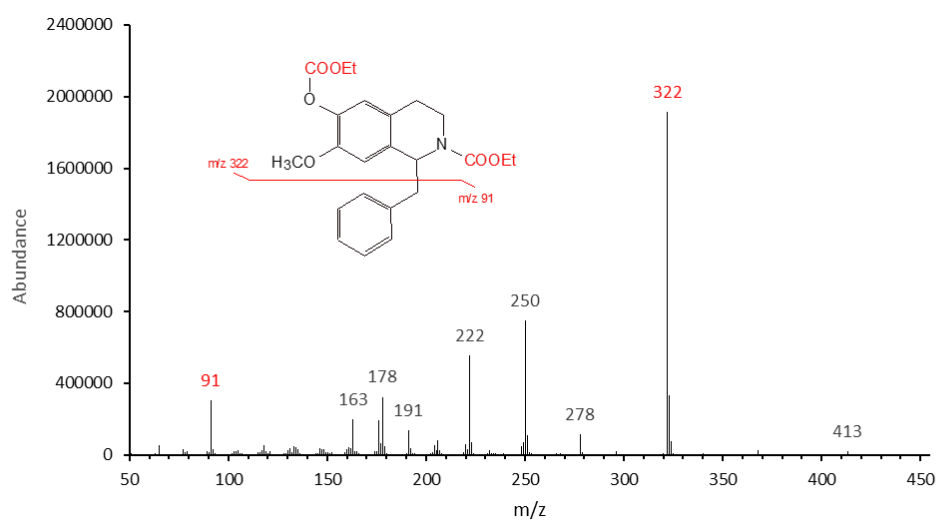
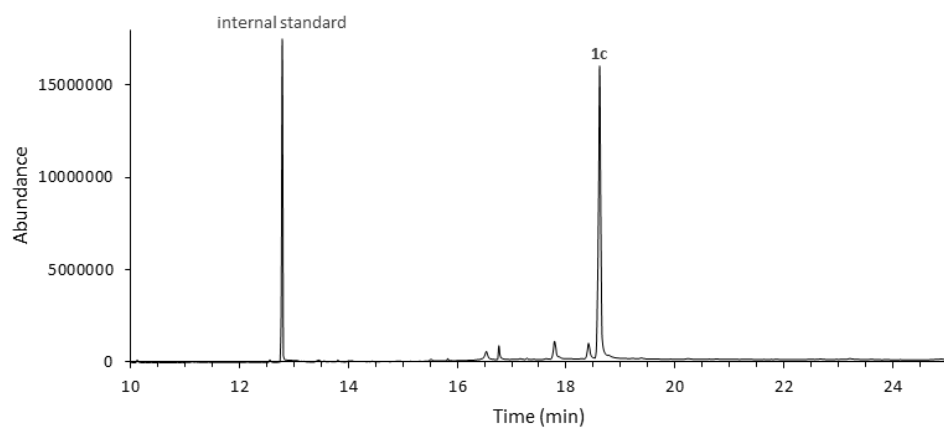


Figure 27 GC/MS chromatogram and EI mass spectrum of 1-benzyl-7-methoxy-1,2,3,4-tetrahydroisoquinolin-6-ol (ethyl chloroformate derivative)

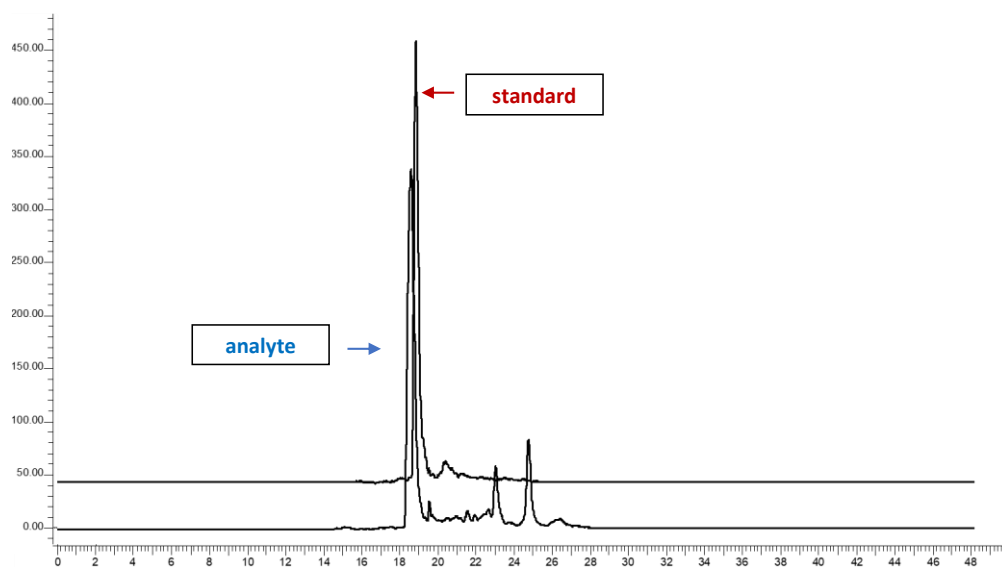
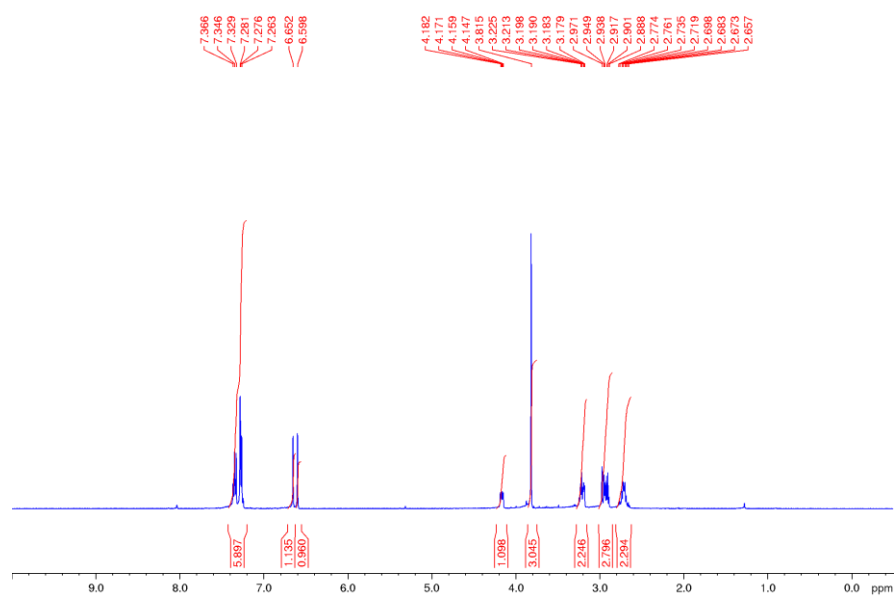


Figure 28 HPLC-DAD analysis of 1-benzyl-7-methoxy-1,2,3,4-tetrahydroisoquinolin-6-ol. The measurement was performed at 280 nm: chromatogram overlapping of authentic standard (upper curve) and analyte (lower curve)

^1H NMR (400.13 MHz), CDCl_3



^{13}C NMR (100.6 MHz), CDCl_3

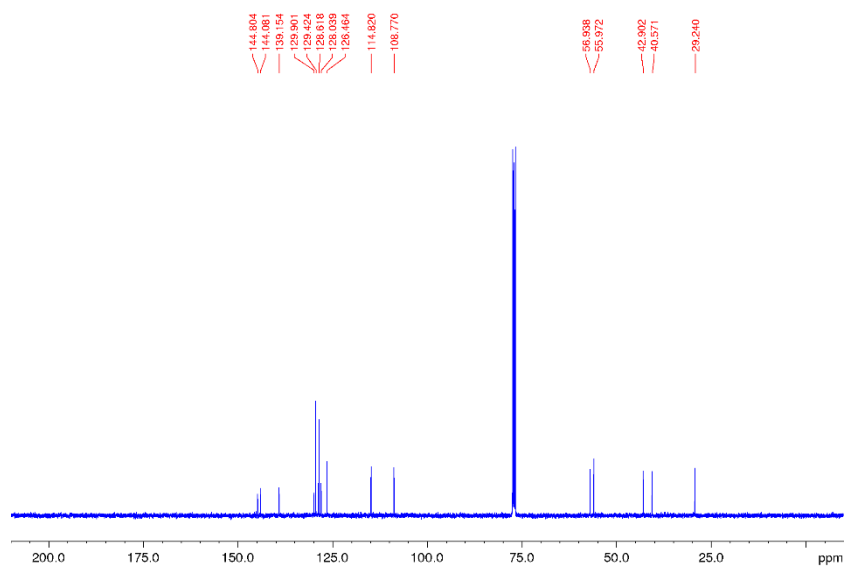


Figure 29 ^1H and ^{13}C NMR spectra of 1-benzyl-7-methoxy-1,2,3,4-tetrahydroisoquinolin-6-ol in CDCl_3

¹³C NMR - DEPT, CDCl₃

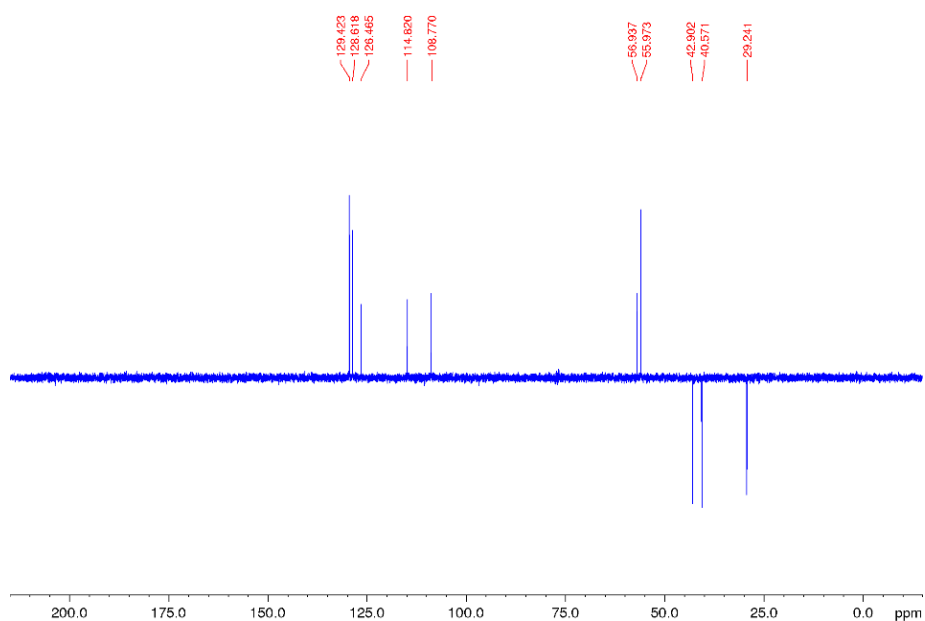


Figure 30 ¹³C NMR spectra of 1-benzyl-7-methoxy-1,2,3,4-tetrahydroisoquinolin-6-ol in CDCl₃. mp: 151- 153 °C; IR (neat): 3305, 3055, 2916, 1604, 1532, 1494, 1334, 1209, 1125, 997 cm⁻¹; ¹H NMR (400.13 MHz) (CDCl₃): δ = 7.36 - 7.24(m, 5 H), 6.65 (s, 1 H), 6.59 (s, 1 H), 4.16 (dd, *J*₁ = 9.4 Hz, *J*₂ = 4.4 Hz, 2 H), 3.8 (s, 3 H), 3.24- 3.17 (m, 2 H), 2.97 – 2.88 (m, 3 H), 2.77 – 2.65 (m, 2 H); ¹³C NMR (100.6 MHz) (CDCl₃): δ = 144.8 (C), 144.1 (C), 139.1 (C), 129.9 (C), 129.4 (CH), 128.6 (CH), 128.0 (C), 126.5 (CH), 114.8 (CH), 108.8 (CH), 56.9 (CH), 55.9 (CH₃), 42.9 (CH₂), 40.6 (CH₂), 29.2 (CH₂).

4.7 LCAO stability in non-aqueous media

Enzymes naturally evolved in the cellular environment, so water is the most suitable medium for biocatalysis. The aqueous solvent maintains the native structure of the enzyme and promotes the conformational mobility required for catalysis. However, some biocatalysts are naturally efficient also in non-aqueous solvents. An explanation lies in the minimum amount of water constituting the layers around the enzyme and that is required to guarantee the catalytic mechanism, which differs for each enzyme.

From a biocatalytic point of view, carrying out reactions in non-aqueous media allows for an increase in the solubility of hydrophobic substrates, an easy recovering of the reaction products and no water-dependent side-reactions.

Given the biocatalytic potential of LCAO, it is important to evaluate whether this enzyme is also active in non-aqueous solvents. The first step is to assess its stability in different organic solvents including biphasic systems.

Activity tests (**Figures 31-32**) show that free LCAO is stable in the presence of at least 70-80% of water-miscible solvent. These results are not surprising if we take into consideration the enzymatic mechanism known as "pH memory". It is reported that [38] protein ionogenic groups retain their last ionization state on dehydration and subsequent placement in organic solvents.

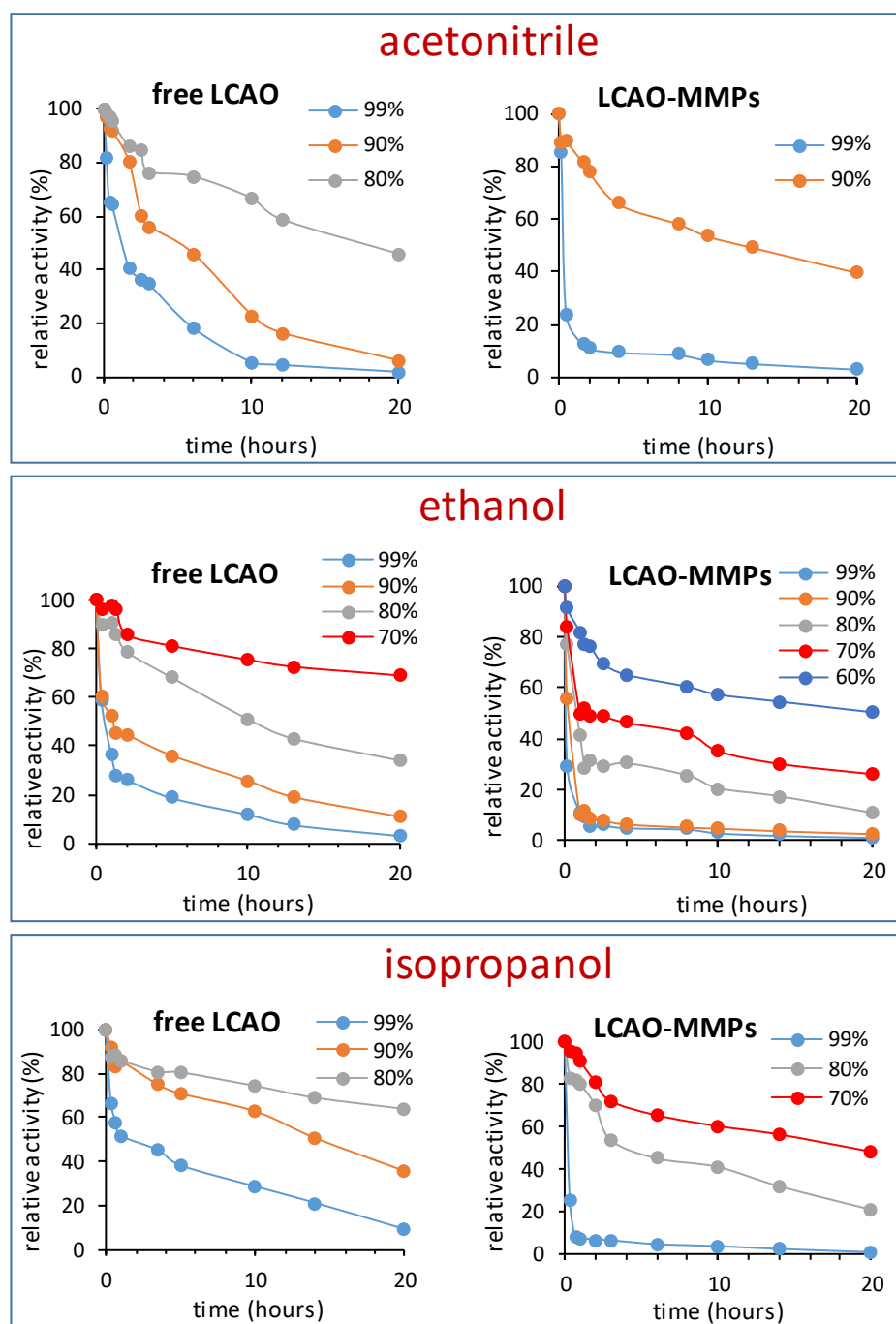


Figure 31 Activity test performed on free and immobilized LCAO in acetonitrile, ethanol and isopropanol. Data are presented as mean \pm SD (n = 3).

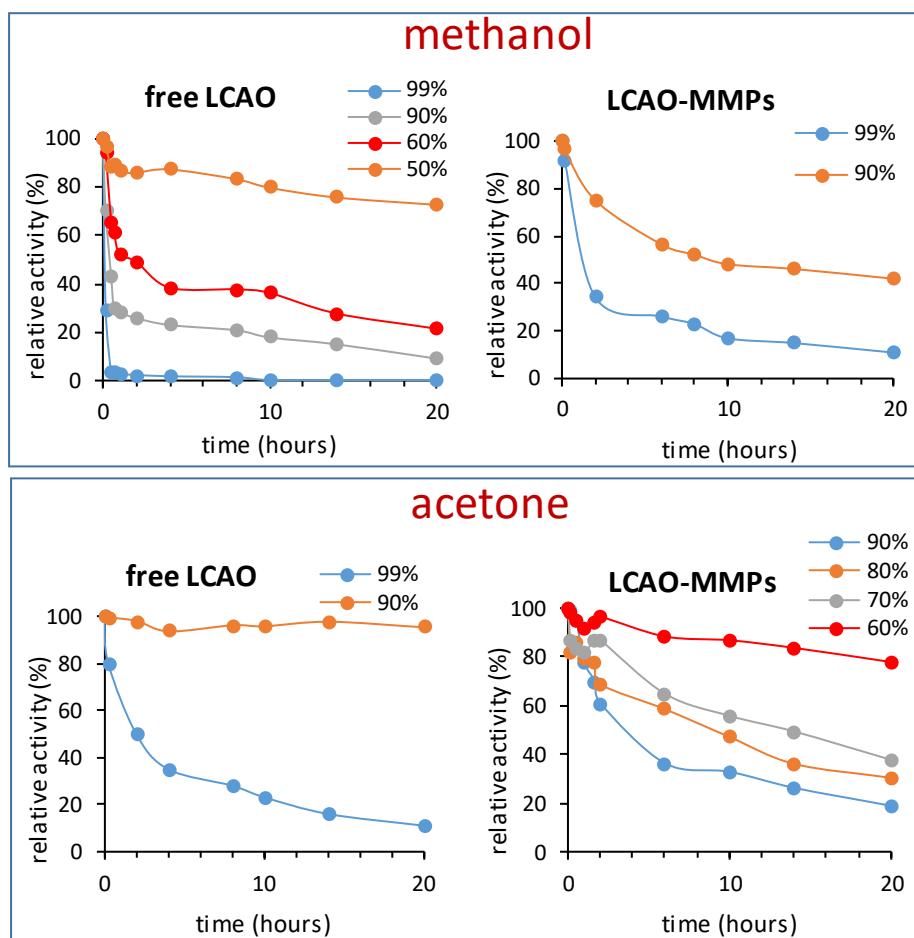


Figure 32 Activity test performed on free and immobilized LCAO in methanol and acetone. Data are presented as mean \pm SD (n = 3).

The most stable condition for free LCAO is in the presence of 90% acetone, while slight instability was observed as the polarity of the organic solvent increased. Furthermore, our results show that the solvent in which LCAO is least stable is methanol: this cannot be used at concentrations higher than 50%. Concerning LCAO-MMP, its stability is comparable to free LCAO in isopropanol, ethanol, and acetonitrile. Using methanol and acetone as co-

solvents, LCAO-MMP stability is reversed compared to the free form of LCAO since the immobilized form is more unstable as the polarity of the solvent decreases. It is well established that the more polar solvents tend to strip the free enzyme of its hydration molecules, functional to catalysis [38]. In addition, hydrophilic solvents may penetrate the catalytic site inducing a conformational change in the secondary and tertiary structure [39]. Subsequently, the protein is more prone to denaturation because of the higher conformational mobility. On the other hand, the organic solvent, such as acetone or acetonitrile, could keep the enzymatic structure of free LCAO more rigid. In such a more apolar medium, the few water molecules of the monolayers around the enzyme will exhibit a lower destabilizing effect in terms of kinetic and thermodynamics. Based on our results, LCAO immobilization is a functional strategy when using the enzyme in a polar medium such as methanol, as it is stable for almost one day in the presence of 90% of this solvent. Probably, methanol confers to immobilized LCAO a rigid and stable conformation avoiding unfolding and conformational changes at the active site.

For a homogeneous system, substrates and products do not accumulate around the enzyme, which therefore remains easily operative [92]. In addition, diffusion resistance at the interface does not occur. However, testing LCAO in water-organic solvent biphasic systems could be advantageous considering that biocatalysis takes place in the aqueous phase, whereas the hydrophobic reaction products are extracted by the organic solvent. In biphasic systems, water is partially dispersed in the organic solvent and partly present on the solid support or the enzyme, and they all compete for water [93]. If there is enough aqueous solvent, a continuous micro-phase could form with the pores of the solid support, so the immobilized enzyme functions as a free enzyme.

At lower concentrations of water, however, the micro-phase does not form: the immobilized enzyme is no longer hydrated and catalytic activity could be altered. Therefore, to evaluate the stability of free and immobilized LCAO in biphasic systems, the catalyst was kept under constant stirring for 20 h in the presence of 1:1 water/water immiscible organic solvent (dichloromethane, hexane, ethyl acetate or diethyl ether). Our results (**Figure 33**) show that, in this conditions, immobilized LCAO is always more stable than the free enzyme. This is evident when hexane and dichloromethane are used: in these cases, while the immobilized enzyme retains good stability, the free form tends to lose it in a shorter time. This is not surprising because, as already mentioned, immobilization typically stabilizes the enzyme to unfold. Hence, also in this case, immobilization of LCAO on amino-functionalized particles somehow diminishes the contact with the denaturing organic solvent. Unlike monophasic systems, the biphasic ones need constant stirring to favour reaction products partition between the two phases. Under these conditions, an emulsion can form which denatures the protein. However, considering that the immobilized enzyme does not lose its activity, the immobilization itself is likely to protect LCAO from denaturation.

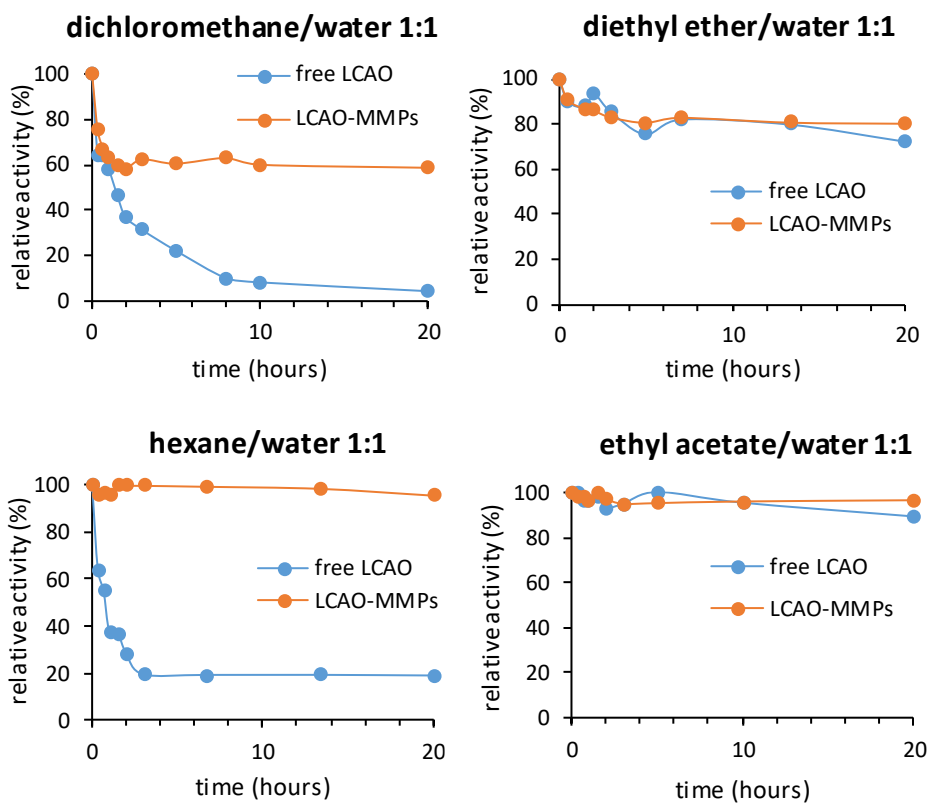


Figure 33 Activity test performed on free and immobilized LCAO in water/organic solvent 1:1. Data are presented as mean \pm SD (n = 3).

CHAPTER 5

CONCLUSIONS

LCAO is a copper-containing plant enzyme whose use, to date, has been mainly confined to the realization of biosensors for the detection of biogenic amines. This enzyme, synthesized by plants as a defence system against pathogens, shows a relaxed substrate specificity as it can accommodate various primary amines in the catalytic site, converting them into the corresponding aldehydes. It is precisely this feature that makes it a good candidate for biocatalytic processes. In various industrial sectors (cosmetics, pharmaceuticals, and food), there is a growing interest in the synthesis of aldehydes labelled as “natural”, and exploiting the catalytic power of LCAO for this purpose could indeed be an advantage.

The first step for LCAO to be used as a biocatalyst is to have an enzyme purification method that can be cost-effective and applicable on a large scale. We have shown that it is possible to purify the enzyme from the etiolated shoots of *Lathyrus cicera* without costly chromatographic steps. Specifically, we have shown that tangential ultrafiltration may fit this purpose. Tangential ultrafiltration replaces classical dialysis and concentration steps, making the whole process fast and efficient. This process can be easily scaled up using suitable crossflow systems equipped with cassettes with larger membrane areas (even square meters), able to filter larger volumes (up to thousands of liters). Considering that tangential flow filtration devices and cassettes can be cleaned

and reused several times, the system is also economical. The whole purification procedure takes about 7 h compared to the 16 h needed for the previously used protocol. The highly purified protein (>95%) is stable for up to 6 months, sterile filtered at 4 °C.

To expand the range of LCAO potential substrates, we tested its activity towards a set of primary aromatic ethyl/propyl amines and linear amines/diamines. The analysis of the kinetic parameters shows that the enzyme is active on all the tested compounds (except dopamine) and, therefore, it is suitable to develop a fully enzymatic synthesis of aldehydes. Despite an excellent conversion (>95%) of all the amine substrate tested, the synthesis of aldehydes is still in the low milligram scale.

To scale up the process and improve the enzyme's performance, we immobilized LCAO onto solid supports, which also has the advantage of allowing its recovery and recycling. The best performance is obtained using amine-functionalized magnetic microparticles as the enzyme retains its activity, greatly improves its thermostability, and can be recycled numerous times with its natural substrate. Furthermore, as well as the free form, immobilized LCAO can be used for biotransformations. Specifically, we used it to synthesize a set of aromatic aldehydes variously substituted, showing that it is possible to scale up the process by recycling the immobilized enzyme a number of times, achieving excellent conversions. As a proof of concept, we have shown that it is possible to use the aldehydes thus produced for the synthesis of complex molecules, such as benzyloquinoline alkaloids.

In the last part of the project, we evaluated the stability of both free and immobilized LCAO in non-aqueous media. Organic solvents are the most

commonly used non-aqueous media for biocatalysis as they facilitate the transformation of substrates that are unstable or poorly soluble in water.

Although the data are preliminary, they show that LCAO is stable both in water-miscible solvents (acetonitrile, acetone, methanol, ethanol, or isopropanol) and in biphasic systems (water-hexane, water -dichloromethane, water-ethyl acetate or water-diethyl ether) for up to 20 hours, at room temperature. Given future biocatalytic applications, this is an important starting point. One of the limitations of LCAO-catalyzed reactions is the poor water solubility of oxygen: running the reaction in the presence of organic solvents could indeed improve its solubility, ensuring an effective scale-up of the entire process.

The data obtained in the present project pave the way for further development of the biocatalytic applications of LCAO. Given its broad substrate specificity, the next step will be expanding it to aromatic amines, precursors of aldehydes that are widely used in the pharmaceutical, food, and cosmetic industries. In this perspective, we could design and develop micro-reactors in which LCAO will be co-immobilized with other enzymes (catalase, norcochlorine synthase, methyl transferase) for the domino synthesis of molecules with high structural complexity. The biocatalytic potential of LCAO will be further expanded by studying its ability to perform biotransformations even in non-aqueous media, such as organic solvents and bio-renewable solvents (NADES, cyrene, etc.).

BIBLIOGRAPHY

1. A.K. Bergquist, K. Söderholm (2014). Industry Strategies for Energy Transition in the Wake of the Oil Crisis. *Business and Economic History On-Line*. 12, 1-18
2. M. Hajian, S.J. Kashani (2021). Evolution of the concept of sustainability. From Brundtland Report to sustainable development goals. *Sustainable Resource Management*, 1-24
3. R.G. Hunt, W.E. Franklin, R.G. Hunt (1996). LCA - How it came about. *The International Journal of Life Cycle Assessment*. 1, 4-7
4. B.M. Trost (1991). The Atom Economy - A Search for Synthetic Efficiency. *Science*, 254(5037), 1471-1477
5. B.M. Trost (1995). Atom economy a challenge for organic synthesis: homogeneous catalysis leads the way. *Angewandte Chemie International Edition in English*. 34(3), 259-281.
6. R.A. Sheldon (1992). Organic synthesis; past, present and future. *Chemistry and Industry*. 23, 903-906
7. R.A. Sheldon (1996). Selective catalytic synthesis of fine chemicals: opportunities and trends. *Journal of Molecular Catalysis A: Chemical*. 107(1-3), 75-83.
8. R.A. Sheldon (2018). Metrics of Green Chemistry and Sustainability: Past, Present, and Future. *ACS Sustainable Chem. Eng.* 6(1), 32-48
9. A. Lapkin, D.J.C. Constable (2008). *Green Chemistry Metrics: Measuring and Monitoring Sustainable Processes*. ISBN: 978-1-405-15968-5
10. A.P. Dicks, A. Hent (2014). Atom Economy and Reaction Mass Efficiency. *Green Chemistry Metrics*. pp 17-44

11. C. Jimenez-Gonzalez, C. S. Ponder, Q. B. Broxterman, J. B. Manley (2011). Using the Right Green Yardstick: Why Process Mass Intensity Is Used in the Pharmaceutical Industry To Drive More Sustainable. *Organic Process Research & Development*. 15(4), 912–917
12. R.A. Sheldon (1994). Consider the environmental quotient. *CHEMTECH (United States)* 24(3).
13. R.A. Sheldon (2017). The E factor 25 years on: the rise of green chemistry and sustainability. *Green Chemistry*. 19, 18-43.
14. J. A. Linthorst (2010). An overview: origins and development of green chemistry. *Foundations of Chemistry*. 12, 55–68.
15. P. Anastas, J. C. Warner (1998). Green Chemistry: Theory and Practice. *Oxford University Press*. 1, ISBN 10: 0198502346.
16. S.L.Y. Tang, R.L. Smith, M. Poliakoff (2005). Principles of green chemistry: PRODUCTIVELY. *Green Chemistry*. 7, 761-762.
17. J. Becker, C. Manske, S. Randl (2002). Chemistry and sustainability metrics in the pharmaceutical manufacturing sector. *Current Opinion in Green and Sustainable Chemistry*. 33
18. M. Santi, L. Sancineto, V. Nascimento, J.B. Azeredo, E.V.M. Orozco, L.H. Andrade, H. Gröger, and C. Santi (2021). Chemistry and sustainability metrics in the pharmaceutical manufacturing Compounds. *International Journal of Molecular Science*. 22(3), 990
19. M.D. Truppo. (2017). Biocatalysis in the Pharmaceutical Industry: The Need for Speed. *ACS Medicinal Chemistry Letters*. 8, 476–480.
20. C.M. Heckmann, F.Paradisi (2020). Looking Back: A Short History of the Discovery of Enzymes and How They Became Powerful Chemical Tools. *ChemCatChem*. 12(24), 6082–6102.

21. S. Wu, R. Snajdrova, J.C. Moore, K. Baldenius, U.T. Bornscheuer (2020). Biocatalysis: Enzymatic Synthesis for Industrial Applications. *Angewandte*. 60(1), 88-119
22. M. Bilal, H.M.N. Iqbal (2020). State-of-the-art strategies and applied perspectives of enzyme biocatalysis in food sector - current status and future trends. *Critical Reviews in Food Science and Nutrition*. 60(12), 2052-2066.
23. R. Singha, S. Langyanb, B. Rohtagic, S. Darjeea, A. Khandelwala, M. Shrivastavaa, R. Kotharid, H. Mohand, S. Rainad, J. Kaurd, A. Singhd (2022). Production of biofuels options by contribution of effective and suitable enzymes: Technological developments and challenges. *Materials Science for Energy Technologies*. 5, 294-310.
24. A. Papadopoulou, C. Peters, S. Borchert, K. Steiner, and R. Buller (2022). Development of an Ene Reductase-Based Biocatalytic Process for the Production of Flavor Compounds. *Organic Process Research & Development*. 26(7), 2102-2110.
25. N.A. Samakabc, Y. Jiaab, M.M. Sharsharab, T. Mua, M. Yanga, S. Peهاب, J. Xingab (2020). Recent advances in biocatalysts engineering for polyethylene terephthalate plastic waste green recycling. *Environment International*. 145, 106-144.
26. T. Ma, W. Kong, Y. Liu, H. Zhao, Y. Ouyang, J. Gao, L. Zhou, Y. Jiang (2022). Asymmetric Hydrogenation of C=C Bonds in a SpinChem Reactor by Immobilized Old Yellow Enzyme and Glucose Dehydrogenase. *Applied Biochemistry and Biotechnology*. doi: 10.1007/s12010-022-03991-9
27. A.R. Alcántara (2019). Biocatalysis and Pharmaceuticals: A Smart Tool for Sustainable Development. *Catalysts*. 9(10), 792.

28. S. Simić, E. Zukić, L. Schmermund, K. Faber, C.K. Winkler, W. Kroutil (2022). Shortening Synthetic Routes to Small Molecule Active Pharmaceutical Ingredients Employing Biocatalytic Methods. *Chemical Reviews ACS Publications*. 122(1), 1052–1126.
29. Y.G. Zheng, H.H. Yin, D.F. Yu, X. Chen, X.L. Tang, X.J. Zhang, Y.P. Xue, Y.J. Wang, Z.Q. Liu (2017). Recent advances in biotechnological applications of alcohol dehydrogenases. *Applied Microbiology and Biotechnology*. 101, 987–1001.
30. J.M. Woodley (2008). New opportunities for biocatalysis: making pharmaceutical processes greener. *Trends in Biotechnology*. Volume 26(6), 321-327.
31. R.A. Sheldon (2008). E factors, green chemistry and catalysis: an odyssey. *Chemical Communication*. 39(29), 3352-3365.
32. H. Sunac, H. Zhangac, E.L. Anga, H. Zhaoab (2018). Biocatalysis for the synthesis of pharmaceuticals and pharmaceutical intermediates. *Bioorganic & Medicinal Chemistry*. 26(7), 1275-1284.
33. L. Wen, K. Huang, Y. Zheng, J. Fang, S.M. Kondengaden, P.G. (2016). Two-step enzymatic synthesis of 6-deoxy-l-psicose. *Tetrahedron Letters*. 57(34), 3819-3822.
34. T. Li, J. Liang, A. Ambrogelly, T. Brennan, G. Gloor, G. Huisman, J. Lalonde, A. Lekhal, B. Mijts, S. Muley, L. Newman, M. Tobin, G. Wong, A. Zaks†, X. Zhang (2012). Efficient, chemoenzymatic process for manufacture of the boceprevir bicyclic [3.1.0] proline intermediate based on amine oxidase-catalyzed desymmetrization. *Journal of the American Chemical Society*. 134(14), 6467-6472
35. V. Köhler, K.R. Bailey, A. Znabet, J. Raftery, M. Helliwell, N.J. Turner (2010). Enantioselective biocatalytic oxidative desymmetrization of substituted pyrrolidines. *Angewandte*. 49(12), 2182-2184

36. R.N. Patel (2008): Synthesis of chiral pharmaceutical intermediates by biocatalysis. *Coordination Chemistry Reviews*. 252 (5-7), 659-701.
37. C. Schnepeland, N. Sewald (2017). Enzymatic Halogenation: A Timely Strategy for Regioselective C-H Activation. *Chemistry Europe Journal*. 23(50), 12064–12086.
38. A. M. Klibanov (2001). Improving enzymes by using them in organic solvents. *Nature*. 409, 241-246.
39. V. Stepankova, S. Bidmanova, T. Koudelakova, Z. Prokop, R. Chaloupkova, J. Damborsky (2013). Strategies for Stabilization of Enzymes in Organic Solvents. *ACS Catalysis*. 3(12), 2823–2836
40. G. Kirchner, M.P. Scollar, A.M. Klibanov (1985). Resolution of racemic mixtures via lipase catalysis in organic solvents. *Journal of the American Chemical Society*. 107(24), 7072-7076.
41. R. Siedentop and K. Rosenthal (2022). Industrially Relevant Enzyme Cascades for Drug Synthesis and Their Ecological Assessment. *International Journal of Molecular Sciences*. 23(7), 3605
42. J. Carro, E. Fernandez-Fueyo, C. Fernández-Alonso, J. Cañada, R. Ullrich, M. Hofrichter, M. Alcalde, P. Ferreira, A.T. Martínez (2018). Self-sustained enzymatic cascade for the production of 2,5-furandicarboxylic acid from 5-methoxymethylfurfural. *Biotechnology for Biofuels*. 11(86).
43. U. T. Bornscheuer, G. W. Huisman, R. J. Kazlauskas, S. Lutz, J. C. Moore & K. Robins (2012). Engineering the third wave of biocatalysis. *Nature*. 485(7397),185-194.
44. Uwe T. Bornscheuer (2017): The fourth wave of biocatalysis is approaching. *The Royal Society*. 376(2110).

45. I. Zachos, C. Nowak, V. Sieber (2019). Biomimetic cofactors and methods for their recycling. *Current Opinion in Chemical Biology*. 49, 59-66.
46. A. Basso, S. Serban (2019). Industrial applications of immobilized enzymes - A review. *Molecular Catalysis*. 479, 110607
47. C. Garcia-Galan, Á. Berenguer-Murcia, R. Fernandez-Lafuente, R.C. Rodrigues (2011). Potential of Different Enzyme Immobilization Strategies to Improve Enzyme Performance. *Advanced Synthesis And Catalysis*. 353(16), 2885-2904
48. R. DiCosimo, J. McAuliffe, A. J. Poulouse, G. Bohlmannb (2013). Industrial use of immobilized enzymes. *Chemical Society Reviews*. 42(15), 6437-6474
49. H.J. Federsel, T.S. Moody, S.J.C. Taylor (2021): Recent Trends in Enzyme Immobilization - Concepts for Expanding the Biocatalysis Toolbox. *Molecules*. 26(9), 2822
50. T. Tosa, T. Mori, N. Fuse, I. Chibata (1967): Studies on continuous enzyme reactions. Preparation of a DEAE-sephadex–aminoacylase column and continuous optical resolution of acyl-DL-amino acids. *Biotechnology & Bioengineering*. 9(4).
51. J. Chapman, A.E. Ismail, C.Z. Dinu (2018) Industrial Applications of Enzymes: Recent Advances, Techniques, and Outlooks. *Catalysts*. 8(6), 238.
52. A.C. Lustosa de Melo Carvalho, T. de Sousa Fonseca, M.C. de Mattos, M. da Conceição Ferreira de Oliveira, T. Leda Gomes de Lemos, F. Molinari, D. Romano, I. Serra (2015). Recent Advances in Lipase-Mediated Preparation of Pharmaceuticals and Their Intermediates. *International Journal of Molecular Sciences*. 16(12), 29682–29716.

53. C.T. Tsai, A.S. Meyer (2014). Enzymatic Cellulose Hydrolysis: Enzyme Reusability and Visualization of β -Glucosidase Immobilized in Calcium Alginate. *Molecules*. 19(12), 19390-19406
54. M. Hall (2021). Enzymatic strategies for asymmetric synthesis. *RSC Chemical Biology*. 2, 958-989
55. V. Resch, J.H. Schrittwieser, E. Siirola, W. Kroutil (2011). Novel carbon-carbon bond formations for biocatalysis. *Current Opinion on Biotechnology*. 22(6), 793-799
56. J. Dong, E. Fernández-Fueyo, F. Hollmann, C.E. Paul, M. Pesic, S. Schmidt, Y. Wang, S. Younes, W. Zhang (2018). Biocatalytic Oxidation Reactions: A Chemist's Perspective. *Angewandte*. 57(30), 6238-9261
57. V. F. Batista, J.L. Galman, D.C.G.A. Pinto, A.M.S. Silva, N.J. Turner (2018). Monoamine Oxidase: Tunable Activity for Amine Resolution and Functionalization. *ACS Catalytyst*. 8(12), 11889–11907
58. D. Ghislieri, A.P. Green, M. Pontini, S.C. Willies, I. Rowles, A. Frank, G. Grogan, N.J. Turner (2013). Engineering an Enantioselective Amine Oxidase for the Synthesis of Pharmaceutical Building Blocks and Alkaloid Natural Products. *Journal of American Society*. 135(29), 10863–10869
59. A. Boffi, G. Favero, R. Federico, A. Macone, R. Antiochia, C. Tortolini, G. Sanz3, F. Mazzei (2015). Amine oxidase-based biosensors for spermine and spermidine determination. *Analytical and Bioanalytical Chemistry*. 407(4):1131-7
60. E. Bonaiuto, M. Magro, D. Baratella, P. Jakubec, E. Sconcerle, M. Terzo, G. Miotto, A. Macone, E. Agostinelli, S. Fasolato, R. Venerando, G. Salviulo, O. Malina, R. Zboril, F. Vianello (2016): Ternary Hybrid γ -Fe₂O₃/Cr(VI)/Amine Oxidase Nanostructure for

- Electrochemical Sensing: Application for Polyamine Detection in Tumor Tissue. *Chemistry*. 22(20), 6846-6852
61. K. Bhagvat, H. Blaschko, D. Richter (1939). Amine Oxidase. *Biochemical Journal*. 33(8), 1338–1341
 62. B.J. Brazeau, B.J. Johnson, C.M. Wilmot (2004) Copper-containing amine oxidases. Biogenesis and catalysis; a structural perspective. *Archives of Biochemistry and Biophysics*. 428(1), 22-31
 63. G. Rea, O. Metoui, A. Infantino, R. Federico, R. Angelini (2002). Copper Amine Oxidase Expression in Defense Responses to Wounding and *Ascochyta rabiei* Invasion. *Plant Physiology*, 128(3), 865-875
 64. M.P. Campestre; C.D. Bordenave; A.C. Origone; A.B. Menendez; O.A. Ruiz; A.A. Rodriguez; S.J. Maiale (2011). Polyamine catabolism is involved in response to salt stress in soybean hypocotyls. *Journal of Plant Physiology*. 128, 1234-1240.
 65. S. Vakal, S. Jalkanen, K.M. Dahlström, and T.A. Salminen (2020). Human Copper-Containing Amine Oxidases in Drug Design and Development. *Molecules*. 25(6), 1293
 66. L. Maintz, V. Schwarzer, T. Bieber, K. van der Ven, N. Novak (2008). Effects of histamine and diamine oxidase activities on pregnancy: A critical review. *Human Reproduction Update*. 14(5), 485-495
 67. B.J. Brazeau, B.J. Johnson, C.M. Wilmot (2004): Copper-containing amine oxidases. Biogenesis and catalysis; a structural perspective. *Archives of Biochemistry and Biophysics*. 428(1), 22-31
 68. A. J. Tipping, M.J. McPherson (1995). Cloning and molecular analysis of pea seedling copper amine oxidase. *The Journal of Biological Chemistry*. 270(28), 16939-16946

69. M. Lunelli, M.L. Di Paolo, M. Biadene, V. Calderone, R. Battistutta, M. Scarpa, A. Rigo, G. Zanotti (2005). Crystal Structure of Amine Oxidase from Bovine Serum. *Journal of Molecular Biology*. 346(4), 991-1004
70. S.Z. Moosavi-Nejad, M. Rezaei-Tavirani, A. Padiglia, G. Floris, A.-A. Moosavi-Movahedi: Amine oxidase from lentil seedlings: Energetic domains and effect of temperature on activity. *The Protein Journal*. 20 (5), 405-411
71. M. Šebela, L. Luhov, I. Frébort, H.G. Faulhammer, S. Hirota, L. Zajoncová, V. Stučka, P. Peč (1998): Analysis of the active sites of copper/topa quinone-containing amine oxidases from *Lathyrus odoratus* and *L. sativus* seedlings. *Phytochemical Analysis*. 9(5), 211-222
72. S.M. Janes, D. Mu, D. Wemmer, A.J. Smith, S. Kaur, D. Maltby, A.L. Burligame, J.P. Klinman (1990). A new redox cofactor in eukaryotic enzymes: 6-Hydroxydopa at the active site of bovine serum amine oxidase. *Science*. 248(4958), 981-987
73. V. Klema, C. Wilmot (2012). The Role of Protein Crystallography in Defining the Mechanisms of Biogenesis and Catalysis in Copper Amine Oxidase. *International Journal of Molecular Science*. 13(5), 5375-5405
74. T. Murakawa, S. Baba, Y. Kawano, H. Hayashi, T. Yano, T. Kumasaka, M. Yamamoto, K. Tanizawa, T. Okajima (2019). In crystallo thermodynamic analysis of conformational change of the topaquinone cofactor in bacterial copper amine oxidase. *Proceedings of the National Academy of Sciences*. 116(1), 135-140



75. A. Padiglia, A. Cogoni, G. Floris (1991). Characterization of amine oxidases from pisum, lens, Lathyrus and Cicer. *Phytochemistry*. 30(12), 3895-3897
76. P. Pietrangeli, R. Federico, B. Mondovì, L. Morpurgo (2007). Substrate specificity of copper-containing amine oxidases. *Journal of Inorganic Biochemistry*. 101(7), 997-1004
77. B. Mondovì, W.A. Fogel, R. Federico, C. Calinescu, M.A. Mateescu, A.C. Rosa, E. Masini (2013). Effects of amine oxidases in allergic and histamine-mediated conditions. *Recent patents on inflammation and allergy drug discovery*. 7(1), 20-34
78. C. Calinescu, B. Mondovi, R. Federico, P. Ispas-Szabo, M.A. Mateescu (2012). Carboxymethyl starch : Chitosan monolithic matrices containing diamine oxidase and catalase for intestinal delivery. *International Journal of Pharmaceutics*. 428(1-2), 48-56
79. P. Pietrangeli, S. Nocera, P. Fattibene, X. Wang, B. Mondovì, L. Morpurgo (2000). Modulation of Bovine Serum Amine Oxidase Activity by Hydrogen Peroxide. *Biochemical and Biophysical Research Communication*. 267(1), 174-178
80. P. Pietrangeli, S. Nocera, R. Federico, B. Mondovì, L. Morpurgo (2004). Inactivation of copper-containing amine oxidases by turnover products. *European Journal of Biochemistry*. 271(1), 146-152
81. S. Longu, A. Mura, A. Padiglia, R. Medda, G. Floris (2005). Mechanism-based inactivators of plant copper/quinone containing amine oxidases. *Phytochemistry*. 66(15),1751-1758
82. J. Dadamio, M. Van Tornout, S. Van den Velde, R. Federico, C. Dekeyser, M. Quiryneen (2011). A novel and visual test for oral malodour: first observations. *Journal of breath research*. 5(4), 046003

83. C. Calinescu, R. Federico, B. Mondovi, M.A. Mateescu (2010). Zymographic assay of plant diamine oxidase on entrapped peroxidase polyacrylamide gel electrophoresis. A study of stability to proteolysis. *Analytical and Bioanalytical Chemistry*. 396(3), 1281–1290
84. M. Di Fusco, R. Federico, A. Boffi, A. Macone, G. Favero, F. Mazzei (2011). Characterization and application of a diamine oxidase from *Lathyrus sativus* as component of an electrochemical biosensor for the determination of biogenic amines in wine and beer. *Analytical and Bioanalytical Chemistry*. 401(2), 707-716
85. A. Bonamore, L. Calisti, A. Calcaterra, O.H. Ismail, M. Gargano, I. D'Acquarica, B. Botta, A. Boffi, A. Macone (2016). A Novel Enzymatic Strategy for the Synthesis of Substituted Tetrahydroisoquinolines. *Chemistry Select*. 1(8), 1525-1528
86. P. Pietrangeli, S. Nocera, B. Mondovì, L. Morpurgo (2003). Is the catalytic mechanism of bacteria, plant, and mammal copper-TPQ amine oxidases identical? *Biochim. Biophys. Acta*. 1647(1-2), 152-156
87. B.R. Lichman, E.D. Lamming, T. Pesnot, J.M. Smith, H.C. Hailes, Ward. One-pot triangular chemoenzymatic cascades for the syntheses of chiral alkaloids from dopamine. *Green Chem*. 17, 852–855.
88. N. Gorgas, A. Ilic, K. Kirchner (2019). Chemoselective transfer hydrogenation of aldehydes in aqueous media catalyzed by a well-defined iron(II) hydride complex. *Monatsh. Chem*. 150, 121–126.
89. W. Wang, S. Wang, X. Qin, J. Li (2005). Reaction of Aldehydes and Pyrazolones in the Presence of Sodium Dodecyl Sulfate in Aqueous Media. *Synth. Commun*. 35, 263–1269

90. S. Kobayashi, T. Endo, T. Yoshino, U. Schneider, M. Ueno. Allylation Reactions of Aldehydes with Allylboronates in Aqueous Media: Unique Reactivity and Selectivity that are Only Observed in the Presence of Water. *Chemistry - An Asian Journal*. 8, 2033–2045.
91. T. Pesnot; M.C. Gershater; J.M. Ward; H.C. Hailes. Phosphate mediated biomimetic synthesis of tetrahydroisoquinoline alkaloids. *Chemical Communications*. 47, 3242.
92. H. Ogino, H. Ishikawa (2001). Enzymes which are stable in the presence of organic solvents. *Journal of Bioscience and Bioengineering* 91(2), 109-116

Article

Biocatalytic Production of Aldehydes: Exploring the Potential of *Lathyrus cicera* Amine Oxidase

 Elisa Di Fabio ¹, Alessio Incocciati ¹ , Alberto Boffi ^{1,2}, Alessandra Bonamore ^{1,*} and Alberto Macone ^{1,*} 
¹ Department of Biochemical Sciences “Alessandro Rossi Fanelli”, Sapienza University of Rome, Piazzale Aldo Moro 5, 00185 Rome, Italy; elisa.difabio@uniroma1.it (E.D.F.); incocciati.1750499@studenti.uniroma1.it (A.I.); alberto.boffi@uniroma1.it (A.B.)

² Center for Life Nano Science@Sapienza, Istituto Italiano Di Tecnologia, V.le Regina Elena 291, 00161 Rome, Italy

* Correspondence: alessandra.bonamore@uniroma1.it (A.B.); alberto.macone@uniroma1.it (A.M.)

Abstract: Aldehydes are a class of carbonyl compounds widely used as intermediates in the pharmaceutical, cosmetic and food industries. To date, there are few fully enzymatic methods for synthesizing these highly reactive chemicals. In the present work, we explore the biocatalytic potential of an amino oxidase extracted from the etiolated shoots of *Lathyrus cicera* for the synthesis of value-added aldehydes, starting from the corresponding primary amines. In this frame, we have developed a completely chromatography-free purification protocol based on crossflow ultrafiltration, which makes the production of this enzyme easily scalable. Furthermore, we determined the kinetic parameters of the amine oxidase toward 20 differently substituted aliphatic and aromatic primary amines, and we developed a biocatalytic process for their conversion into the corresponding aldehydes. The reaction occurs in aqueous media at neutral pH in the presence of catalase, which removes the hydrogen peroxide produced during the reaction itself, contributing to the recycling of oxygen. A high conversion (>95%) was achieved within 3 h for all the tested compounds.

Keywords: aldehydes; primary amines; copper-containing amine oxidase; crossflow ultrafiltration; biocatalysis; oxidative deamination; *Lathyrus cicera*



Citation: Di Fabio, E.; Incocciati, A.; Boffi, A.; Bonamore, A.; Macone, A. Biocatalytic Production of Aldehydes: Exploring the Potential of *Lathyrus cicera* Amine Oxidase. *Biomolecules* **2021**, *11*, 1540. <https://doi.org/10.3390/biom11101540>

Academic Editor: Vladimir N. Uversky

Received: 6 September 2021
Accepted: 16 October 2021
Published: 18 October 2021

Publisher’s Note: MDPI stays neutral with regard to jurisdictional claims in published maps and institutional affiliations.



Copyright: © 2021 by the authors. Licensee MDPI, Basel, Switzerland. This article is an open access article distributed under the terms and conditions of the Creative Commons Attribution (CC BY) license (<https://creativecommons.org/licenses/by/4.0/>).

1. Introduction

Aldehydes are extremely interesting chemical compounds due to their numerous industrial applications. The high reactivity of the carbonyl group of aldehydes makes them versatile feedstocks for the synthesis of resins, dyes, pharmaceutical intermediates through carbonylation, condensation, hydrocyanation, transamination, and α -alkylation [1–5]. They can also be used as flavors and fragrances in the cosmetic and food industry [6–8]. Many aldehydes, especially those used by the perfume industry, are extracted from natural sources. However, this procedure is typically limited by their intrinsic lability and low bioaccumulation. Given the high-value applications and large markets for several aldehydes and considering the high demand for “natural” labeled compounds, research on their green and sustainable synthesis is taking center stage [9–11]. In this frame, biocatalysis occupies a privileged place, being a valid alternative compared to the conventional physical (extraction) or chemical synthetic routes. To date, a variety of engineered microorganisms and isolated enzymes for the de novo biosynthesis of aldehydes have been described and characterized [12,13]. Although microbial aldehyde biosynthetic pathways are well known, their production is typically hindered by their endogenous reduction to the corresponding alcohols [14]. Even if it is possible to limit the production of these unwanted byproducts through microbial engineering (reduced aromatic aldehyde reduction or RARE strain) [15], the resulting accumulation of aldehydes is generally toxic, as they covalently modify proteins, nucleic acids, and coenzymes, affecting the survival of the microorganism itself [16].

A valid alternative to microbial factories is represented by isolated enzymes, both extracted from natural sources and obtained by recombinant protein expression technology [17–19].

Aldehydes can be enzymatically synthesized by oxidation of the corresponding primary alcohols [20] and primary amines [21] or by reduction of the corresponding carboxylic acids [22–24]. Aldehyde synthesis starting from the corresponding alcohols can be performed by alcohol oxidases, which are typically active on a broad range of alcohols, such as primary and secondary alcohols, allylic and aryl alcohols, sterols, and carbohydrates [25,26]. However, the major drawback of these enzymes is the overoxidation of the aldehydes to carboxylic acids. In addition, they are not active on functionalized β -ethyl alcohols [27]. Conversely, alcohol dehydrogenases require expensive cofactors and are active on a limited selection of substrates [28]. Aldehydes can be also obtained starting from the corresponding carboxylic acids through the action of broad substrate specificity carboxylic acid reductases [29,30]. However, enzymatic reduction of the carboxylic acids to the corresponding aldehydes is an energetically demanding reaction that requires the use of ATP as a co-substrate. In addition, this reaction is hard to control due to the further reduction of aldehydes to alcohols. Thus, in industrial syntheses, carboxylic acid reductases are typically coupled to other enzymes in domino processes to quickly carry out decarbonylation, reduction, or transamination of the newly synthesized aldehydes. A further way for the enzymatic synthesis of aldehydes is the oxidative deamination of the corresponding amines. From a biocatalysis point of view, this is still a rather unexplored field. To date, the enzymes capable of catalyzing this reaction, amine oxidases, have been mainly used in the development of biosensors [31,32]. More recently, plant diamine oxidases (DAO) are emerging as attractive biocatalysts for the one-step bioconversion of primary amines to the corresponding aldehydes. These enzymes, belonging to the family of copper-containing amine oxidases, catalyze the oxidative deamination of polyamines such as putrescine, cadaverine and spermidine, with the concomitant production of H_2O_2 . The production of hydrogen peroxide is physiologically involved in cell wall maturation during plant development as well as in defense mechanisms during pathogen invasion [33,34]. Unlike mammalian and prokaryotic DAOs, plant enzymes display higher chemical stability and turnover rate, making them attractive for biotransformations. To date, plant DAOs from various species have been purified to homogeneity and characterized, the best known and studied being those from *Leguminosae* sp [35,36]. However, until now, the use of these DAOs as biocatalysts has been little explored. Our research group used *Lathyrus cicera* diamine oxidase (LCAO) in a domino process for the synthesis of new non-natural benzylisoquinoline alkaloids [19]. In this frame, LCAO showed a relaxed substrate specificity, being active on four different β -substituted ethylamines. However, in this catalytic process, aldehydes did not accumulate as they were transient intermediates in the Pictet–Spengler condensation catalyzed by *T. flavum* noroclaurine synthase recombinantly expressed in *E. coli* [37].

In the present work, we have explored the biocatalytic potential of LCAO by developing a general method for the synthesis of pure aldehydes starting from differently substituted aliphatic and aromatic primary amines. The synthesis of these aldehydes is particularly interesting for several reasons: (i) they are not commercially available; (ii) some of them are biogenic aldehydes that can be used as pure standards for measurements in human and animal tissues; (iii) they can be used in domino reactions as substrates of other enzymes to produce intermediates of active pharmaceutical ingredients [38]. In addition, to make the whole process fast, easy, and scalable, we developed a new chromatography-free purification protocol of LCAO extracted from *Lathyrus cicera* seedlings.

2. Materials and Methods

2.1. Chemicals

Reagents and solvents obtained from commercial suppliers were used without further purification. All chemicals were purchased from Sigma-Aldrich Srl, Milan, Italy.

2.2. LCAO Chromatography-Free Purification

Lathyrus cicera seeds (300 g) were soaked for 12 h in tap water and then spread in a monolayer on trays lined with moistened filter paper. The trays were covered tightly with aluminum foils. The germinated seeds were watered every 2 days with 100 mL of tap water. After 10 days, the etiolated seedlings (about 500 g) were harvested above the roots, cut in small pieces (about 2 mm) and washed with 1 L of ice-cold deionized water for 15 min. After washing, the ground plant sample was kept in 1.5 L of ice-cold extraction buffer (50 mM pH 5.5 phosphate buffer containing 0.3 M NaCl) for 30 min and then filtered through a 20 Micron Nylon Mesh and squeezed by hand to remove the debris. To allow quantitative recovery, the pellet was extracted again as described above and the resulting crude mixtures were combined. To remove insoluble material, the crude enzyme extract (3 L) was clarified by disposable Sartolab[®] Vacuum Filters System (Polyethersulfone, 0.22 µm) using 30 g of Sartoclear Dynamics[®] Lab Filter Aid (Sartorius) containing highly pure diatomaceous earth (Celpure[®] C300—pharmaceutical grade) pre-wetted with ultrapure water. The buffer was exchanged with 20 mM phosphate buffer pH 6.5 through diafiltration by means of crossflow ultrafiltration using a single Vivaflow 200 module (Sartorius) with a 50 kDa cutoff, coupled to a Masterflex L/S pump system. The same device was also used to concentrate the enzyme extract to 100 mL. The feed flow rate was set to 40 mL/min both in concentration and diafiltration modes. As the last purification step, the sample was subjected to heat treatment at 65 °C for 15 min. Denatured proteins were removed by centrifugation (12,000 rpm, 20 min, 20 °C). All purification steps were monitored by SDS-PAGE (12% SDS) and measuring the enzyme's specific activity. Enzyme activity (LCAO Units) was used to determine the recovery after each purification step. Total soluble protein concentration was determined using the method of Bradford with bovine serum albumin as a standard. LCAO content throughout the purification procedure was also monitored by high-performance size exclusion chromatography (HP-SEC). HP-SEC was performed using an Agilent Infinity 1260 HPLC apparatus equipped with a UV detector. Separation was carried out using an Agilent AdvanceBio SEC 300 Å, 7.8 × 150 mm, 2.7 µm, LC column connected to an AdvanceBio SEC 300 Å, 7.8 × 50 mm, 2.7 µm, LC guard column. Isocratic analysis was carried out with 20 mM phosphate buffer pH 6.5 containing 150 mM NaCl as mobile phase. The flow rate was 0.7 mL/min over an elution window of 7 min. Protein elution was followed using UV detection at 220 nm and 445 nm (TPQ-phenylhydrazine adduct).

2.3. LCAO Activity

LCAO activity was assayed by a coupled diamine oxidase/peroxidase spectrophotometric test at 25 °C with 10 mM putrescine in 20 mM phosphate buffer at pH 6, 7, and 8 in the presence of 150 nM enzyme. H₂O₂ produced by LCAO was monitored following horse radish peroxidase catalyzed coupling of 4-aminoantipyrine (AAP) and sodium 3,5-dichloro-2-hydroxybenzenesulfonate (DCHBS) as oxygen acceptor. The enzymatic activity, which led to the formation of colored product, was measured at 515 nm for 60 s and expressed as U/mL per mg protein. Initial rates of reaction at the various substrate concentrations were determined at three different pH values (6, 7, 8), and the kinetic parameters were calculated by non-linear regression fitting of the data to the Michaelis–Menten equation $V = V_{max}(S)/(K_m + (S))$. All curve fitting was carried out using Kaleidagraph software (Synergy Software, Reading, PA, USA).

2.4. Enzymatic Synthesis of Aldehydes

The biocatalytic synthesis of the aldehydes was carried out starting from the corresponding primary amines in the presence of LCAO. Twenty different substituted ethyl amines were tested. A solution of 5 mM of amine substrate was prepared in 50 mM HEPES buffer pH 7.0 in the presence of 250 U/mL of catalase from bovine liver (Sigma-Aldrich) to a final volume of 10 mL. LCAO was added to a final concentration of 2 U/mL and the reaction was carried out at room temperature under stirring. To ensure constant cat-

alytic efficiency, the enzyme is supplied (5 U) at regular time intervals (30 min). The substrate consumption was monitored by HPLC or GC/MS, whereas aldehyde formation was monitored by purpald[®] assay.

Aromatic amine consumption was followed by HPLC using an Agilent Infinity 1260 HPLC apparatus equipped with UV and fluorometric detectors. The separation was carried out using a Halo C18 AQ column (3 × 150 mm, 2.7 μm) connected to the C18 AQ guard column (3 × 5 mm, 2.7 μm). The elution was performed at a flow rate of 0.8 mL/min, with solvent A (0.1% trifluoroacetic acid in water) and solvent B (0.1% trifluoroacetic acid in acetonitrile). The mobile phase was linearly increased from 0% to 100% of solvent B in 15 min and then run isocratically for 5 min. Afterward, buffer A was reintroduced in the mobile phase up to 100%, and the column was allowed to equilibrate for 10 min. The elution profile of aromatic amines was monitored by setting the UV detector at 280 nm.

Aliphatic amine consumption was followed by GC/MS. Derivatization with ethyl chloroformate (ECF) was conducted in a single step by adding to 0.1 mL of the reaction mixture 20 μL of ECF dissolved in 0.5 mL of dichloromethane. The biphasic system was stirred vigorously for 2 min, saturated with NaCl and extracted sequentially with 1 mL of ethyl ether and 1 mL of ethyl acetate. The organic extracts were combined, dried under nitrogen flow, resuspended in dichloromethane, and analyzed by GC/MS. GC/MS analyses were performed with an Agilent 6850A gas chromatograph coupled to a 5973N quadrupole mass selective detector (Agilent Technologies, Palo Alto, CA, USA). Chromatographic separations were carried out with an Agilent HP-5ms fused silica capillary column (30 m × 0.25 mm id) coated with 5% phenyl-95% dimethylpolysiloxane (film thickness 0.25 μm) as stationary phase. Injection mode: splitless at a temperature of 280 °C. Column temperature program: 100 °C for 2 min and then to 300 °C at a rate of 15 °C/min and held for 5 min. The carrier gas was helium at a constant flow of 1.0 mL/min. The spectra were obtained in the electron impact mode at 70 eV ionization energy; ion source 280 °C; ion source vacuum 10⁻⁵ Torr. Mass spectrometric analysis was performed in the range m/z 50 to 500 at a rate of 0.42 scans s⁻¹.

2.5. Purpald[®] Colorimetric Assay

Substrate conversion efficiency was calculated through the reaction of the newly formed aldehyde with 4-Amino-5-hydrazino-1,2,4-triazole-3-thiol (purpald[®]), a reagent for the colorimetric detection of aldehydes. A volume of 50 μL of the reaction mix were added to 1 mL NaOH 2 M containing 5 mg of purpald[®], vortexed for 5 min and read at 550 nm after 15 min. The calibration was carried out using phenylacetaldehyde commercial standard in the concentration range 0.28–7 mM.

3. Results and Discussion

3.1. LCAO Purification

In the present paper, we have developed a new protocol for the purification of LCAO, which has significant advantages over the generally used one, as it is chromatography-free, fast, and easily scalable. Sprouts of *L. cicera* were selected because they show higher specific activity than other common Leguminosae, such as *Pisum sativum*, *Lens culinaris*, and *Phaseolus vulgaris* (data not shown). Recently, our research group has developed a protocol that involves the combined use of diatomaceous earth filter aid and tangential ultrafiltration for the purification of recombinant proteins [39]. Now, for the first time, these techniques are being used on plant material for the purification of LCAO. According to this purification strategy, the crude plant extract is vacuum filtered using diatomaceous earth as a filter aid. This step replaces the classic centrifugation steps which are time-consuming and limit the amount of plant material that can be processed. As shown in Table 1, this allows an almost total recovery of the enzymatic activity with a concomitant increase in specific activity. The subsequent diafiltration/ultrafiltration step has a dual objective: (i) exchange the buffer, bringing the pH and ionic strength values to those that guarantee greater stability of the enzyme and, (ii) concentrate the enzyme itself. In addition, in

this case, all the enzymatic activity is maintained and there is a 12-fold increase in the specific activity. Tangential ultrafiltration replaces classical dialysis and concentration steps, making the whole process fast and efficient. This process can be easily scaled up using suitable crossflow systems equipped with cassettes with larger membrane areas, able to filter larger volumes (up to thousands of liters). Considering that tangential flow filtration devices and cassettes can be cleaned and reused several times, the system is also economical. Since the stability of the enzyme is not affected by temperatures up to 60 °C (Figure 1A), the last purification step consists of a mild heat treatment, which leads to a 22-fold increase in specific activity, comparable to that obtained by classical chromatographic purification.

Table 1. Purification procedure for *Lathyrus cicera* amine oxidase. The recovery (%) was determined by evaluating the total activity (enzyme units) after each purification step.

Purification Step	Total Activity (Units)	Total Protein (mg)	Specific Activity (units × mg ⁻¹ Protein)	Recovery (%)	Purification (-fold)
Crude extract	2630	2706	0.97	100	1
Filtration on Celpure® C300	2590	1546	1.68	98.47	1.73
Vivaflow200 diafiltration/ ultrafiltration	2606	217	12.01	99.08	12.38
Heat treatment (65 °C)	2100	97.3	21.58	79.85	22.24

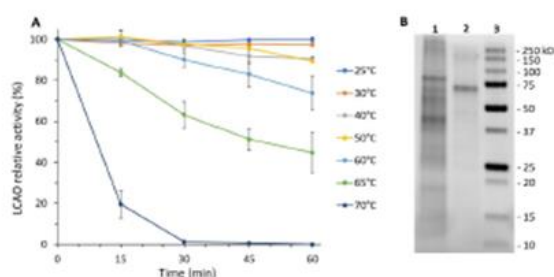
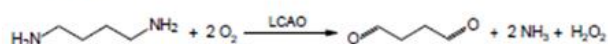


Figure 1. Heat treatment was used as the last step of LCAO purification. (A) Thermal stability of LCAO in the range 25–70 °C. (B) SDS-PAGE of LCAO after the heat treatment at 65 °C for 15 min. Lane 1: insoluble fraction; lane 2: soluble fraction; lane 3: protein ladder.

As demonstrated by SDS-PAGE and HP-SEC analysis (Figures 1B, S1 and S2) LCAO is highly purified (>95%). The whole purification procedure takes about 7 h compared to the 16 h needed for the previously used protocol. The purified protein is stable for up to 6 months, sterile filtered at 4 °C (Figure S3).

3.2. Exploring LCAO Activity toward Aliphatic and Aromatic Primary Amines

LCAO typically uses as a substrate of choice small polyamines such as putrescine, cadaverine, and spermidine, which are oxidatively deaminated with the production of hydrogen peroxide (Scheme 1).



Scheme 1. LCAO catalyzed conversion of putrescine into the corresponding aldehyde.

Similarly, to other copper amine oxidases, it has been reported that this enzyme is also able to accept substrates of a different nature (e.g., histamine, tyramine, benzylamine, etc.) although with lower catalytic performances [36,40]. We, therefore, decided to test the enzymatic activity of LCAO against a larger number of substrates to obtain a variety of aldehydes that may be used as intermediates for the synthesis of molecules with potentially interesting pharmacological profiles. Since this biocatalytic process occurs in aqueous media, aldehydes can be actually used in domino processes by adding other enzymes that use them as substrates [19,40,41] or in other organic transformations that can be carried out directly in water [42–44]. In this study, we tested the activity of LCAO toward different classes of commercially available primary amines: 14 substituted β -ethylamines, three substituted γ -propylamines and three linear amines (Table 2 and Figure S6).

Table 2. Steady-state kinetic parameters for LCAO-catalyzed oxidative deamination of primary amines.

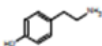
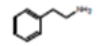
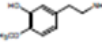
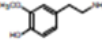
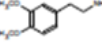
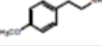
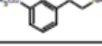




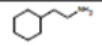
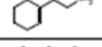
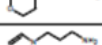


n.	Structure	pH 7				pH 8			
		K_M (mM)	k_{cat} (s^{-1})	k_{cat}/K_M ($M^{-1}s^{-1}$)	Relative Activity (%)	K_M (mM)	k_{cat} (s^{-1})	k_{cat}/K_M ($M^{-1}s^{-1}$)	Relative Activity (%)
1a		0.60	29.24	49.00	100	0.49	13.30	26.94	100
2a		1.20	18.35	14.25	62.8	0.60	9.16	15.92	68.9
3a		1.58	0.27	0.21	0.9	1.66	0.17	0.10	1.3
4a		1.31	2.00	1.53	6.8	1.35	0.96	0.69	7.2
5a		1.00	1.54	1.53	5.3	1.80	2.31	1.26	17.4
6a		5.37	2.53	0.45	8.7	5.60	4.02	0.70	30.2
7a		0.47	6.20	13.04	21.2	1.20	1.80	1.48	13.5
8a		3.83	2.95	0.77	10.1	1.44	1.21	0.78	9.1
9a		ND	ND	0.49	ND	ND	ND	ND	ND
10a		3.38	10.15	3.15	34.7	1.30	1.98	1.45	14.9
11a		0.42	5.53	0.79	18.9	0.70	0.73	0.23	5.5
12a		6.46	5.63	0.72	19.3	0.75	0.17	0.41	1.3
13a		1.44	1.06	0.79	3.6	0.70	0.29	0.80	2.2
14a		1.90	1.47	12.93	5.0	0.23	0.19	1.04	1.4
15a		17.00	1.27	0.07	4.3	ND	ND	0.00	ND
16a		0.61	2.77	4.92	9.5	0.25	0.40	1.60	3.0

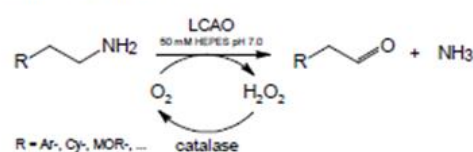
Table 2. Cont.

n.	Structure	pH 7				pH 8			
		K_M (mM)	k_{cat} (s^{-1})	k_{cat}/K_M ($M^{-1}s^{-1}$)	Relative Activity (%)	K_M (mM)	k_{cat} (s^{-1})	k_{cat}/K_M ($M^{-1}s^{-1}$)	Relative Activity (%)
17a		2.30	5.08	2.14	17.4	ND	ND	0.46	0.0
18a		0.23	1.27	2.05	4.3	0.11	2.20	2.19	16.5
19a		8.80	17.9	1.29	61.2	0.33	0.73	5.47	5.5
20a		2.59	3.51	5.35	12.0	2.12	11.8	20.00	88.7

LCAO kinetic parameters were determined at pH 6, 7, and 8. The enzyme is inactive at pH 6, while it is active at pH 7 on all the tested substrates with the exception of compound **9a**, which can be considered a poor substrate. This molecule is processed slowly by the enzyme, and it was not possible to accurately measure the kinetic parameters. This could be probably due to the presence of the hydroxyl groups in the catechol moiety. The enzyme is active in the absence of substituents on the aromatic ring (**2a**), in the presence of substituents in the para position (**1a**, **10a**), or when the catechol -OH are singly or both methylated (**3a–9a**). Besides phenylethylamines, LCAO can also transform non-aromatic or heterocyclic ethyl- or propylamines (**11a–17a**) as well as linear amines (**18a–20a**). Conversely, the enzyme is generally less performing at pH 8. At this pH value, compounds **9a**, **15a** and **17a** are not transformed at all. To date, LCAO crystal structure is not yet available, and it is challenging to establish the structural determinants of the interaction between the enzyme and these unnatural substrates. Although the catalytic performance of LCAO toward all the tested amino substrates is lower than that measured for putrescine, the natural substrate ($k_{cat} = 262 s^{-1}$ and $K_M = 2.7 \times 10^{-4} M$) [36], the kinetic data indicate that this enzyme can actually be used for synthetic purposes.

3.3. Biocatalytic Production of Aldehydes

Considering that LCAO shows the best catalytic performance at pH 7, the synthesis of the aldehydes was carried out at this pH value starting from the corresponding primary amines (Scheme 2).



Scheme 2. Biocatalytic conversion of primary amines (compounds **1a–20a**) into the corresponding aldehydes (compounds **1b–20b**) in the presence of LCAO and catalase.

In the biocatalytic production of aldehydes, LCAO is coupled with catalase, which decomposes hydrogen peroxide, a co-product of the reaction, to water and oxygen. Hydrogen peroxide must be quickly removed from the reaction medium because it can inactivate the proteins and oxidize the substrates and the reaction products. Thus, catalase preserves LCAO activity, while contributing to the recycling of oxygen which is co-substrate of the reaction.

The production of the aldehydes was monitored by the purpald[®] colorimetric assay that, unlike the time-consuming GC and HPLC methods, is typically fast, while preserving high specificity and sensitivity. The assay was set up using the commercially available phenylacetaldehyde as a standard (Figure S4). The reaction products were also character-

used by GC-MS by comparison with the fragmentation profiles of the NIST2017 database (Figure S8).

As shown in Table 3 (and Table S1), all the tested amides are almost completely converted into the corresponding aldehydes (10–200) in a time ranging from 0.5 to 1 h. The formation of byproducts, such as amine derivatives (stemming from the reaction between aldehydes and primary amines or ammoniac, which typically forms at pH 8–9), is not observed at pH 7.

Table 3. Conversion of the primary amides (a–h, 10a–20a) to the corresponding aldehydes (10–200).

a	Reaction Product	EC ₅₀ (Total) (μM)	Conversion (%)			
			0.5 h	1 h	2 h	3 h
10		25	100	100		
10a		25	100	100		
11		40	100	100	100	100
11a		40	100	100	100	100
12		40	100	100	100	100
12a		40	100	100	100	100
13		40	100	100	100	100
13a		40	100	100	100	100
14		40	100	100	100	100
14a		40	100	100	100	100
15		75	100	100	100	100
15a		75	100	100	100	100
16		40	100	100	100	100
16a		40	100	100	100	100
17		75	100	100	100	100
17a		75	100	100	100	100
18		40	100	100	100	100
18a		40	100	100	100	100
19		20	100	100		
19a		20	100	100		

The enzyme is efficient in the conversion of linear amides (compounds 10a and 20a), structurally similar to the natural substrate, and with para-substituted phenylethylamine (compounds 1a and 30a). For these compounds, the transformation occurs within an hour.

To ensure constant catalytic efficiency, the enzyme is supplied at regular time intervals (30 min). This is necessary because, over longer reaction times, the newly synthesized aldehydes may partially inactivate the enzyme. Considering the intrinsic reactivity and instability of aldehydes, this biosynthetic method is particularly suitable for their use as short-living intermediates in domino processes where the aldehydes can be quickly processed in enzymatic cascades [19,41]. However, to evaluate the scalability of the process, we applied the synthesis protocol described above to the conversion of a 10-fold amount of **2a** to the corresponding aldehyde. In addition, in this case, we had an almost total conversion. The extraction of aldehyde from the aqueous reaction media resulted in yield of isolated product of 43 mg (71.6%, purity > 95%) (Figure S7).

4. Conclusions

Aldehydes are extremely interesting chemical compounds for their numerous industrial applications. Considering the high demand for “naturally” synthesized aldehydes, especially in food and cosmetic industries as well as their use for pharmaceutical application, the development of a new green enzymatic protocol for their production is of great interest. In this study, we set up a fully enzymatic strategy for the synthesis of aldehydes by means of a plant extracted amine oxidase. We have shown that this enzyme has a broader substrate specificity than that known thus far, and it is able to catalyze the oxidative deamination of all the amines tested except for dopamine. Structural and site-specific mutagenesis studies will help to gain a deeper understanding of the structural determinants need for recognition of the substrate and its subsequent transformation. Despite an excellent substrate conversion (>95%), the synthesis of aldehydes is still limited to low milligram scale. However, the immobilization and/or modification of the enzyme surface to minimize aldehyde-enzyme interactions could make the scale-up of the process feasible. In addition, the chromatography-free LCAO purification protocol developed here will help make the overall synthetic process easy and cost-effective.

Supplementary Materials: The following are available online at <https://www.mdpi.com/article/10.3390/biom11101540/s1>, Figure S1: HP-SEC analysis of purified LCAO, Figure S2: UV spectrum of purified LCAO with or without phenylhydrazine, Figure S3: Overtime stability of sterile-filtered LCAO, stored at 4 °C, Figure S4: Purpald[®] reaction scheme and calibration plot using standard phenylacetaldehyde, Figure S5: electron impact (70 eV) mass spectra of compounds **1a–8a**, **10a–20a**, Figure S6: Kinetic plots of LCAO catalyzed deamination of compounds **1a–8a**, **10a–20a**, Figure S7: enzymatic synthesis of compound **2b**: HPLC and GC/MS analyses, Table S1: Conversion (%) of the amines **1a–8a**, **10a–20a** to the corresponding aldehydes **1b–8b**, **10b–20b**. Table S2: HPLC and GC/MS retention times of compounds **1a–8a**, **10a–20a**, **1b–8b**, **10b–20b**.

Author Contributions: Conceptualization, E.D.F., A.B. (Alessandra Bonamore), and A.M.; methodology, E.D.F. and A.L.; formal analysis, E.D.F.; investigation, E.D.F. and A.L.; data curation, E.D.F. and A.L.; writing—original draft preparation, E.D.F., A.M. and A.B. (Alessandra Bonamore); writing—review and editing, A.M., A.B. (Alessandra Bonamore) and A.B. (Alberto Boffi); supervision, A.B. (Alessandra Bonamore) and A.M.; project administration, A.B. (Alessandra Bonamore) and A.M.; funding acquisition, A.M. All authors have read and agreed to the published version of the manuscript.

Funding: This research was funded by Sapienza University of Rome, Ricerche Universitarie 2020, “Biocatalytic production of high value-added aldehydes”, protocol number RP120172A3B1AE3E.

Institutional Review Board Statement: Not applicable.

Informed Consent Statement: Not applicable.

Data Availability Statement: All data related to the manuscript are available in the manuscript and in the Supplementary Information in the form graphs, figures, and tables.

Acknowledgments: We thank Francesco Malatesta (Department of Biochemical Sciences “Alessandro Rossi Farelli”, Sapienza University of Rome) for invaluable assistance in the analysis of kinetic parameters.

Conflicts of Interest: The authors declare no conflict of interest.



Article

Immobilization of *Lathyrus cicera* Amine Oxidase on Magnetic Microparticles for Biocatalytic Applications

Elisa Di Fabio ¹, Antonia Iazzetti ^{2,3}, Alessio Incocciati ¹, Valentina Caseli ⁴, Giancarlo Fabrizi ²,
Alberto Boffi ^{1,4}, Alessandra Bonamore ^{1,*} and Alberto Macone ^{1,*}

¹ Department of Biochemical Sciences "Alessandro Rossi Fanelli", Sapienza University of Rome, Piazzale Aldo Moro 5, 00185 Rome, Italy; elisa.difabio@uniroma1.it (E.D.F.); alessio.incocciati@uniroma1.it (A.I.); alberto.boffi@uniroma1.it (A.B.)

² Department of Chemistry and Technology of Drugs, Sapienza University of Rome, Piazzale Aldo Moro 5, 00185 Rome, Italy; antonia.iazzetti@uniroma1.it (A.I.); giancarlo.fabrizi@uniroma1.it (G.F.)

³ Dipartimento di Scienze Biotechnologiche di Base, Cliniche Interventive e Perioperatorie, Università Cattolica del Sacro Cuore, L.go Francesco Vito 1, 00168 Rome, Italy

⁴ Center for Life Nano Science@Sapienza, Istituto Italiano Di Tecnologia, V.le Regina Elena 291, 00161 Rome, Italy; valentina.caseli@iit.it

* Correspondence: alessandra.bonamore@uniroma1.it (A.B.); alberto.macone@uniroma1.it (A.M.)

† These authors contributed equally to this work.



Citation: Di Fabio, E.; Iazzetti, A.; Incocciati, A.; Caseli, V.; Fabrizi, G.; Boffi, A.; Bonamore, A.; Macone, A. Immobilization of *Lathyrus cicera* Amine Oxidase on Magnetic Microparticles for Biocatalytic Applications. *Int. J. Mol. Sci.* **2022**, *23*, 6529. <https://doi.org/10.3390/ijms23126529>

Academic Editor: Jesús Fernández Lucas

Received: 17 May 2022

Accepted: 9 June 2022

Published: 10 June 2022

Publisher's Note: MDPI stays neutral with regard to jurisdictional claims in published maps and institutional affiliations.



Copyright: © 2022 by the authors. Licensee MDPI, Basel, Switzerland. This article is an open access article distributed under the terms and conditions of the Creative Commons Attribution (CC BY) license (<https://creativecommons.org/licenses/by/4.0/>).

Abstract: Amine oxidases are enzymes belonging to the class of oxidoreductases that are widespread, from bacteria to humans. The amine oxidase from *Lathyrus cicera* has recently appeared in the landscape of biocatalysis, showing good potential in the green synthesis of aldehydes. This enzyme catalyzes the oxidative deamination of a wide range of primary amines into the corresponding aldehydes but its use as a biocatalyst is challenging due to the possible inactivation that might occur at high product concentrations. Here, we show that the enzyme's performance can be greatly improved by immobilization on solid supports. The best results are achieved using amino-functionalized magnetic microparticles: the immobilized enzyme retains its activity, greatly improves its thermostability (4 h at 75 °C), and can be recycled up to 8 times with a set of aromatic ethylamines. After the last reaction cycle, the overall conversion is about 90% for all tested substrates, with an aldehyde production ranging between 100 and 270 mg depending on the substrate used. As a proof of concept, one of the aldehydes thus produced was successfully used for the biomimetic synthesis of a non-natural benzylisoquinoline alkaloid.

Keywords: enzyme immobilization; amine oxidase; magnetic particles; aldehydes; biocatalysis; oxidative deamination; primary amines

1. Introduction

The last few decades have witnessed a dramatic development of biocatalysis as a competitive and cost-effective technology for the synthesis of fine chemicals and active pharmaceutical intermediates [1–6]. The use of enzymes from both natural sources or produced in recombinant form, as raw or highly purified extracts, is also becoming increasingly common [7–9]. Enzymes can be used in cascades that mimic synthetic biochemical pathways, or they can replace some steps in the total synthesis of natural and non-natural molecules with high structural complexity [10–14]. However, the use of enzymes can be challenging on a large scale due to their high production costs, low operational stability, and difficulties in recovering them from the reaction mixtures [15]. Thus, a promising way to improve their performance is the immobilization onto solid supports, which also has the advantage of allowing their recovery and recycling [16–18]. Depending on the support on which they are immobilized, enzymes often improve their biochemical and kinetic properties, and, being recyclable, they can also be used in the scale-up of synthetic

processes [19,20]. For quite a long time, successful immobilization of biocatalysts has been largely confined to hydrolytic enzymes [21–23], but this scenario is changing with the development of enzymes for a wider range of biotransformations, including asymmetric reduction, carbon–carbon bond formation, and oxidation [24–26]. In this regard, increasing attention is paid to amine oxidases, enzymes belonging to the class of oxidoreductases that are widespread in nature (from bacteria to humans). These enzymes have recently appeared in the landscape of biocatalysis: they have shown good potential in both amine resolution and functionalization [27] and in the green synthesis of aldehydes [28]. To date, however, very few of them (namely those using FAD as a cofactor) have been immobilized on solid supports, mainly to develop biosensors for diagnostic purposes [29,30]. In this paper, we focus our attention on a plant Cu-containing amine oxidase (LCAO, *Lathyrus cicera* amine oxidase), which our research group has been studying for the biocatalytic productions of aldehydes. In nature, LCAO catalyzes the oxidative deamination of primary biogenic amines (i.e., putrescine and cadaverine) into the corresponding aldehydes [31]. We have shown that this enzyme has a relaxed substrate specificity, as it can convert a wide range of aliphatic and aromatic amines [28]. Although very promising, this system has some limitations, which include the low solubility of the oxygen co-substrate of the reaction, and the possible inactivation of the enzyme that may occur at high aldehyde concentration. One of the ways to overcome these issues could be the immobilization of the enzyme. Typically, immobilization improves the overall catalytic performance, allowing enzyme recycling, and a reduction in the overall process costs [32]. Among the different support materials, magnetic nanoparticles are considered the future of enzyme immobilization, due to their exceptional ease of handling, recovery, and reuse [33,34]. Thus, the present work aims at evaluating the activity of LCAO immobilized on various supports, including magnetic particles. As a proof of concept, we showed that the aldehydes produced with the immobilized enzyme can be easily used for the biomimetic synthesis of new berzylisoquinolines, structurally complex alkaloids that typically require a challenging chemical synthetic sequence [35].

2. Results and Discussion

2.1. Immobilization of LCAO

Cu-containing amine oxidases are enzymes highly expressed in *Leguminosae* sp. Among them, *Lathyrus cicera* is an extremely abundant source of this enzyme, where it is produced at high yields and accumulates in the periplasmic space of the etiolated sprouts. In a recent paper, we demonstrated that LCAO can be purified using an easily scalable chromatography-free protocol [28]. The purified enzyme is naturally active on biogenic primary amines, but it can be also used for the biocatalytic synthesis of a wide range of aliphatic and aromatic aldehydes, starting from the corresponding amines. Typically, biotransformation of non-natural substrates requires more enzyme with respect to the natural substrates, and this could be a problem when considering a large-scale synthesis. In this regard, LCAO immobilization may overcome this issue, by allowing its recycling/reuse, and at the same time, by avoiding the possible inactivation due to the accumulation of the aldehyde. Optimal immobilization strategies have to be tailored for each specific enzyme; thus, we tested which solid support was the most suitable for immobilizing LCAO. As a first step, we selected a series of resins and differently functionalized magnetic and non-magnetic particles, to test the binding capacity of the enzyme and its activity. Specifically, we chose different types of solid supports: a DEAE Sepharose resin, chloromethyl latex microparticles, and three different magnetic beads (COOH- or NH₂-functionalized microparticles (COOH-MMPs and NH₂-MMPs), and TurboBeads amine nanoparticles).

The surface lysine residues of the enzyme are used to covalently bind the selected supports using different strategies. Glutaraldehyde and 1-ethyl-3-(3-dimethylaminopropyl) carbodiimide hydrochloride (EDC) crosslinkers were used for amine-functionalized supports (DEAE, NH₂-MMPs, and TurboBeads amine nanoparticles) and COOH-MMPs, respectively; chloromethyl latex nanoparticles do not require crosslinker agents as they display an

their surface chloromethyl groups which yield a stable covalent bond with amino groups of LCAO, in a one-step process under mild aqueous conditions. As shown in Figure 1, all the selected supports were able to bind the enzyme which, in all cases, was active.

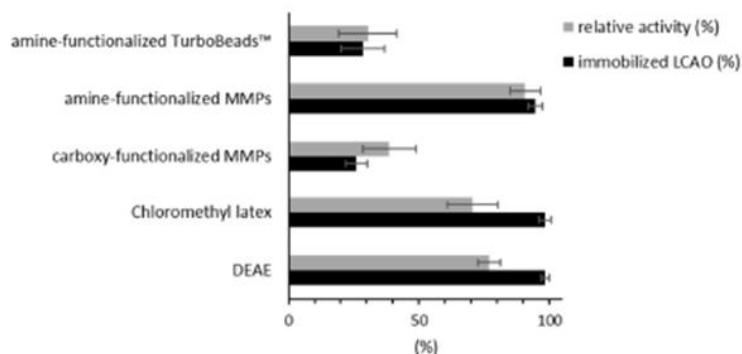


Figure 1. LCAO immobilization on different supports. Data are presented as mean \pm SD ($n = 3$).

Greater difficulties were encountered with the TurboBeads magnetic nanoparticles that, due to the low diameter (≤ 50 nm), are quite difficult to handle and tend to aggregate. This results in a low degree of protein binding, even though the linked enzyme is still active. A similar result was obtained when using the COOH-MMPs. In this case, although the relative activity is higher than expected based on the immobilized enzyme, this system is not convenient due to the large loss of protein that occurs during the crosslinking process. LCAO immobilization occurred efficiently on all the other tested solid supports. On chloromethyl latex nanoparticles and DEAE Sepharose resin very similar results were obtained: about 100% of the enzyme was bound with an enzymatic activity of about 70–80%. Both systems have advantages: chloromethyl latex beads are easy to prepare while DEAE resin can be packed on a column to generate a kind of flow reactor, in which the amino substrate present in the mobile phase can be converted into the aldehyde by the crosslinked enzyme. The best performance in terms of immobilization and activity was achieved with NH_2 -MMPs. In this case, the amount of immobilized enzyme is comparable to chloromethyl latex and DEAE resin, while the relative activity is definitely higher ($>90\%$). These results can be explained by the use of glutaraldehyde as the crosslinker: it typically promotes the formation of multipoint bonds with the enzyme while allowing it to maintain high conformational mobility, likely mimicking its free form. The superparamagnetic property of these micro-sized magnetic beads is useful because individual microparticles become magnetized only when exposed to an external magnetic field, but no magnetization occurs when the field is removed. These unique features can be exploited for enzyme separation from the reaction mixture and its reuse, making them competitive especially for large-scale industrial uses. Given these results, the NH_2 -MMPs were selected as the support of choice for LCAO immobilization.

LCAO-catalyzed oxidative deamination can be easily followed by monitoring hydrogen peroxide by a spectrophotometric assay coupled with peroxidase. The latter, in the presence of AAP and DCHBS, generates a typical purple-colored adduct. This assay can be promptly used to check LCAO immobilization on the surface of MMPs. As shown in Figure 2B, the solution turns purple starting from the particles that gather when a magnetic field is applied.

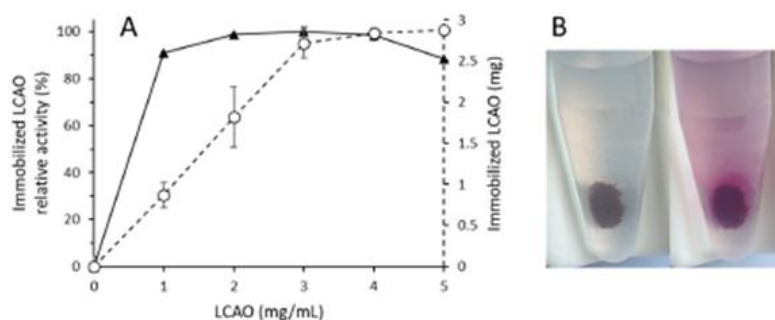


Figure 2. LCAO immobilization on NH_2 -MMPs. (A) Effect of LCAO concentration on the immobilization on NH_2 -MMPs (data are presented as the mean \pm SD of two experiments). (B) LCAO immobilized on NH_2 -MMPs in the absence (left) or the presence (right) of the reagents used for the peroxidase coupled assay. The purple halo around the microparticles grouped by the effect of the magnet indicates that LCAO is immobilized on them.

Alongside these qualitative data, we carried out a quantitative analysis of the immobilization process. The immobilization was performed according to the manufacturer's instructions, starting from a fixed concentration of particles (10 mg) and glutaraldehyde (10%), varying the amount of enzyme. The parameters used to evaluate the efficiency of the process were the amount of protein bound and its relative activity. Soluble LCAO activity at its optimum (pH 7, 25 °C) was considered 100%. As shown in Figure 2A, we tested enzyme concentrations ranging from 1 to 5 mg/mL, measuring at the same time the activity of immobilized LCAO.

In our experimental setting, MMPs are saturated using 3 mg of protein. A further increase in enzyme concentration did not improve the immobilization yield. In addition, in the range of 1–4 mg, the relative activity of the immobilized LCAO was close to 100%. Further increase in enzyme concentration resulted in a 15% loss of LCAO activity that may be explained by reduced accessibility of the substrate to the active site, probably due to a crowding of the enzyme on the surface of the support. Based on these results, the best immobilization yield is achieved by using 3 mg of the free enzyme. The LCAO-MMPs thus obtained were used for the performance study.

2.2. Characterization and Performance Study of LCAO-MMPs

The effect of reaction pH on the relative activity of both soluble and immobilized enzymes was investigated at different pH values (Figure 3A). As previously reported [28], soluble LCAO has an optimum pH towards its natural substrate putrescine between 7 and 8 while is significantly less active at pH 5.5 and 6. The immobilized enzyme does not show a shift in the optimum pH, while at pH different from 7, the activity is always higher than in the free enzyme (T-test, $p < 0.05$). This might be due to the change in the electrostatic charge of the enzyme after immobilization. Based on these results, the performance study was carried out at this pH value.

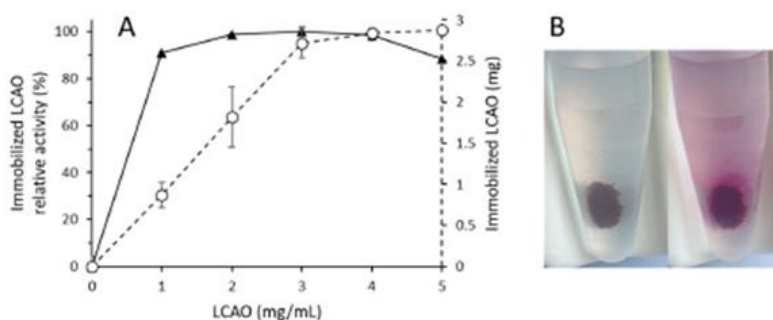


Figure 2. LCAO immobilization on NH₂-MMPs. (A) Effect of LCAO concentration on the immobilization on NH₂-MMPs (data are presented as the mean \pm SD of two experiments). (B) LCAO immobilized on NH₂-MMPs in the absence (left) or the presence (right) of the reagents used for the peroxidase coupled assay. The purple halo around the microparticles grouped by the effect of the magnet indicates that LCAO is immobilized on them.

Alongside these qualitative data, we carried out a quantitative analysis of the immobilization process. The immobilization was performed according to the manufacturer's instructions, starting from a fixed concentration of particles (10 mg) and glutaraldehyde (10%), varying the amount of enzyme. The parameters used to evaluate the efficiency of the process were the amount of protein bound and its relative activity. Soluble LCAO activity at its optimum (pH 7, 25 °C) was considered 100%. As shown in Figure 2A, we tested enzyme concentrations ranging from 1 to 5 mg/mL, measuring at the same time the activity of immobilized LCAO.

In our experimental setting, MMPs are saturated using 3 mg of protein. A further increase in enzyme concentration did not improve the immobilization yield. In addition, in the range of 1–4 mg, the relative activity of the immobilized LCAO was close to 100%. Further increase in enzyme concentration resulted in a 15% loss of LCAO activity that may be explained by reduced accessibility of the substrate to the active site, probably due to a crowding of the enzyme on the surface of the support. Based on these results, the best immobilization yield is achieved by using 3 mg of the free enzyme. The LCAO-MMPs thus obtained were used for the performance study.

2.2. Characterization and Performance Study of LCAO-MMPs

The effect of reaction pH on the relative activity of both soluble and immobilized enzymes was investigated at different pH values (Figure 3A). As previously reported [28], soluble LCAO has an optimum pH towards its natural substrate putrescine between 7 and 8 while is significantly less active at pH 5.5 and 6. The immobilized enzyme does not show a shift in the optimum pH, while at pH different from 7, the activity is always higher than in the free enzyme (T-test, $p < 0.05$). This might be due to the change in the electrostatic charge of the enzyme after immobilization. Based on these results, the performance study was carried out at this pH value.

One of the main reasons for the immobilization of an enzyme for biocatalytic purposes is its reusability and this is important to reduce the overall costs in any industrial application. While free LCAO can be used once, immobilized LCAO can be recycled efficiently. As shown in Figure 4, the enzyme can be reused up to 15 times with its natural substrate putrescine ($10.87 \pm 1.83\%$ relative activity at cycle 15).

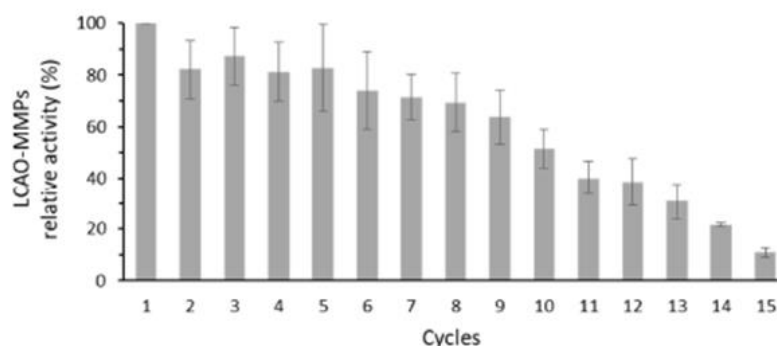
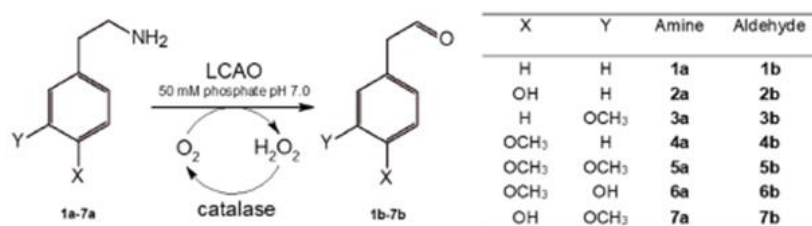


Figure 4. Reusability of LCAO immobilized on NH₂-MMPs. The reaction was carried out with putrescine as a substrate in the presence of catalase. Data are presented as mean \pm SD ($n = 3$).

The loss of activity observed during the cycles could be due to the partial inactivation of the enzyme caused by the accumulation of the aldehyde product which can react with the amino groups on the surface of the enzyme itself. However, the immobilized enzyme is more stable with respect to the free one probably because these surface amino groups are already involved in the crosslinking with the MMPs.

2.3. Biocatalytic Application of the Immobilized LCAO

The greater stability of the immobilized enzyme paves the way for its better use for biocatalytic purposes. Free LCAO has a relaxed substrate specificity, being able to process variously substituted aromatic and aliphatic primary amines [28]. In this paper, we aim to test whether the immobilized enzymes can be used for the biocatalytic production of aldehydes starting from a selection of aromatic ethylamines according to Scheme 1.



Scheme 1. Biocatalytic conversion of primary amines (compounds 1a–7a) into the corresponding aldehydes (compounds 1b–7b) in the presence of LCAO and catalase.

As a first step, we determined the Michaelis–Menten constant of the immobilized enzyme towards compounds 1a–7a comparing them with the natural substrate putrescine.

The K_m values are reported in Table 1 and compared with those previously obtained with the free enzyme.

Table 1. Michaelis–Menten constant of free and immobilized LCAO towards 1a–7a and putrescine.

Substrate	K_m Free LCAO (mM) *	K_m LCAO-MMPs (mM)
putrescine	0.27	0.36
1a	1.20	0.51
2a	0.60	0.79
3a	0.47	1.81
4a	5.37	4.74
5a	1.00	2.19
6a	1.58	0.64
7a	0.47	0.47

* [28].

The immobilized LCAO is active on all the substrates being able to convert all the amines tested in the corresponding aldehydes. K_m values for LCAO-MMPs are in the same low millimolar range of free enzyme and the small differences observed may be due to a series of factors including stabilization of the enzyme in more active conformations, different accessibility to the catalytic site, and different diffusion rate of substrates on the surface of the nanoparticle.

Based on these data, we tested whether immobilized LCAO could be eligible for scaling up the biocatalytic production of more complex aldehydes (Scheme 1). In a previous paper [28], we showed that LCAO can oxidatively deaminate a variety of aliphatic and aromatic primary amines with almost total conversion. In that case, we used an amine concentration equal to 5 mM as the accumulation of reaction product aldehyde tended to inactivate the enzyme. To overcome this drawback, more units of LCAO were added at regular intervals until the reaction was completed. The immobilized enzyme is less susceptible to inactivation by the accumulation of the reaction products, probably because its surface amino groups are instead used to bind to the magnetic microparticle.

A strong indication of this behavior comes from the actual studies on the natural putrescine substrate (see Figure 4), where the increased stability of the enzyme allowed up to 15 reaction cycles. Based on both these observations and the kinetic parameters (Table 1), we decided to scale up the process using an initial 20 mM amine concentration (15 mL final volume) in the presence of catalase, then using the same condition at each reaction cycle. The results are shown in Figure 5 and Table 2.

Table 2. Reusability of LCAO immobilized on NH_2 -MMPs in the synthesis of 1b–7b.

Product	Cycles	% Conversion	Total Amount (mg)
1b	8	92.85	267.40
2b	3	89.46	109.50
3b	6	91.50	247.05
4b	6	88.83	239.85
5b	4	89.93	194.25
6b	5	90.82	226.15
7b	5	89.48	222.80

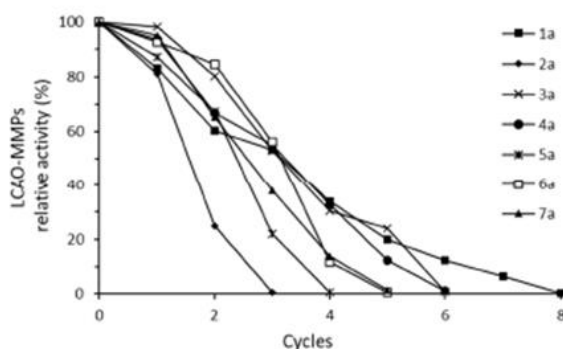
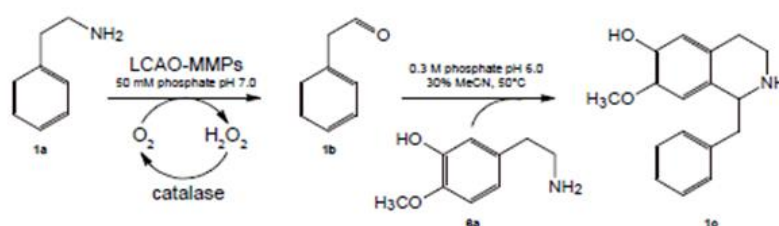


Figure 5. Reusability of LCAO immobilized on NH_2 -MMPs using compounds **1a–7a** as substrates in the presence of catalase. Data are presented as the mean of two experiments.

LCAO-MMPs quantitatively convert all tested substrates, although the number of times they can be reused varies. The conversion at the end of each reaction cycle was evaluated by determining the concentration of aldehyde by means of a colorimetric assay with Purpald[®]. The overall conversion at the end of all cycles is about 90% for all tested substrates, with an aldehyde production ranging between 100 and 270 mg depending on the substrate used. These values show an increase in aldehyde yield up to 45 times higher than the previously published method with the free enzyme [28]. These yields can be further increased by excluding the last reaction cycle. In the last cycle, in fact, the residual relative activity is always very low while the quantity of amine is equal to that of the previous cycles (20 mM). This implies that the complete transformation is slower and that the aldehyde formed, over long reaction times, can generate by-products that reduce the overall yields. Therefore, excluding the last cycle, a purer product would be obtained, albeit in a smaller quantity. With this protocol, the aldehydes are obtained in aqueous media ready to be used in domino processes, without further extraction and purification.

In this regard, as a proof of concept, we used one of the aldehydes thus produced to synthesize a new non-natural benzyloquinoline alkaloid. In nature, the first committed step for the synthesis of benzyloquinoline alkaloids is the Pictet–Spengler cyclization between *p*-OH phenylacetaldehyde and dopamine, catalyzed by norcoclaurine synthase [36]. Pesnot et al. found that this reaction can be catalyzed by phosphate ions as well, although yielding the racemic product [37]. This can be a very convenient method for the synthesis of racemic benzyloquinolines, as metabolic engineering and total chemical synthesis approaches, though occasionally applied, fail to meet industry standards in sustainability and efficiency. Other research groups have shown that the phosphate biomimetic catalysis may be suitable for the synthesis of different benzyloquinolines, starting from dopamine (or analogs with a free OH in position 3) and a series of variously substituted aldehydes. Based on these findings, we decided to synthesize a benzyloquinoline (**1c**), starting from **1b** (produced with LCAO-MMPs) and **6a** using phosphate ions as a catalyst (Scheme 2).



Scheme 2. Biomimetic synthesis of compound 1c.

This reaction takes place in the same reaction pot as the aldehyde (after removing the immobilized enzyme), lowering the pH to 6 and increasing the ionic strength of the buffer (up to 0.3 M). Under these conditions, in the presence of acetonitrile as cosolvent and at a temperature of 50 °C, the Pictet–Spengler reaction takes place. In about 2 h the reaction is complete providing 1c with a yield of 80%. Reaction yield was determined based on HPLC analyses, according to the method described in Section 4.

3. Conclusions

In this paper, we showed that it is possible to immobilize LCAO on different supports and that the best performance is obtained by using amine-functionalized magnetic particles. The enzyme immobilized on this support retains its activity, greatly improves its thermostability, and can be recycled numerous times with its natural substrate. Furthermore, immobilized LCAO can be used for biocatalytic applications. Specifically, this enzyme was used for the synthesis of a variety of aromatic aldehydes variously substituted starting from the corresponding amines. We showed that it is possible to scale up the process by recycling the immobilized enzyme a number of times and that it is possible to use the aldehydes thus produced for the synthesis of complex molecules, such as benzyloquinoline alkaloids.

4. Materials and Methods

4.1. Chemicals

Reagents and solvents obtained from commercial suppliers were used without further purification. All chemicals were purchased from Merck KGaA (Darmstadt, Germany). CDCl_3 (99.80% D) was obtained from Eurisotop (Saint Aubin, France).

4.2. LCAO Extraction and Purification

LCAO was extracted and purified by means of a chromatography-free protocol as reported by Di Fabio et al. [28]. Etiolated shoots (14 days old) were separated from the seed and roots and then shredded. Upon maceration in 0.3 M sodium chloride, the crude extract was filtered with the Sartolab[®] Vacuum Filters System (Polyethersulfone, 0.22 μm) using highly pure diatomaceous earth (Sartoclear Dynamics[®]) as a filter aid (Sartorius). The extract was then subjected to tangential ultrafiltration using a Vivaflow 200 module (Sartorius), exchanging the buffer with 50 mM phosphate pH 6.5. The sample was heated for 15 min at 65 °C and centrifuged to remove the precipitated proteins. Enzyme purity was checked using SDS-PAGE.

4.3. LCAO Immobilization

LCAO immobilization was performed using different commercial solid supports (DEAE resin, amino- and carboxy-functionalized magnetic microparticles, chloromethyl latex, and amino-functionalized Turbobeads), using standard protocols.

The amount of immobilized enzyme was measured by the Bradford assay by determining the concentration of soluble protein before and after the immobilization procedure.

DEAE fast flow resin: 2.47 g of Sepharose fast flow resin (Ge Healthcare) were washed twice with deionized water, activated with 0.5 M sodium chloride, and equilibrated with 10 mL of 50 mM sodium phosphate pH 7.0. LCAO (180 U—3.2 mg) and 0.2% glutaraldehyde (final concentration) were then added, and the mix was left in gentle agitation for 1 h. The resin was extensively washed with 50 mM sodium phosphate pH 7.0, resuspended in the same buffer to a final volume of 6 mL, and stored at 4 °C.

Chloromethyl latex beads: 0.25 mL of chloromethyl latex beads solution (Thermo Fisher Scientific) were activated with 1 mL 25 mM MES buffer pH 6.0, then centrifuged at 6000 rpm for 20 min. The beads (30 mg) were resuspended in 1 mL 25 mM MES buffer pH 6.0 containing 1.7 mg of LCAO (94 U) and incubated overnight at room temperature under gentle stirring. Then, the particle solution was centrifuged for 15 min at 5000 rpm and the beads were washed twice with 2 mL PBS and stored at 4 °C in 2 mL of the same buffer containing 0.1% glycine and 1% Tween 20.

Carboxy-functionalized magnetic microparticles (COOH-MMPs): 0.2 mL of carboxy-functionalized magnetic microparticles (Merck KGaA) were washed with 2 mL 0.1 M MES buffer pH 5.3. Magnetic particles (4 mg) recovered using the LifeSep magnetic separation unit (Dexter Magnetic Technologies, Inc.) were resuspended in 2 mL of the same buffer containing EDC (10 mM) and left under gentle stirring for 30 min at room temperature. The activated particles were washed with 50 mM sodium phosphate pH 7.3. Immobilization took place by adding 2.7 mg of LCAO (150 U) dissolved in 2 mL of the washing buffer and leaving the particles under stirring at room temperature for 3 h. The mix was washed with phosphate buffer and then resuspended in 2 mL 50 mM sodium phosphate pH 7.0 containing 30 mM glycine (quencher) and 0.5% Tween 20. After 30 min under gentle stirring, the microparticles were recovered, washed with phosphate buffer, and stored at 4 °C in 50 mM sodium phosphate pH 7.0 containing 0.1% Tween 20.

Turbobeads amine: 30 mg of Turbobeads nanoparticles (Merck KGaA) were washed with deionized water, recovered using the LifeSep magnetic separation unit, resuspended in 1 mL 0.1 M MES buffer pH 6.0 and then sonicated for 1 min. The nanoparticles were extensively washed in the sonication buffer, resuspended in 2 mL of the same buffer containing 10% glutaraldehyde, and stirred for 1.5 h. The particles were then washed with 50 mM phosphate buffer pH 7.3 and incubated with 1.5 mg of LCAO (82 U) under gentle stirring at room temperature. After 3 h, the reaction was quenched exchanging the buffer with 50 mM phosphate pH 7.3 containing 30 mM glycine and 0.5% tween 20. After an additional 30 min, the particles were recovered, washed with phosphate buffer, resuspended in 2 mL 50 mM phosphate buffer pH 7.0 containing 0.1% tween 20, and stored at 4 °C.

Amino-functionalized magnetic microparticles (NH₂-MMPs): 0.2 mL of amino-functionalized magnetic microparticles solution (Merck KGaA) were activated twice with 0.1 M MES buffer pH 6.0. After separation using the LifeSep magnetic separation unit, the particles (10 mg) were resuspended in the same buffer containing 10% glutaraldehyde and left under stirring for 1 h at room temperature. The magnetic beads were then recovered, washed with 50 mM phosphate buffer pH 7.3, and resuspended in 1 mL of the same buffer containing different amounts of LCAO (from 1 to 5 mg; 55–275 U). After 2.5 h, the reaction was quenched exchanging the buffer with 50 mM sodium phosphate pH 7.3 containing 30 mM glycine and 0.5% Tween 20. After further 30 min under gentle stirring, the magnetic particles were washed with 50 mM sodium phosphate pH 7 and 0.1% Tween 20 and stored at 4 °C in the same buffer.

4.4. LCAO Activity

Enzymatic activity of both free and immobilized LCAO was determined by a coupled diamine oxidase/peroxidase spectrophotometric assay. Relative activity was obtained by calculating the percentage of immobilized enzyme units versus the total units used in the immobilization reaction.

The enzymatic assay was carried out in the presence of 10 mM putrescine at 25 °C and in 20 mM phosphate buffer pH 7.0. Enzymatic activity of LCAO immobilized on NH₂-MMPs was also assayed using 2 U LCAO at different pH values (ranging between 5.5 and 8.0). The production of H₂O₂ was monitored following the increasing absorption at 515 nm, due to the coupling between 1 mM 4-aminoantipyrine (AAP) and 10 mM sodium-3,5-dichloro-2-hydroxybenzenesulfonate (DCHBS) catalyzed by horseradish peroxidase (2 U/mL). The initial rates of the reaction at different substrate concentrations (0.1–10 mM) were determined and the kinetic parameters were calculated by non-linear regression fitting the data to the Michaelis–Menten equation $V = V_{max}[S]/(K_m + [S])$. All curve fitting was carried out using Kaleidagraph software (Synergy Software, Reading, PA).

4.5. Enzymatic Synthesis of Aldehydes

The biocatalytic synthesis of the seven different aldehydes (compounds **1b–7b**) was carried out starting from the corresponding primary amines (compounds **1a–7a**) in the presence of LCAO immobilized on the surface of NH₂-MMPs (LCAO-MMPs). A 20 mM solution of amine substrate was prepared in 50 mM sodium phosphate buffer pH 7.0 in the presence of 30 U of LCAO-MMPs and 250 U/mL of catalase to a final volume of 15 mL. At the end of each reaction cycle, the particles were recovered using the magnetic separation unit, extensively washed with phosphate buffer pH 7, and reused for the next reaction cycle.

The substrate consumption was monitored by GC/MS, whereas aldehyde formation was monitored by Purpald[®] assay and GC/MS.

GC/MS analysis: amine substrates (**1a–7a**) were analyzed as ethoxy carbonyl derivatives. Derivatization with ethyl chloroformate (ECF) was conducted by adding to 50 µL of the reaction mixture, 25 µL of 7 M sodium hydroxide, and 25 µL ECF dissolved in 50 µL of dichloromethane. The biphasic system was stirred vigorously for 2 min, saturated with NaCl, and extracted with 125 µL of ethyl acetate. After centrifugation, 100 µL of the organic phase were analyzed by GC/MS using methyl-C17 as the internal standard. Aldehydes (**1b–7b**) were analyzed without derivatization: 100 µL of reaction mix were extracted with 400 µL of diethyl ether and directly analyzed by GC/MS. GC/MS analyses were performed with an Agilent 6850A gas chromatograph coupled to a 5973N quadrupole mass selective detector (Agilent Technologies, Palo Alto, CA, USA). Chromatographic separations were carried out with an Agilent HP-5ms fused silica capillary column (30 m × 0.25 mm id) coated with 5% phenyl–95% dimethylpolysiloxane (film thickness 0.25 µm) as a stationary phase. Injection mode: splitless at a temperature of 280 °C. Column temperature program: 70 °C for 4 min and then to 240 °C at a rate of 25 °C min⁻¹ and held for 4 min. The carrier gas was helium at a constant flow of 1.0 mL min⁻¹. The spectra were obtained in the electron impact mode at 70 eV ionization energy; ion source 280 °C; ion source vacuum 10⁻⁵ Torr. Mass spectrometric analysis was performed in the range m/z 50–500 at a rate of 0.42 scans s⁻¹.

Purpald[®] colorimetric assay: Aldehyde production was monitored by a colorimetric assay following the reaction between the newly synthesized aldehyde and 4-Amino-5-hydrazino-1,2,4-triazole-3-thiol (Purpald[®]) [28].

4.6. Biomimetic Synthesis of Compound **1c**

Compound **1b** was synthesized starting from **1a** as described above. The immobilized enzyme was reused up to 8 times. After each reaction cycle, LCAO-MMPs were recovered and reused, while the newly synthesized aldehyde (15 mL 20 mM) was stored at –20 °C. At the end of the last cycle, the reaction fractions of each cycle were pooled, the pH was adjusted to 6.0, and the ionic strength of the buffer was increased to 0.3 M. Compound **6a** was added stoichiometrically to **1b** and the phosphate mediated Pictet Spengler cyclization was carried out for 2 h at 50 °C in the presence of 30% acetonitrile.

The production of the benzyloisoquinoline alkaloid (**1c**) was monitored by GC/MS after ECF derivatization (see above). Column temperature program: 70 °C for 1 min and then to 300 °C at a rate of 15 °C min⁻¹ and held for 10 min.

The enzymatic assay was carried out in the presence of 10 mM putrescine at 25 °C and in 20 mM phosphate buffer pH 7.0. Enzymatic activity of LCAO immobilized on NH₂-MMPs was also assayed using 2 U LCAO at different pH values (ranging between 5.5 and 8.0). The production of H₂O₂ was monitored following the increasing absorption at 515 nm, due to the coupling between 1 mM 4-aminoantipyrine (AAP) and 10 mM sodium-3,5-dichloro-2-hydroxybenzenesulfonate (DCHBS) catalyzed by horseradish peroxidase (2 U/mL). The initial rates of the reaction at different substrate concentrations (0.1–10 mM) were determined and the kinetic parameters were calculated by non-linear regression fitting the data to the Michaelis–Menten equation $V = V_{max}[S]/(K_m + [S])$. All curve fitting was carried out using Kaleidagraph software (Synergy Software, Reading, PA).

4.5. Enzymatic Synthesis of Aldehydes

The biocatalytic synthesis of the seven different aldehydes (compounds **1b–7b**) was carried out starting from the corresponding primary amines (compounds **1a–7a**) in the presence of LCAO immobilized on the surface of NH₂-MMPs (LCAO-MMPs). A 20 mM solution of amine substrate was prepared in 50 mM sodium phosphate buffer pH 7.0 in the presence of 30 U of LCAO-MMPs and 250 U/mL of catalase to a final volume of 15 mL. At the end of each reaction cycle, the particles were recovered using the magnetic separation unit, extensively washed with phosphate buffer pH 7, and reused for the next reaction cycle.

The substrate consumption was monitored by GC/MS, whereas aldehyde formation was monitored by purpald[®] assay and GC/MS.

GC/MS analysis: amine substrates (**1a–7a**) were analyzed as ethoxy carbonyl derivatives. Derivatization with ethyl chloroformate (ECF) was conducted by adding to 50 µL of the reaction mixture, 25 µL of 7 M sodium hydroxide, and 25 µL ECF dissolved in 50 µL of dichloromethane. The biphasic system was stirred vigorously for 2 min, saturated with NaCl, and extracted with 125 µL of ethyl acetate. After centrifugation, 100 µL of the organic phase were analyzed by GC/MS using methyl-C17 as the internal standard. Aldehydes (**1b–7b**) were analyzed without derivatization: 100 µL of reaction mix were extracted with 400 µL of diethyl ether and directly analyzed by GC/MS. GC/MS analyses were performed with an Agilent 6850A gas chromatograph coupled to a 5973N quadrupole mass selective detector (Agilent Technologies, Palo Alto, CA, USA). Chromatographic separations were carried out with an Agilent HP-5ms fused silica capillary column (30 m × 0.25 mm id) coated with 5% phenyl–95% dimethylpolysiloxane (film thickness 0.25 µm) as a stationary phase. Injection mode: splitless at a temperature of 280 °C. Column temperature program: 70 °C for 4 min and then to 240 °C at a rate of 25 °C min⁻¹ and held for 4 min. The carrier gas was helium at a constant flow of 1.0 mL min⁻¹. The spectra were obtained in the electron impact mode at 70 eV ionization energy; ion source 280 °C; ion source vacuum 10⁻⁵ Torr. Mass spectrometric analysis was performed in the range m/z 50–500 at a rate of 0.42 scans s⁻¹.

Purpald[®] colorimetric assay: Aldehyde production was monitored by a colorimetric assay following the reaction between the newly synthesized aldehyde and 4-Amino-5-hydrazino-1,2,4-triazole-3-thiol (Purpald[®]) [28].

4.6. Biomimetic Synthesis of Compound **1c**

Compound **1b** was synthesized starting from **1a** as described above. The immobilized enzyme was reused up to 8 times. After each reaction cycle, LCAO-MMPs were recovered and reused, while the newly synthesized aldehyde (15 mL, 20 mM) was stored at –20 °C. At the end of the last cycle, the reaction fractions of each cycle were pooled, the pH was adjusted to 6.0, and the ionic strength of the buffer was increased to 0.3 M. Compound **6a** was added stoichiometrically to **1b** and the phosphate mediated Pictet Spengler cyclization was carried out for 2 h at 50 °C in the presence of 30% acetonitrile.

The production of the benzylisoquinoline alkaloid (**1c**) was monitored by GC/MS after ECF derivatization (see above). Column temperature program: 70 °C for 1 min and then to 300 °C at a rate of 15 °C min⁻¹ and held for 10 min.

Article

Rapid and Simultaneous Determination of Free Aromatic Carboxylic Acids and Phenols in Commercial Juices by GC-MS after Ethyl Chloroformate Derivatization

Alessio Incocciati , Elisa Di Fabio, Alberto Boffi, Alessandra Bonamore  and Alberto Macone 

Department of Biochemical Sciences, "Sapienza" University of Rome, p.le A. Moro 5, 00185 Rome, Italy; alessio.incocciati@uniroma1.it (A.I.); elisa.difabio@uniroma1.it (E.D.F.); alberto.boffi@uniroma1.it (A.B.)
 * Correspondence: alessandra.bonamore@uniroma1.it (A.B.); alberto.macone@uniroma1.it (A.M.)

Abstract: Natural phenol and phenolic acids are widely distributed in the plant kingdom and the major dietary sources include fruits and beverages derived therefrom. Over the past decades, these compounds have been widely investigated for their beneficial effects on human health and, at the same time, several analytical methods have been developed for their determination in these matrices. In the present paper, 19 different aromatic carboxylic acids and phenols were characterized by GC-MS using ethyl chloroformate as the derivatizing agent. This procedure occurs quickly at room temperature and takes place in aqueous media simultaneously with the extraction step in the presence of ethanol using pyridine as a catalyst. The analytical method herein developed and validated presents excellent linearity in a wide concentration range (25–3000 ng/mL), low LOQ (in the range 25–100 ng/mL) and LOD (in the range 12.5–50 ng/mL), and good accuracy and precision. As a proof of concept, ethyl chloroformate derivatization was successfully applied to the analysis of a selection of commercial fruit juices (berries, grape, apple, pomegranate) particularly rich in phenolic compounds. Some of these juices are made up of a single fruit, whereas others are blends of several fruits. Our results show that among the juices analyzed, those containing cranberry have a total concentration of the free aromatic carboxylic acids and phenols tested up to 15 times higher than other juices.

Keywords: phenolic acids; benzoic acids; phenols; ethyl chloroformate; GC-MS; fruit juices



Citation: Incocciati, A.; Di Fabio, E.; Boffi, A.; Bonamore, A.; Macone, A. Rapid and Simultaneous Determination of Free Aromatic Carboxylic Acids and Phenols in Commercial Juices by GC-MS after Ethyl Chloroformate Derivatization. *Separations* 2022, 5, 9. <https://doi.org/10.3390/separations5010009>

Article

Ethylchloroformate Derivatization for GC–MS Analysis of Resveratrol Isomers in Red Wine

Elisa Di Fabio, Alessio Inocciati, Federica Palombarini, Alberto Boffi, Alessandra Bonamose ^{*}† and Alberto Macone ^{*}† 

Department of Biochemical Sciences, “Sapienza” University of Rome, p.le A.Moro 5, 00185 Rome, Italy;

elisa.difabio@uniroma1.it (E.D.F.); inocciati.1750499@studenti.uniroma1.it (A.I.);

federica.palombarini@uniroma1.it (F.P.); alberto.boffi@uniroma1.it (A.B.)

^{*} Correspondence: alessandra.bonamose@uniroma1.it (A.B.); alberto.macone@uniroma1.it (A.M.)

† These authors contributed equally to this work.

Received: 17 September 2020; Accepted: 9 October 2020; Published: 9 October 2020




Abstract: Resveratrol (3,5,4'-trihydroxystilbene) is a natural compound that can be found in high concentrations in red wine and in many typical foods found in human diet. Over the past decades, resveratrol has been widely investigated for its potential beneficial effects on human health. At the same time, numerous analytical methods have been developed for the quantitative determination of resveratrol isomers in oenological and food matrices. In the present work, we developed a very fast and sensitive GC–MS method for the determination of resveratrol in red wine based on ethylchloroformate derivatization. Since this reaction occurs directly in the water phase during the extraction process itself, it has the advantage of significantly reducing the overall processing time for the sample. This method presents low limits of quantification (LOQ) (25 ng/mL and 50 ng/mL for *cis*- and *trans*-resveratrol, respectively) and excellent accuracy and precision. Ethylchloroformate derivatization was successfully applied to the analysis of resveratrol isomers in a selection of 15 commercial Italian red wines, providing concentration values comparable to those reported in other studies. As this method can be easily extended to other classes of molecules present in red wine, it allows further development of new GC–MS methods for the molecular profiling of oenological matrices.

Keywords: resveratrol; red wine; ethylchloroformate; gas chromatography–mass spectrometry

Review

Ferritin Nanocages for Protein Delivery to Tumor Cells

Federica Palombarini, Elisa Di Fabio, Alberto Boffi, Alberto Macone *  and Alessandra Bonamore *

Department of Biochemical Sciences "Alessandro Rossi Fanelli", Sapienza University of Rome, Piazzale Aldo Moro 5, 00185 Rome, Italy; federica.palombarini@uniroma1.it (F.P.); elisa.difabio@uniroma1.it (E.D.F.); alberto.boffi@uniroma1.it (A.B.)

* Correspondence: alberto.macone@uniroma1.it (A.M.); alessandra.bonamore@uniroma1.it (A.B.)

Received: 17 January 2020; Accepted: 13 February 2020; Published: 13 February 2020



Abstract: The delivery of therapeutic proteins is one of the greatest challenges in the treatment of human diseases. In this frame, ferritins occupy a very special place. Thanks to their hollow spherical structure, they are used as modular nanocages for the delivery of anticancer drugs. More recently, the possibility of encapsulating even small proteins with enzymatic or cytotoxic activity is emerging. Among all ferritins, particular interest is paid to the *Archaeoglobus fulgidus* one, due to its peculiar ability to associate/dissociate in physiological conditions. This protein has also been engineered to allow recognition of human receptors and used in vitro for the delivery of cytotoxic proteins with extremely promising results.

Keywords: ferritin; drug delivery; therapeutic proteins; nanocarrier; *Archaeoglobus fulgidus*; TfR1 receptor; tumor cells

RESEARCH

Open Access



Self-assembling ferritin-dendrimer nanoparticles for targeted delivery of nucleic acids to myeloid leukemia cells

Federica Palombanini^{1†}, Silvia Masciarelli^{2,4†}, Alessio Incocciati¹, Francesca Liccardo², Elisa Di Fabio³, Antonia Iazzetti², Giancarlo Fabrizi², Francesco Fazi^{2*}, Alberto Macone^{1*}, Alessandra Bonamore^{1*} and Alberto Boffi^{1,5}

Abstract

Background: In recent years, the use of ferritins as nano-vehicles for drug delivery is taking center stage. Compared to other similar nanocarriers, *Archaeoglobus fulgidus* ferritin is particularly interesting due to its unique ability to assemble-disassemble under very mild conditions. Recently this ferritin was engineered to get a chimeric protein targeted to human CD71 receptor, typically overexpressed in cancer cells.

Results: *Archaeoglobus fulgidus* chimeric ferritin was used to generate a self-assembling hybrid nanoparticle hosting an aminic dendrimer together with a small nucleic acid. The positively charged dendrimer can indeed establish electrostatic interactions with the chimeric ferritin internal surface, allowing the formation of a protein-dendrimer binary system. The 4 large triangular openings on the ferritin shell represent a gate for negatively charged small RNAs, which access the internal cavity attracted by the dense positive charge of the dendrimer. This ternary protein-dendrimer-RNA system is efficiently uptaken by acute myeloid leukemia cells, typically difficult to transfect. As a proof of concept, we used a microRNA whose cellular delivery and induced phenotypic effects can be easily detected. In this article we have demonstrated that this hybrid nanoparticle successfully delivers a pre-miRNA to leukemia cells. Once delivered, the nucleic acid is released into the cytosol and processed to mature miRNA, thus eliciting phenotypic effects and morphological changes similar to the initial stages of granulocyte differentiation.

Conclusion: The results here presented pave the way for the design of a new family of protein-based transfecting agents that can specifically target a wide range of diseased cells.

Keywords: Ferritin, Protein nanoparticles, Self-assembly, Targeted delivery, Dendrimers, PAMAM, miRNA